# MATHEMATICAL MODELING OF SOLAR AIR HEATER WITH DIFFERENT GEOMETRIES

A thesis submitted in partial fulfillment of
the requirement for the award of degree of

**MASTER OF ENGINEERING**

**in**

**CAD/CAM & ROBOTICS**


**Submitted By**

**ASHISH KUMAR**
**(80781005)**

**Under the guidance of**

**Mr. SUMEET SHARMA**
**Sr. Lecturer, Mechanical Engg. Deptt.**
**Thapar University, Patiala**



**Mechanical Engineering Department**

**THAPAR UNIVERSITY PATIALA-147004**


**JULY, 2009**

# CERTIFICATE

I hereby declare that the work which is being presented in this thesis entitled, **"MATHEMATICAL MODELING OF SOLAR AIR HEATER WITH DIFFERENT GEOMETRIES"** in partial fulfillment of requirement for the award of the **MASTER OF ENGINEERING IN CAD/CAM & ROBOTICS** submitted in the **MECHANICAL ENGINEERING DEPARTMENT OF THAPAR UNIVERSITY, PATIALA,** is an authentic record of the initial work carried out by me under the guidance of **Mr. SUMEET SHARMA, Sr. Lecturer, Mechanical Engineering Department, TU, Patiala** and refers other researcher's works which are duly listed in the references section.

The matter presented in this thesis has not been submitted in part or full to any other university or institute for the award of any degree.

**Dated:** 15/07/2009

**(ASHISH KUMAR)**

This is to certify that above declaration made by the student concerned is correct to the best of my knowledge & belief.

**Mr. SUMEET SHARMA**
**Sr. Lecturer, MED**
**Thapar University, Patiala**

**Countersigned by**

**Dr. S. K. MOHAPATRA**
**Professor & Head, MED**
**Thapar University, Patiala**

**Dr. R. K. SHARMA**
**Dean, Academic Affairs**
**Thapar University, Patiala**

# ACKNOWLEDGEMENT

Words are often less to revels one's deep regards. With an understanding that work like this can never be the outcome of a single person, I take this opportunity to express my profound sense of gratitude and respect to all those who helped me through the duration of this work.

I am highly grateful to the authorities of Thapar University, Patiala for providing this opportunity to carry out the thesis work.

I would like to express a deep sense of gratitude and thank profusely to my thesis guide **Mr. SUMEET SHARMA** for their sincere & invaluable guidance, suggestions and attitude which inspired me to submit thesis report in the present form. His feedback and editorial comments were also invaluable for the writing of this thesis. I am also thankful to **Dr. Mohd. KALEEM KHAN**, Asst. Prof., MED, IIT Patna, for their sincere & invaluable guidance and time to time suggestions. I am thankful to **Dr. S. K. MOHAPATRA,** Prof. & Head, Mechanical Engineering Department for providing the facilities for the completion of the work.

At last, I would like to thanks all the members and employees of Mechanical Engineering Department, Thapar University, Patiala for their everlasting support.

Regards,

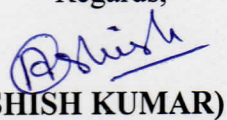

**(ASHISH KUMAR)**

# ABSTRACT

The intent of the present study is to study the behavior of counter flow solar air heaters and to compare their performance with the conventional solar air heaters under different set of conditions, obtained by changing the various governing parameters like air mass flow rate, inlet air temperature, spacing between top cover and absorber plate and intensity of solar radiation. Four types of solar air heaters have been taken into consideration i.e. single glazing solar air heater, double glazing solar air heater, counter flow solar air heater and counter flow with porous matrix solar air heater. The problem have been solved by the Finite Difference Method. It has been found that the counter flow solar air heater is more efficient than the conventional solar air heaters. The efficiency of counter flow with porous matrix solar air heater is highest among all four types of solar air heaters which are been taken into consideration.

# NOMENCLATURE

| SYMBOLS | DESCRIPTION |
|---|---|
| $A_f$ | Frontal area |
| $a_v$ | Specific area |
| $c_p$ | Specific heat |
| D | Depth of the duct |
| $D_e$ | Equivalent diameter |
| $D_h$ | Hydraulic diameter |
| $d_w$ | Wire diameter |
| h | Heat transfer coefficient |
| I | Intensity of solar radiation |
| k | Thermal conductivity |
| L | Length of the duct |
| m’ | Air mass flow rate per unit duct width |
| m | Air mass flow rate |
| N | No. of screens |
| $n_1$ | Refractive index |
| Nu | Nusselt number |
| P | Porosity |
| p | Perimeter of duct cross section |
| Pr | Prandtl number |
| Re | Reynolds number |
| $r_h$ | Hydraulic radius |
| T | Temperature |
| U | Overall heat transfer coefficient |
| V | Ambient air velocity |
| W | Pumping power |

## GREEK LETTERS

| | |
|---|---|
| $\varepsilon$ | Emissivity |
| $\tau$ | Transmissivity |
| $\alpha$ | Absorptivity |
| $\sigma$ | Diffusivity |
| $\beta$ | Stefan-Boltzmann constant |
| $\rho$ | Extinction coefficient |
| $\mu$ | Dynamic viscosity |
| $\nu$ | Kinematic viscosity |
| $\eta$ | Thermal efficiency |
| $\Delta$ | Difference of two quantities |

## SUBSCRIPTS

| | |
|---|---|
| a | Ambient |
| b | Bottom |
| c | Cover |
| e | Effective |
| f | Fluid |
| p | Packing, plate |
| r | Radiation |
| t | Top |
| 1 | First glass cover / air in first passage |
| 2 | Second glass cover / air in second passage |

# TABLE OF CONTENT

# LIST OF FIGURES

# LIST OF TABLES

# CHAPTER 1
# INTRODUCTION

With the rapid rise in the population and the living standards, the world seems to engulf into major crisis, called energy crisis. If this growth continues with the same pace the condition would go from bad to worse. The reverse of conventional sources of energy like coal, petroleum and natural gas are depleting at a very fast rate to fulfill the demand of the growing population. So there is a need to look for some other energy sources that could meet this growing demand. One such source is solar energy, which is cheap available in abundance. Solar energy has been utilized in many ways. Some of its thermal applications are as follows

1. Water heating
2. Space heating
3. Power generation
4. Space cooling and refrigeration
5. Distillation
6. Drying, and
7. Cooking

## 1.1 THERMAL ENERGY COLLECTION AND STORAGE DEVICES

In any solar-thermal collection device, the principle usually followed is to expose a dark surface to solar to solar radiation so that most of the solar radiation is absorbed and converted heat energy. A part of this heat energy is then transferred to a fluid like water or air. When no optical concentration of radiation is done, the device in which the collection is achieved is called the flat plate collector. In other words, when the area of interception of solar radiation is same as that of absorption then the collection device is called flat-plate collector else it is concentrating collector. The flat plate collector is the most important type of solar collector because it is simple in design, has no moving parts and requires little maintenance. It can be used for variety of applications in which temperature of required heat energy ranges from 40-100$^0$C.

When the temperature above$100^0$C are required, it usually becomes necessary to concentrate the radiation. This is achieved by concentrating collector.

In this chapter, the utilization of solar energy into useful thermal energy has been discussed. The devices which are used for this purpose are known as solar collectors.

## 1.2 SOLAR COLLECTOR

A solar thermal collector is a solar collector specifically intended to collect heat, that is, to absorb sunlight to provide heat.

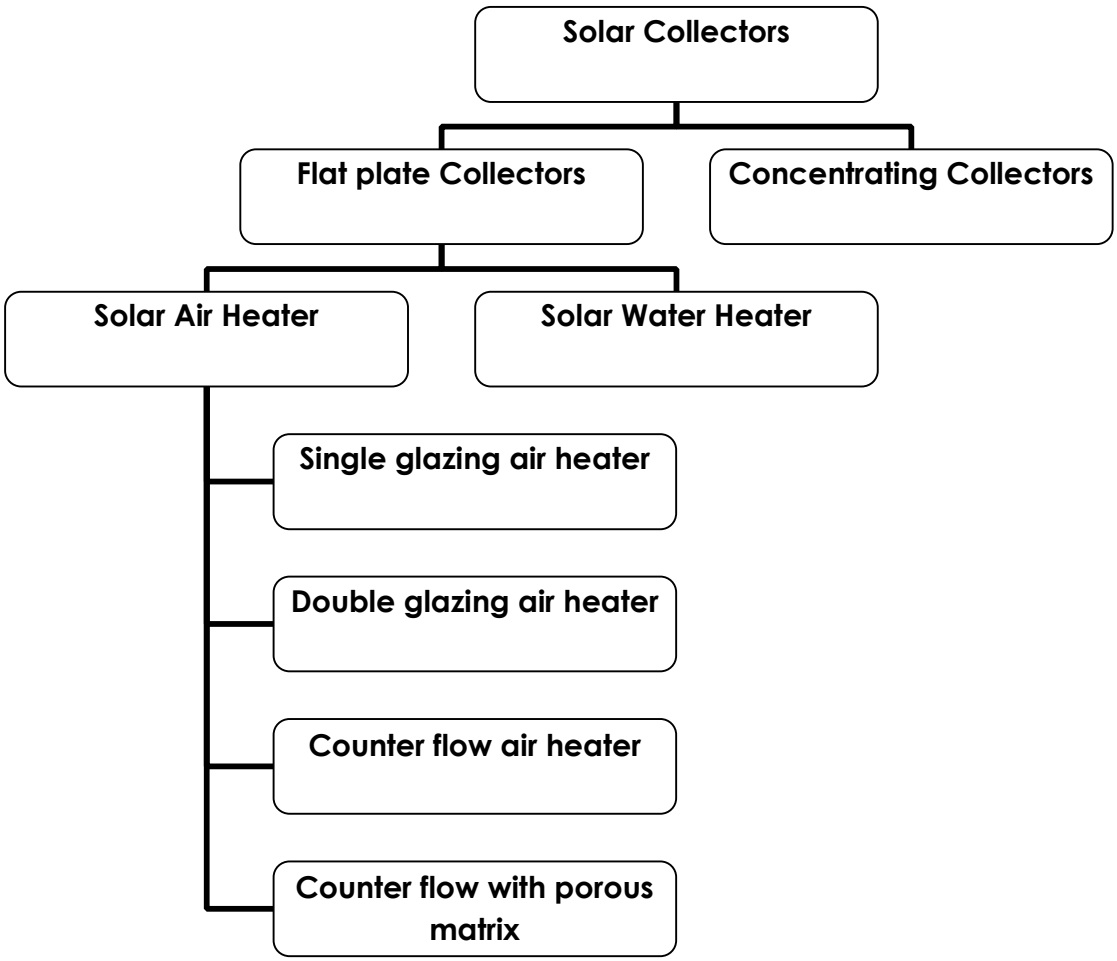


**Fig.1.1 Classification of solar collectors**

There are various types of thermal collectors, such as solar parabolic, solar trough and solar towers. These types of collectors are generally used in solar power plants where

solar heat is used to generate electricity by heating water to produce steam and driving a turbine connected to the electrical generator. Fig. 1.1 shows the classification of solar collectors.

### 1.2.1 Concentrating collector

Concentrating collectors use mirrored surfaces to concentrate the sun's energy on an absorber called a receiver as shown in figure 1.2. Concentrating collectors also achieve high temperatures, but unlike evacuated-tube collectors, they can do so only when direct sunlight is available. The mirrored surface focuses sunlight collected over a large area onto a smaller absorber area to achieve high temperatures. Some designs concentrate solar energy onto a focal point, while others concentrate the sun's rays along a thin line called the focal line. The receiver is located at the focal point or along the focal line. A heat-transfer fluid flows through the receiver and absorbs heat. These collectors reach much higher temperatures than flat-plate collectors. However, concentrators can only focus direct solar radiation, with the result being that their performance is poor on hazy or cloudy days. Concentrators are most practical in areas of high insolation (exposure to the sun's rays), such as those close to the equator and in the desert southwest United States.

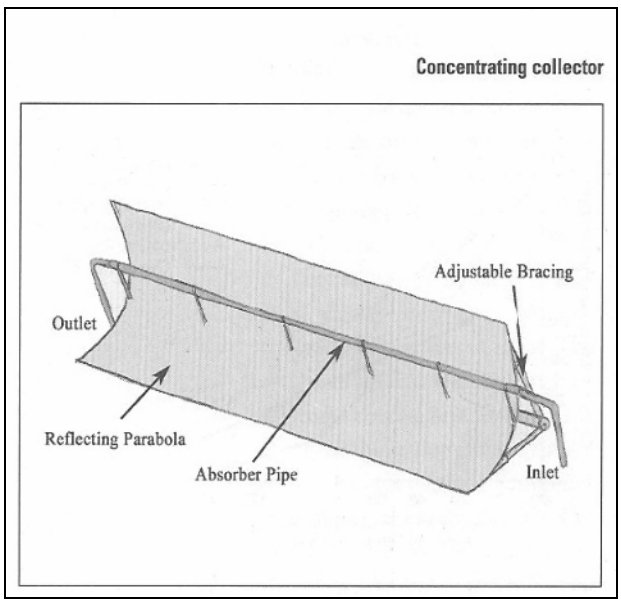


**Figure1.2 concentrating collector**

There are four basic types of concentrating collectors:

- Parabolic trough
- Parabolic dish
- Power tower
- Stationary concentrating collectors

### 1.2.2 Flat-plate collectors

Flat-plate collectors are very common and are available as liquid-based and air-based collectors. These collectors are better suited for moderate temperature applications where the demand temperature is 30-$70^0$C and/or for applications that require heat during the winter months. The air-based collectors are used for the heating of buildings, ventilation air and crop-drying. In this type of collector a flat absorber plate efficiently transforms sunlight into heat. To minimize heat escaping, the plate is located between a glazing (glass pane or transparent material) and an insulating panel. The glazing is chosen so that a maximum amount of sunlight will pass though it and reach the absorber. figure 1.3 represents the constructional features of flat plate collectors.

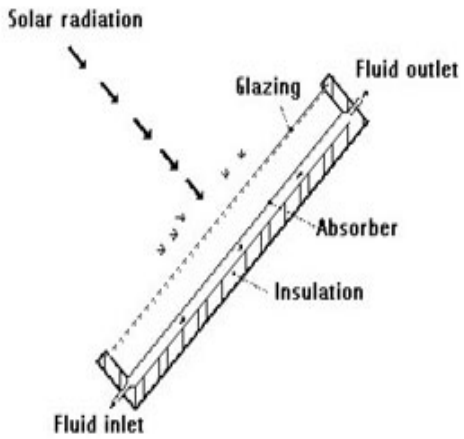


**Figure 1.3 Flat plate collector**

#### 1.2.2.1 Solar water heater

In Solar water heater water is heated by the use of solar energy. Solar heating systems are generally composed of solar thermal collectors, a fluid system to move the heat from the collector to its point of usage. figure 1.4 shows the different parts of solar water heater. The system may use electricity for pumping the fluid, and have a reservoir or tank for heat storage and subsequent use. The systems may be used to heat water for a wide variety of uses, including home, business and industrial uses.

Heating swimming pools, under floor heating or energy input for space heating or cooling are more specific examples.

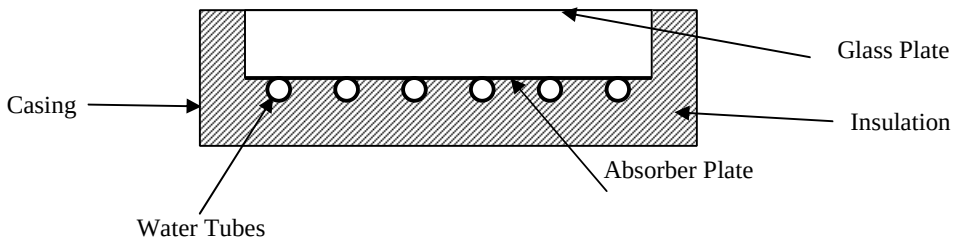


**Figure 1.4: Solar water heater**

### 1.2.2.2 Solar Air Heater

A solar air heater is a simple device to heat air by utilizing solar energy, which has many applications in drying agricultural products, such as seeds, fruits and vegetables, and as a low-temperature energy source. Also, solar air heaters are utilized for heating buildings with auxiliary heaters to save energy in winter-time. Solar air heaters can also be used for industrial purposes. Radiation energy of sun is absorbed by a absorber plate and then transferred to air. This heated air can be used further according to our requirement.

Different configurations are possible for air flow in the passage. Solar air heaters are simple in design and maintenance. Depending upon the air passage in the solar air heater the air heaters can be classified in the following ways

#### 1.2.2.2.1 Single glass cover air heater

In this type of air heater there is only one glass surface on the top and the absorber is below the glass plate as shown in figure1.5. The air flows between the glass plate and the absorber plate.

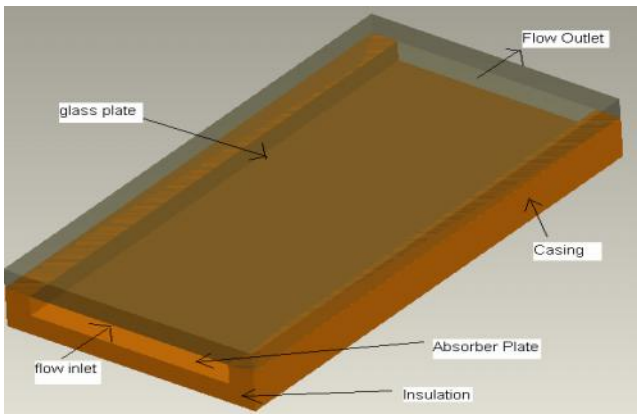


**Figure 1.5 Single Glass cover air heater**

#### 1.2.2.2.2 Double glass cover air heater

This type of air heater includes two glass cover on the top surface and the air flows between the glass cover and the absorber plate. The figure 1.6 shows the constructional features of double glass cover air heater.

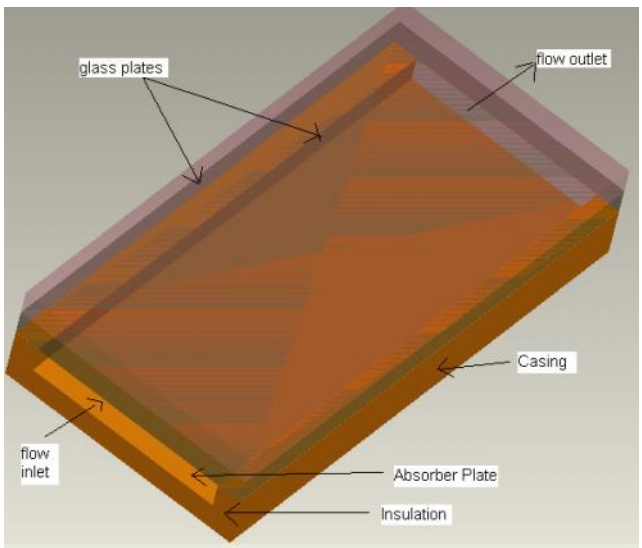


**Figure 1.6 Double glass cover air heater**

#### 1.2.2.2.3 Counter air heater without porous matrix

As the name suggest there is counter flow of air in the heater. First air flows between two glass plate in one direction and then between the glass plate and the absorber plate in the opposite direction as shown in figure 1.7.

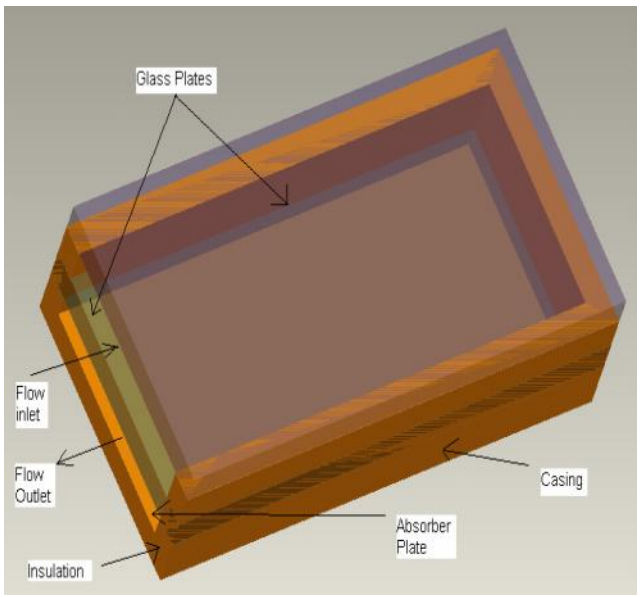


**Figure 1.7 Counter solar air heater**

### 1.2.2.2.4 Counter air heater with porous matrix

The constructional part is same as for the above air heater but in this type of air heater we use porous matrix in the second pass of the air flow as shown in figure 1.8.

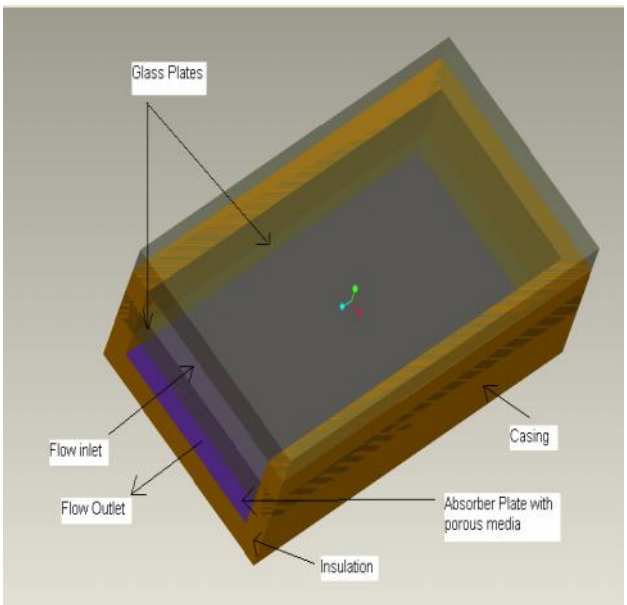


**Figure 1.8 Counter air heater with porous matrix**

## 1.3 TRANSMISSIVITY-ABSORPTIVITY PRODUCT

Tranimissivity-Absorptivity product is defined as the ratio of the flux absorbed in the absorber plate to the flux incident on the cover system, and is denoted by the symbol $(\tau\alpha)$. Out of fraction $\tau$ transmitted through the cover system, a part is absorbed and a part reflects back diffusively. Out of the reflected part, a portion is transmitted through the cover system and a portion reflected back to the absorber plate. The process of absorption and reflection at the absorber plate surface (Fig.1.9) goes on indefinitely, the quantities involved being successively smaller.

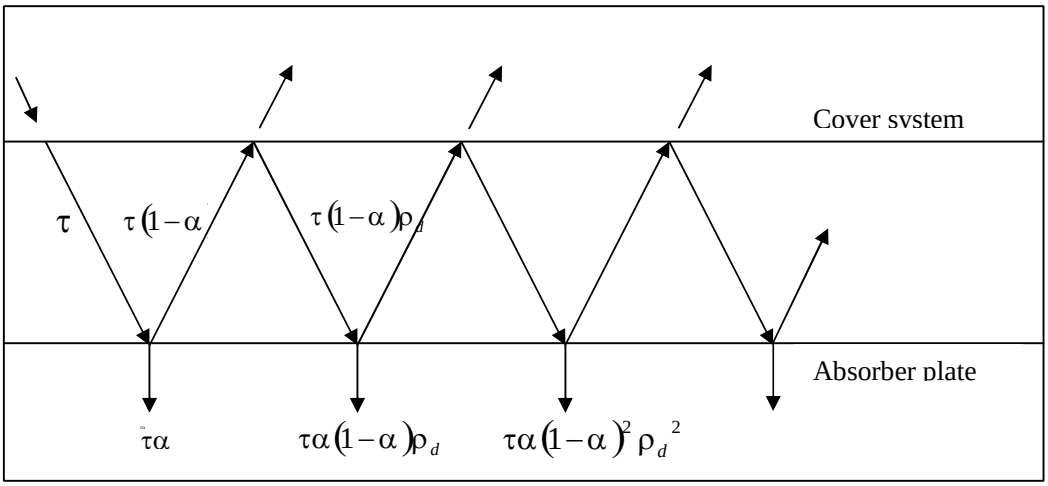


**Fig 1.9 Absorption and reflection at the absorber plate**

Thus the net fraction absorbed $(\tau\alpha)$

$$= \tau\alpha\left[1 + (1-\alpha)\rho_d + (1-\alpha)^2\rho^2{}_d + .....\right]$$

$$= \frac{\tau\alpha}{1-(1-\alpha)\rho_d} \qquad ...1.1$$

## 1.4 OVERALL LOSS COEFFICIENT

The heat loss from the collector in terms of overall loss coefficient defined by the equation

$$q_1 = U_1 A_p (T_{pm} - T_a) \qquad ...1.2$$

Where $U_1$ = Overall loss coefficient

$A_p$ = Area of absorber plate,

$T_{pm}$ = Average temperature of absorber plate,

$T_a$ = Ambient Temperature

The heat loss from the collector is the sum of heat loss from the top, bottom and the sides. Thus,

$$q_1 = q_t + q_b + q_s \quad \text{...1.3}$$

where the subscripts t, b and s represented top, bottom and sides.

$$q_t = U_t A_p (T_{pm} - T_a) \quad \text{...1.4}$$

$$q_b = U_b A_p (T_{pm} - T_a) \quad \text{…1.5}$$

$$q_s = U_s A_p (T_{pm} - T_a) \quad \text{…1.6}$$

$$U_1 = U_t + U_b + U_s$$

Typical values of $U_1$ range from 2 to 10 W/m$^2$-K.

### 1.4.1 Top loss coefficient $U_t$

The top loss coefficient is evaluated by considering convection and re-radiation losses from the absorber plate in the upward direction. For the purpose of calculation, it is assumed that the transparent covers and the absorber plate constitute a system of infinite parallel surfaces and that the flow of heat is one-dimensional and steady. It is further assumed that the temperature drop across the thickness of the covers is negligible and the interaction between the incoming solar radiation absorbed by the covers and the outgoing loss may be neglected. The outgoing re-radiation is of larger wavelength. For these wavelengths, the transparent cover is assumed to be opaque. This is a very good assumption if the material is glass.

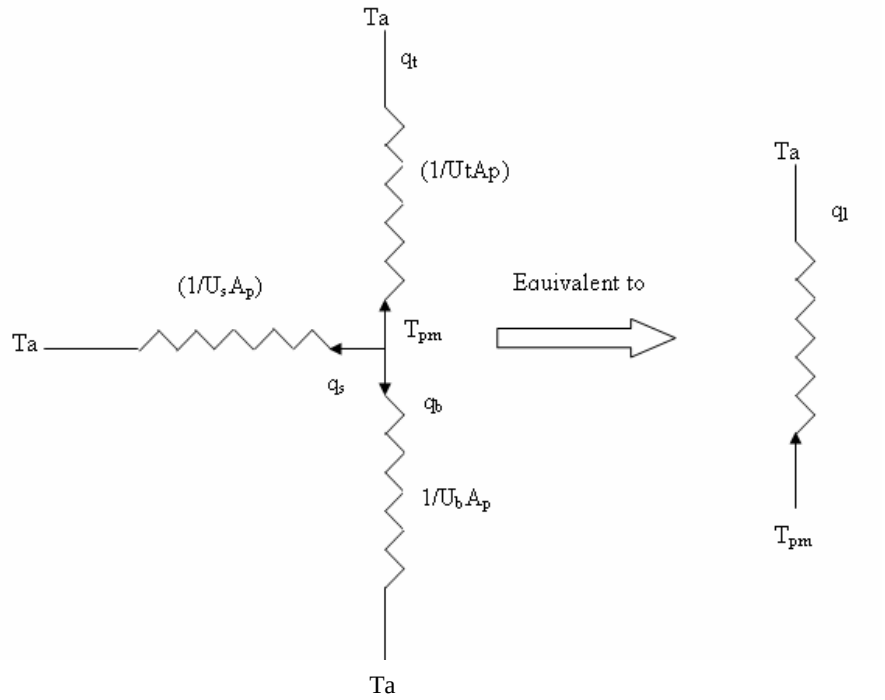


**Fig1.10 Thermal resistance network showing losses**

A schematic diagram of two cover system is shown in Fig.1.10. In a steady state, the heat transferred by convection and radiation between (a) the absorber plate and the cover (b) the two covers (c) the front cover and the surroundings must be equal.

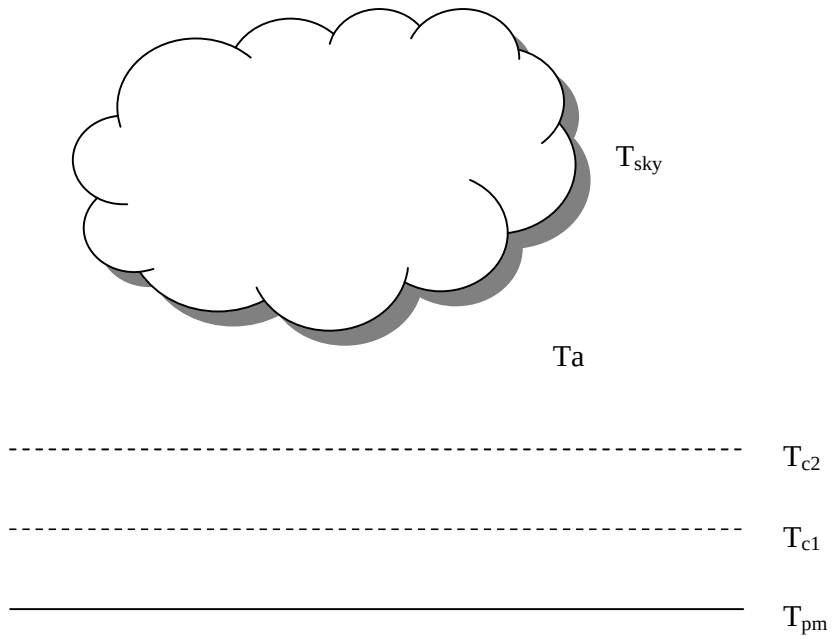


**Fig1.11 Calculation of the $U_t$**

Heat transferred by convection and re- radiation as suggested by Sukhatme [2] between

(i) The absorber plate and the first cover

$$\frac{q_1}{A_p} = h_{p-c1}\left(T_{pm} - T_{c1}\right) + \sigma \frac{\left(T_{pm}^4 - T_{c1}^4\right)}{1/\varepsilon_p + 1/\varepsilon_c - 1} \quad \text{...1.7}$$

(ii) The two glass covers

$$\frac{q_1}{A_p} = h_{c1-c2}\left(T_{c1} - T_{c2}\right) + \sigma \frac{\left(T_{c1}^4 - T_{c2}^4\right)}{1/\varepsilon_c + 1/\varepsilon_c - 1} \quad \text{…1.8}$$

(iii) The second glass cover and the sky

$$\frac{q_1}{A_p} = h_a\left(T_{c2} - T_a\right) + \sigma\varepsilon_c\left(T_{c2}^4 - T_{sky}^4\right) \quad \text{…1.9}$$

The above three non linear equations are solved simultaneously for the evaluation of $q_t$, $T_{c1}$, $T_{c2}$ the empirical relation for the top loss coefficient as suggested by Sukhatme [2] is given as

$$U_t = \left[\frac{M}{\left(\frac{C}{T_{pm}}\right)\left(\frac{T_{pm} - T_a}{M + f}\right)^{0.33}} + \frac{1}{h_a}\right]^{-1} + \left[\frac{\sigma\left(T_{pm}^2 + T_a^2\right)\left(T_{pm} + T_a\right)}{\frac{1}{\varepsilon_p + 0.05M\left(1 - \varepsilon_p\right)} + \frac{2M + f - 1}{\varepsilon_c} - M}\right] \quad \text{…1.10}$$

Where $f = \left(1 - 0.04h_a + 0.0005h_a^2\right)\left(1 + 0.091\right)M$ …1.11

$$C = 365.9\left(1 - 0.00883\beta + 0.0001298\beta^2\right) \quad \text{…1.12}$$

M=number of glass covers

**Heat transfer coefficient at the top cover:**

The convective heat transfer coefficient ($h_a$) at the top cover has been generally calculated so far from the following empirical correlation suggested by McAdams [3],

$$h_a = 5.7 + 3.8V \quad \text{…1.13}$$

where $V$ is the wind speed in m/s

Sparrow and his coworkers [1] have suggested the following dimensionless correlation,

$$j = 0.86(\mathrm{Re}^* L)^{-1/2} \quad \text{…1.14}$$

Where j=j-factor given by $\frac{h_a}{\rho C_p V}\Pr^{2/3}$ …1.15

$\mathrm{Re}_L^*$ =Reynolds number ($VL/\nu$ ) based on the characteristics dimension

$$L=4A_c/C_c \quad \ldots 1.16$$

$A_c$=Collector gross area

$C_c$=Circumference associated with the collector gross area

**Sky Temperature**

Sky temperature is usually calculated from the following simple empirical relation in which temperature are expressed in kelvin as suggested by Sukhatme [2],

$$T_{sky}=Ta-6 \quad \ldots 1.17$$

### 1.4.2 Bottom loss coefficient, $U_b$:

The bottom loss coefficient is calculated by considering conduction and convection losses from the absorber plate in the downward direction. It will be assumed that the heat flow is one dimensional and steady (Fig.1.12). In most cases, the thickness of thermal insulation is provided such that the thermal resistance associated with conduction dominates. Thus, neglecting the convective resistance at the bottom surface of the collector casing,

$$U_b=K_i/\delta_b \quad \ldots 1.18$$

Where $K_i$=Thermal conductivity of the insulation

$\delta_b$ = Thickness of the insulation

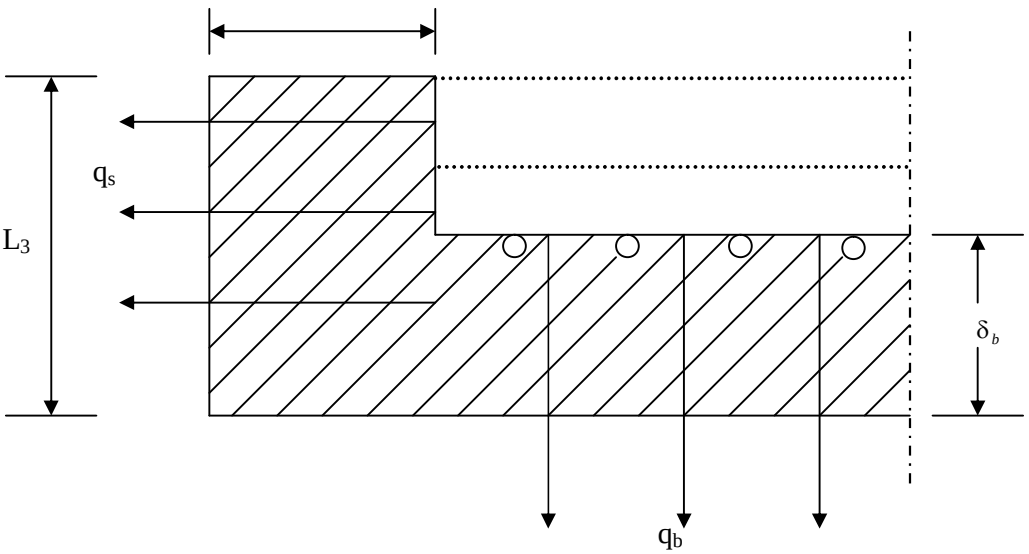


**Fig1.12 Bottom and side losses from a flat-plate**

### 1.4.3 Side loss coefficient, $U_s$

Here also the same assumptions, which are applied for bottom loss coefficient, i.e., conduction resistance dominate and that the flow of heat is one dimensional and steady state. The one-dimensional approximation can be justified on the grounds that the $U_s$ is always much smaller than the $U_t$.

If the dimensions of the absorber plate is $L_1$ x $L_2$ and the height of the collector is $L_3$ and assuming that the average temperature drop across the insulation is $(T_{pm}-T_a)/2$ and that the thickness of this insulation is $\delta_s$

$$q_s = \frac{2L_3(L_1 + L_2)k_i(T_{pm} - T_a)}{2\delta_s} \quad \text{...1.19}$$

$$U_s = \frac{2L_3(L_1 + L_2)k_i(T_{pm} - T_a)}{L_1 L_2 \delta_s} \quad \text{…1.20}$$

## 1.5 THE FINITE DIFFERENCE METHOD

In this method, the physical domain is first discretized into computational domain by the method of grid generation. The grid consists of the linear elements with nodes at the point of intersection. The following steps describe the whole procedure:

**STEP I:** Differential Equations can be obtained by the application of governing conservation laws over a system.

**STEP II:** Applying finite difference schemes to transform the given differential equations into the difference equations.

**STEP III:** Algebraic equations in nodal unknowns are thus obtained.

**STEP IV:** These simultaneous algebraic equations can be solved by any numerical method.

**STEP V:** The solution of these algebraic equations is the solution at the nodes.

**STEP VI:** Finally, quantities of interest can be calculated.

### 1.5.1 Discrete Approximation of Derivatives by Taylor's Series:

Basic equation for Taylor's Series Equation

$$f(x_0+\Delta x)= f(x_0)+\frac{df}{dx}_{x=x_0}\Delta x+\frac{d^2f}{dx^2_{x=x_0}}\frac{(\Delta x)^2}{2!}+\ldots\ldots \quad \ldots 1.21$$

$$f(x_0-\Delta x)= f(x_0)-\frac{df}{dx}_{x=x_0}\Delta x+\frac{d^2f}{dx^2_{x=x_0}}\frac{(\Delta x)^2}{2!}-\ldots\ldots \quad \ldots 1.22$$

**Approximation of the first derivative:**

Using equation 1.22

$$\frac{df}{dx}_{x=x_o}=\frac{f(x_0+\Delta x)-f(x_0)}{\Delta x}-\frac{d^2f}{dx^2}_{x=x_0}\frac{\Delta x}{2!}-\ldots\ldots \quad \ldots 1.23$$

Formally we can write,

$$\frac{df}{dx}_{x=x_o}=\frac{f(x_0+\Delta x)-f(x_0)}{\Delta x}-0(\Delta x) \quad \ldots 1.24$$

Finite Difference Approximation:

$$\frac{df}{dx}_{x=x_o}\approx\frac{f(x_0+\Delta x)-f(x_0)}{\Delta x} \text{ order of accuracy is } O(\Delta x) \quad \ldots 1.25$$

$O(\Delta x)$ is called **'Truncation Error'**

For convenience,

$f(x_0)= f_1$

$f(x_0+\Delta x)= f_{i+1}$

$f(x_0+2\Delta x)= f_{i+2}$

$f(x_0-\Delta x)= f_{i-1}$ ……..and so on.

Or $f_i^{'}=\frac{f_{i+1}-f_i}{h}$ order of accuracy is 0(h). …1.26

Equation 1.25 (or 1.26) is called **'Forward Difference Approximation'**

Similarly using equation 1.22, we get

$$f_i=\frac{f_i-f_{i=1}}{h} \text{ order of accuracy is 0(h)} \quad \ldots 1.27$$

This is called **'Backward Difference Approximation'**

Similarly, subtracting 1.22 from 1.21 and dividing throughout by 2h, we get

$$f_i^{'}=\frac{f_{i+1}-f_{i-1}}{2h} \text{ Order of accuracy is } O(h^2) \quad \ldots 1.28$$

This is called **'Central Difference Approximation'**

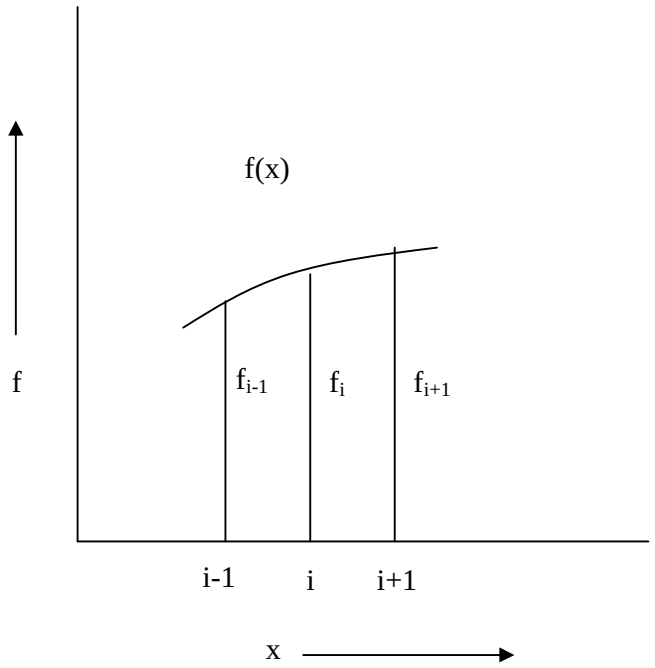


**Fig 1.13 Finite difference representation**

**Approximation for Second Derivatives:**

Forward Difference Approximation:

$$f_i'' = \frac{f_{i+2} - 2f_{i+1} + f_i}{h^2} \text{ order of accuracy O(h)} \quad \ldots 1.29$$

Backward Difference Approximation:

$$f_i'' = \frac{f_{i-2} - 2f_{i-1} + f_i}{h^2} \text{ order of accuracy O(h)} \quad \ldots 1.30$$

Central Difference Approximation:

$$f_i'' = \frac{f_{i+1} - 2f_i + f_{i-1}}{h^2} \text{ order of accuracy O(h)} \quad \ldots 1.31$$

# CHAPTER 2
# LITERATURE REVIEW

A lot of research work has been carried out throughout the world to investigate and analyze the thermal performance of air heaters. A brief review of literature is presented here.

**Zhao *et al.* [1]** proposed a computer model derived from basic laws governing thermal energy exchanges between surfaces for the transient simulation of flat plate collectors. The model works under the transient conditions and doesn't require the assumption of constant fluid properties. The radiation exchanges between the surfaces in the collector and the outmost glazing surface and the ambient air are calculated without linearization. The time interval used can be small or large (a commonly used time interval for simulation is one hour). The temperature profile along the collector, of the cover plates, of the absorbing plate, and of the insulation surface, as well as of the fluid can be determined at each time interval. The concept of subdivisions is introduced in the development of governing equations for air type collectors but could be readily applied to water type collectors as well. In the approach presented in the paper, starting from the basic laws of energy balance, a set of algebraic equations are obtained and solved simultaneously for each sub-region along the collector. Due to non-linearity of convective and radiant heat transfer coefficient used, the model requires an iterative solution procedure.

**Choudhary *et al.* [2]** analyze in detail one pass corrugated bare plate solar air heater. The result obtained from the study can be used to calculate the performance, to optimize the design and to improve the efficiency without increasing the cost of system. A series of experiments have been carried out to determine the comparative performance of air heaters with different widths of air channel and different mass flow rates. Too small the channel width with a large air velocity results in excessive fan running cost. So, the optimum channel width would be that which corresponds to an efficient and cost effective design of the system. They discussed the optimization procedure which was used to obtain optimum performance and optimum design parameters for any amount of air flowing through the heater channel.

**Nasr *et al.* [3]** studied forces convection heat transfer from cylinder embedded in a packed bed numerically. The local volume averaged conservation equations are used to examine the effect of the effects oft the Reynolds(Re), the Darcy(Da), Forchheimer(Fs) and effective Prandtl numbers. An increase in either Re or $Pr_{eff}$ results in the heat transfer enhancement. This enhancement is found to be consistent with that obtained from the prediction of boundary layer theory, which shows the Nusselt number (Nu) dependence on the Re to the one half power. The effect of decreasing Da is an increase in Nu and increasing Da decreases the heat transfer. The effect of Fs is found to depend on the product (DaRe). A comparison between the numerical predictions and experimental data gives the values of effective thermal conductivities and quantified the average thermal dispersion. They utilized the finite element for the computation of the various parameters. The packing surrounding cylinder is discretized into triangular elements to form the computational domain. In the paper they defined the effective thermal conductivity ($K_{eff}$) as the superposition of stagnant conductivity (independent of flow) and flow-dependent dispersion conductivity. If the thermal dispersions are present the value of $k_{eff}$ is found to increase. Thermal dispersion ia s result of simultaneous existence of temperature and velocity gradient within the pores of porous medium. Also, an attempt is made to quantify its contribution to heat transfer from an embedded cylinder is presented in this paper. They found out that the value of $k_{eff}$ is about ten times the thermal conductivity of air, (0.3 W/mK).

**Gupta *et al.* [4]** studied the thermo hydraulic performance of solar air heaters with roughened absorber plates. However, such as air heaters are accompanied by increased pumping power, their work involves the effect of roughness and operating parameters on thermal as well as hydraulic performance of roughened solar air heaters. Also performance is compared with the conventional type air heater. The optimum design and operating parameters have been determined. They reported that roughened heaters are advantageous for low Reynolds number (Re), though a smooth solar air heater will perform better hydraulically. Although thermal efficiency of the roughened solar air heater may be more them that of a smooth heater. Beyond a certain limiting value of Reynolds number (13000-19000), the actual value depends upon the relative roughness height and insolation. They also worked out the optimum design conditions for roughened solar air heaters for relative roughness height and

insolation and relative roughness pitch of 10 and for an angle of attack of $60^0$. They developed the following empirical relationship to yield the optimum conditions:

$$\mathrm{Re} = 1311.2(I)^{0.281}(e/D)^{-0.121} \quad \ldots 2.1$$

where I is the intensity of solar radiation, e is the relative roughness height, D is the hydraulic diameter.

**Jannot *et al* [5]** presented a new set of equations for radiative balance of the absorber plate and the transparent cover of a solar air heater covered with plastic film. Air is supposed to flow through the passage between the absorber plate and the bottom of the collector. Glass is commonly used as a front cover in the solar collectors because it absorbs almost all the infrared radiations re-emitted by the absorber plate, resulting in the enhancement of thermal efficiency of the solar collector by creating the green house effect. However , the use of glass covers in rural areas of the developing countries has two major disadvantages, its high cost and its fragility during transportation and in service. It is the reason why, for several years , transparent plastic covers have been widely used in the zones to construct moderate cost solar heaters. The transparent plastic covers also have two major shortcomings:

1. The collector performance is highly sensitive to air leakage and it is quite difficult to obtain perfect air tightness with a plastic cover.
2. During the dry season the dust content in tropical countries is quite high and this causes dust deposits on both lower face of the plastic cover and on the upper face of the absorber , exposed to the solar radiation , thee result is lowering of its transmittance and absorptance towards solar radiation.

**Mohammad *et al.* [6]** presented an analysis for novel type solar air heater. The main idea is to minimize the heat losses from the top glass cover of the collector and maximize heat extraction from the absorber. This can be done by forcing the air flow over the front glass cover before passing through the absorber. Hence, they proposed the design in which extra cover is employed to form a counter flow heat exchanger. In order to make it more efficient, porous media is placed in the second passage. The porous absorber forms an extensive area for heat transfer, where the volumetric heat transfer coefficient is very high. Hence, use of porous absorber increases the rate of heat transfer from the absorber to the air stream. In the proposed design, which

combines double air passage and porous media, care should be taken to minimize pressure drop. The pressure drop is not high if high porous medium is used. However, the thermal efficiency of the proposed design is found significantly high.

**Akhtar *et al.* [7]** developed an improved equation for computing the glass cover temperature of the flat plate solar collectors with single glazing. A semi-analytical correlation for the factor 'f' –the ratio of inner to outer heat transfer coefficients-as a function of collector parameter and atmospheric variables has been obtained by regression analysis. This relation readily provides the glass cover temperature ($T_g$). The results have been compared with those obtained by numerical solution of heat balance equations. Computational error in $T_g$ and $U_t$ are reduced by factor of five or more. With such low errors in the computation of $T_g$ and $U_t$, the numerical solution of heat balance equation is not required. The error in the computation of $U_t$ was within 2% with the range of air gap spacing 8mm to 90mm the range of ambient temperature was $0^0$C-$45^0$C.

**Kolb *et al.* [8]** described the development and testing of an efficient and single glazed solar matrix air collector. This collector is designed in order to overcome physical problems of conventional flat plate air collectors as well as technical problems of matrix air collectors. The absorber consists of two parallel black galvanized industrial woven fine meshed copper wire screens. The collector is very durable and flexible regarding mass flow rate and collector duct height and yielded high thermal performance at very low-pressure losses. Matrix collectors offer large heat transfer area to volume ratio and large heat transfer coefficients due to small hydraulic diameters. In this way the operating temperatures of the system, and thus the heat losses from the collector are reduced which results in higher collector efficiencies.

**Karwa [9]** in his paper has critically reviewed the various correlations employed by researchers to predict the heat transfer coefficient for air floe in solar air heater duct in the range $2300<Re<15000$. Some of the correlations have been basically developed for circular section ducts or for ducts with high aspect ratio. All of them do not take into account the effect of the combined thermal and hydrodynamic development length and also do not cover the complete range of Reynolds number of interest. The Nusselt number values predicted by this correlation differ by as much as 30 to 40%.

The study established the need of a reliable heat transfer coefficient correlation applicable from transition to early turbulent flow regime in asymmetrically heated rectangular section ducts of solar air heaters, which includes the effect of development length and aspect ratio on the heat transfer coefficient.

**Muluwork *et al.* [10]** in his paper presented experimental results for air flow in the rectangular duct with repeated discrete rib roughness on the upper broad wall, which is subjected to uniform heat flux. The effect of relative roughness length ratio on tanton number and friction factor for V-down and V-up and traverse discrete rib roughened surfaces have been studied for Reynolds number about 2000<Re<15500. The use of artificial roughness results in considerable enhancement in the heat transfer. The Stanton number ratio enhancement obtained is between 1.32 to 2.47 in the range of system and operating parameters covered in the investigation.

**Mittal *et al.* [11]** investigates the thermo hydraulic performance on a packed bed solar air heater having its duct packed with blackened wire screen matrices of different geometrical parameters(wire diameter and pitch) as shown in fig.2.1. To obtain the effective efficiency a mathematical model has been developed on the basis of energy transfer mechanism in the bed. The following assumptions have been made during the development of the mathematical model

- Edge and back losses have been neglected
- Environmental temperature and wind velocity have been assumed to be constant.

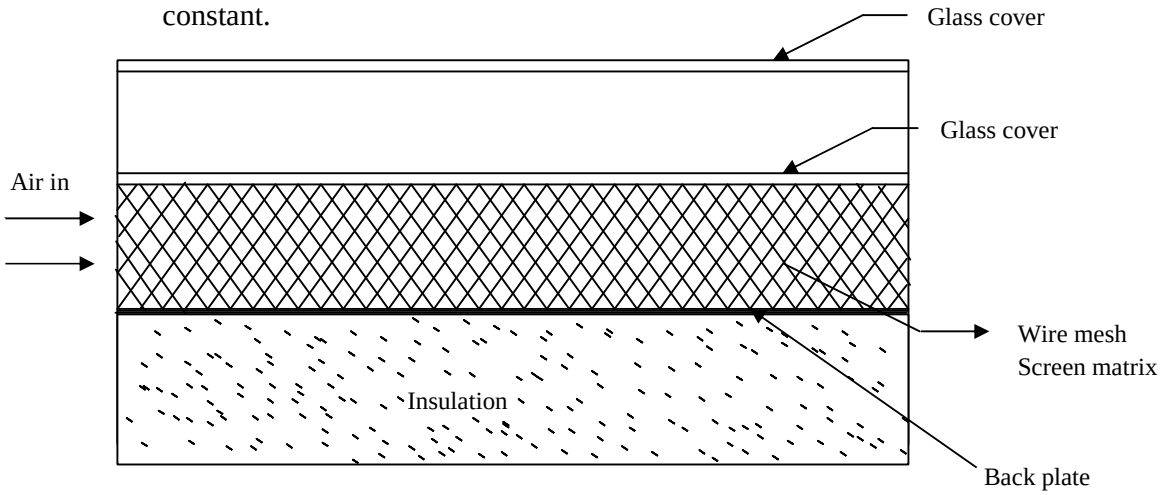


**Fig 2.1 Packed bed solar air heater**

After the thermodynamic investigations of a packed bed solar air heater packed with wire screen matrix indicate that the thermal gain of such collectors is relatively higher as compare to smooth collectors, although the pressure drop across the duct also increases significantly. This paper suggested that the porosity of the bed does not govern the performance of the solar air heater.

**Mittal *et al.* [12]** in his paper studied the effect of roughness elements on the effective efficiency of the solar air heater. As we know the solar air heater is widely used collection devices but the thermal efficiency of solar air heaters has found to be generally poor because of their inherently low heat transfer capability between the absorber plate and air flowing in the duct. This heat transfer capability can be improved by using the roughness elements on the absorber plate. In his paper the research has been done on the various roughness elements and their effect on the thermal efficiency of the solar air heaters proposed by different investigators. To compare the effective thermal efficiency of the solar air heaters having different types of geometry of roughness elements on the absorber plate a expression has been developed

$$\eta_e = \frac{q_u - P/C}{IA_c} \qquad \ldots 2.2$$

where $\eta_e$ = effective efficiency

$q_u$ = useful thermal energy gain

P = mechanical power

C = conversion efficiency

I = Solar radiation

$A_c$=Area of absorber plate

By using the expression the effective thermal efficiency have been compared and found that solar air heater having inclined ribs as roughness elements is found to have better effective efficiency in the higher range of Reynolds number, however expanded metal mesh is found suitable roughness element in the lower range of Reynolds number.

**Aharwal *et al.* [13]** experimentally reviewed the effect of artificial roughness in the form of repeated ribs for the enhancement of thermal performance of solar air heaters.

This paper experimentally examines the heat transfer and friction factor characteristics of a rectangular duct roughened with repeated square cross-section split-rib with a gap. The various parameters used as width to height ratio (W/H), relative roughness pitch (P/e), relative roughness height ($e/D_h$) and angle of attack. An experimental test facility has been designed and fabricated to study the effect of gap position and gap width of inclined rib geometry for the Reynolds number in the range of $3000<Re<18,000$ and it is been found that the inclined rib arrangement enhances the heat transfer and friction factor of the roughened ducts. The thermo-hydraulic performance analysis of roughened ducts shows that the relative gap width of 1.0 and a relative gap position of 0.25 results in a higher value of efficiency parameter.

# CHAPTER 3
# PROBLEM FORMULATION

A literature review of solar air heaters shows that that the different type of solar air heaters have been investigated experimentally under different systems and operating conditions by several researchers. A comparison of performance of these heaters become difficult without identical values of parameters such a ambient conditions, inlet air temperature, air mass flow rate per unit collector width, gap between the absorber and cover plates, intensity of solar radiation etc. Thus to compare the performance of these heaters under identical values of parameters, their simulation becomes necessary. In view of the above, simulation of four different type of solar air heaters has been done in the present work. The four solar air heaters selected for this purpose are single-glazing, double glazing, counter flow without porous matrix and counter flow with porous matrix solar air heaters. Air flows above the absorber plate in all these solar air heaters. Computer program in C++ language has been developed to simulate the behavior of aforesaid solar air heaters. Also, the evaluation of various performance parameters will be carried out through the same. Moreover, the performance of all these solar air heaters will be analyzed and compared.

In the present study, at first mathematical model is obtained by the application of the governing conservation laws. The heat balance is accomplished across each component of given solar air heater i.e., the glass covers, the air stream and the absorber plate. The heat balance for the air stream yields the governing differential equations and the associated boundary conditions. The heat and fluid flow are assumed steady and one dimensional. It is because of the radiation heat exchange terms that render the problem non-linear hence making the exact solution cumbersome. So a numerical approach is applied which would give a solution with a fairly good accuracy. The finite difference method (FDM) will be used to solve the differential equations and hence to simulate a given solar air heater. In FDM technique, the first step involves the transformation of the actual physical domain into the computational grid. Second step is to transform the differential equations into difference equations, which along with the equations obtained by heat balance across

the covers and the absorber are the simultaneous non linear algebraic equations. The third step is to solve the equations using gauss elimination method. The solution is obtained in the form of nodal temperatures for the covers, the air stream and the absorber. Study has been extend by changing the various governing parameters like the air mass flaw rate, the inlet air temperature, the depth of the collector duct and the intensity of solar radiation and finally the performance characteristics have been obtained.

# CHAPTER 4
# MODELING AND ANALYSIS

Simulation in a crude sense is the method of predicting the output of a proposed system or an existing system with out conducting experiment on it. System simulation involves the development of the mathematical model for a given problem which should be dynamic in nature. The mathematical model is then solved numerically.

## 4.1 ANALYSIS

Energy balance analysis have been done here for four types of solar air heaters, conventional with single glass cover, conventional with double-glazing, counter-flow without matrix and counter flow with porous matrix solar air heaters. The analysis of conventional type solar air heater is done so that the performance of other heaters can be compared with it. The analysis is based on the assumption that heat and the fluid flow are one-dimensional and in steady state. A numerical approach is applied to obtain the solution of the given problem.

In the present study first a mathematical model is obtained by the application of the governing conservation laws. The heat balance is accomplished across each component of a given air heater, i.e., the glass covers, the air streams and the absorber plate. The heat balance for the air stream yields the governing differential equations and the associated boundary conditions. It is because of the radiation heat exchange terms that render the problem non-linear hence making the exact solution cumbersome. So a numerical approach which would give a solution with a fairly good accuracy is needed. The finite difference (FDM) has been employed to solve the differential equations. In FDM technique the first step involves the transformation of the actual physical domain into the computational grid. Second step is to transform the differential equations into difference equations. Which along with the equations obtained by heat balance across the covers and the absorber are the simultaneous non linear algebraic equations. The next step is to solve them numerically using gauss elimination method . The solution is obtained in the form of nodal temperatures for

the covers, the air streams and the absorber. Study has been extended by changing the various governing parameters like the air mass flow rate, the inlet air temperature, the depth of the collector duct and the intensity of solar radiation and finally the performance characteristics have been obtained.

Following are the assumptions made in the analysis of the mentioned heaters:

1. The air flow is forced, steady and one-dimensional and the thermo-physical properties of air and packed bed are independent of temperature.
2. The plug flow condition exists throughout the length of heater, i.e., the air velocity in the channel at any section is constant.
3. The flow of heat is one-dimensional and steady.
4. The temperature drop across the thickness of the covers is negligible.
5. Heat loss from the sides of the duct is very small and hence neglected.
6. The temperature distribution within each packed element and glass cover is uniform.
7. Conductive heat transfer in the flow directions is negligibly small and is ignored except in case of counter flow solar air heater with porous matrix.
8. The porous absorber and the air stream are in thermal equilibrium because the value of volumetric heat transfer coefficient in the pores of the porous matrix is very high.

Under steady state operating conditions, the energy balance for the conventional and counter flow collectors as suggested by Mohammad [6] and applying the finite difference method on the proposed four models of air heaters are as follows

### 4.1.1 Conventional Solar Air Heater with single glazing

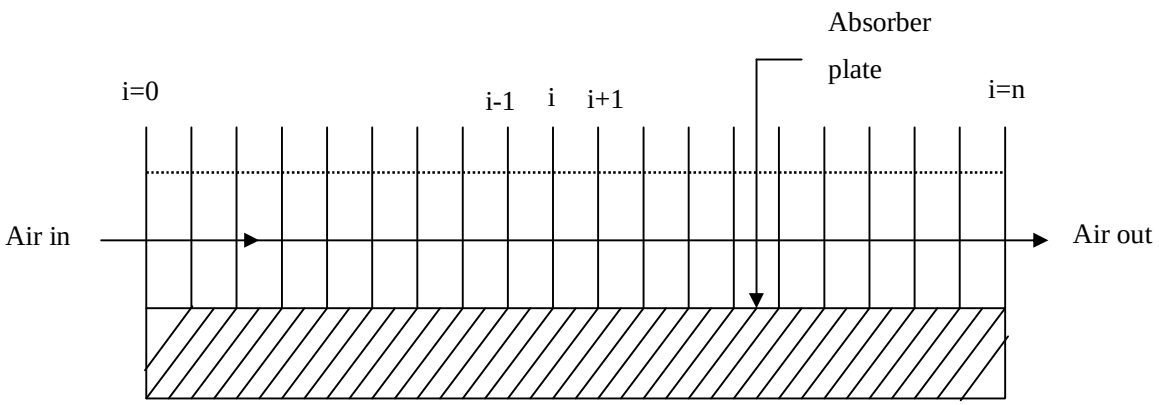


**Fig 4.1 Computational domain for conventional heater with single glazing**

**For i-th node,**

**For Glass cover:**

The governing equation (G.E.)

$$I\alpha_c = h_a(T_c - T_a) + h_{fc}(T_c - T_f) + h_{r.pc}(T_c - T_p) \quad \ldots 4.1a$$

The finite difference equation (F.D.E)

$$I\alpha_c = h_a(T_c[i] - T_a) + h_{fc}(T_c[i] - T_f[i]) + h_{r.pc}(T_c[i] - T_p[i]) \quad \ldots 4.1b$$

$$T_c[i] = \frac{I\alpha_c + h_a T_a + h_{fc} t_f[i] + h_{r.pc} T_p[i]}{h_a + h_{fc} + h_{r.pc}} \quad \ldots 4.1c$$

**For air stream:**

The governing differential equation (G.D.E.)

$$m' c \frac{dT_f}{dx} = h_{fc}(T_c - T_f) + h_{fp}(T_p - T_f) \quad \ldots 4.2a$$

The finite difference equation using forward difference formulation,

$$m' c \frac{T_f[i+1] - T_f[i]}{\Delta x} = h_{fc}(T_c[i] - T_f[i]) + h_{fp}(T_p[i] - T_f[i]) \quad \ldots 4.2b$$

$$T_f[i+1] = \{1 - \frac{\Delta x}{m' c}(h_{fc} + h_{fp})\} T_f[i] + h_{fc} \frac{\Delta x}{m' c} T_c[i] + h_{fp} \frac{\Delta x}{m' c} T_p[i] \quad \ldots 4.2c$$

The associated boundary condition (B.C.) is

$$T_f[0] = T_1$$

**For absorber plate:**

$$\text{G.E.: } I\alpha_p\tau_c = h_{fp}(T_p - T_f) + h_{r.pc}(T_p - T_c) + U_a(T_p - T_a) \quad \ldots 4.3a$$

$$\text{F.D.E.: } I\alpha_p\tau_c = h_{fp}(T_p[i] - T_f[i]) + h_{r.pc}(T_p[i] - T_c[i]) + U_a(T_p[i] - T_a) \quad \ldots 4.3b$$

$$T_p[i] = \frac{I(\alpha_p\tau_c) + h_{fp} T_f[i] + h_{r.pc} T_c[i] + U_b T_a}{U_b + h_{fp} + h_{r.pc}} \quad \ldots 4.3c$$

### 4.1.2 Conventional Solar Air Heater with double glazing

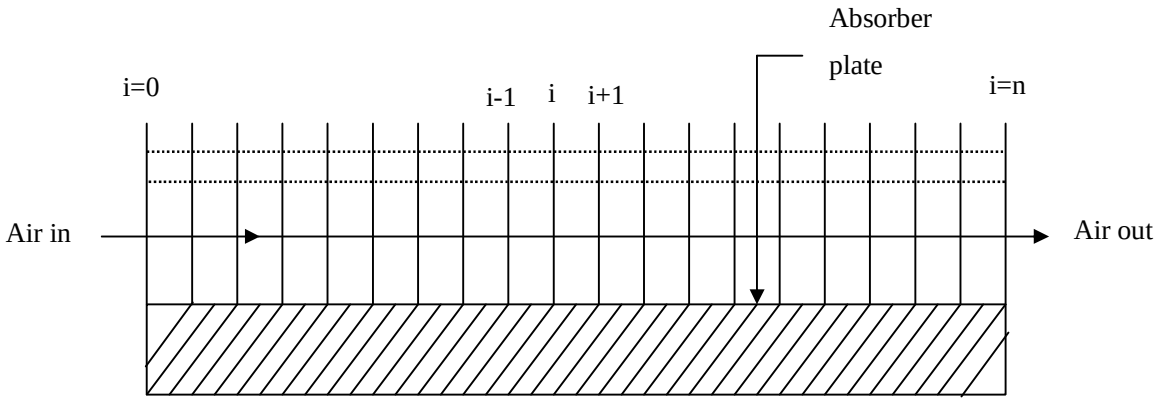


**Fig 4.2 Computational domain for conventional heater with double glazing**

**For top glass cover:**

G.E.: $I\alpha_{c1} = h_a(T_{c1} - T_a) + h_{cc}(T_{c1} - T_{c2}) + h_{r.cc}(T_{c1} - T_{c2})$ …4.4a

F.D.E.: $I\alpha_{c1} = h_a(T_{c1}[i] - T_a) + h_{cc}(T_{c1}[i] - T_{c2}) + h_{r.cc}(T_{c1}[i] - T_{c2}[i])$ …4.4b

$$T_{c1}[i] = \frac{I\alpha_c + h_a T_a + h_{cc} T_{c2}[i] + h_{r.cc} T_{c2}[i]}{h_a + h_{cc} + h_{r,cc}} \quad \text{…4.4c}$$

**For second glass cover:**

G.E.: $I\alpha_c\tau_c = (h_{r.cc} + h_{cc})(T_{c2} - T_{c1}) + h_{fc2}(T_{c2} - T_f) + h_{r.pc}(T_{c2} - T_p)$ …4.5a

F.D.E.:

$$I\alpha_c\tau_c = (h_{r.cc} + h_{cc})(T_{c2}[i] - T_{c1}[i]) + h_{fc2}(T_{c2}[i] - T_f[i]) + h_{r.pc}(T_{c2}[i] - T_p[i])$$

…4.5b

$$T_{c2}[i] = \frac{I\alpha_c\tau_c + h_{fc2} T_f[i] + h_{cc} T_{c1}[i] + h_{r,cc} T_{c1}[i] + h_{r,pc} T_p[i]}{h_{fc2} + h_{cc} + h_{r,cc} + h_{r,pc}} \quad \text{…4.5c}$$

**For air stream:**

G.D.E.: $m'c\frac{dT_f}{dx} = h_{fc2}(T_{c2} - T_f) + hf_p(T_p - T_f)$ …4.6a

F.D.E.: $m'c\frac{T_f[i+1] - T_f[i]}{\Delta x} = h_{fc2}(T_{c2}[i] - T_f[i]) + hf_p(T_p[i] - T_f[i])$ …4.6b

$$T_f[i+1] = \{1 - \frac{\Delta x}{m' c}(h_{fc2} + h_{fp})\}T_f[i] + h_{fc2}\frac{\Delta x}{m' c}T_{c2}[i] + h_{fp}\frac{\Delta x}{m' c}T_p[i] \quad \text{...4.6c}$$

**For absorber plate:**

G.E.: $I\alpha_p\tau_c\tau_c = h_{fp}(T_p - T_f) + h_{r.pc2}(T_p - T_{c2}) + U_a(T_p - T_a)$ …4.7a

F.D.E.: $I\alpha_p\tau_c\tau_c = h_{fp}(T_p[i] - T_f[i]) + h_{r.pc2}(T_p[i] - T_{c2}[i]) + U_a(T_p[i] - T_a)$

…4.7b

$$T_p[i] = \frac{I(\alpha_p\tau_c\tau_c) + h_{fp}T_f[i] + h_{r,pc}T_{c2}[i] + U_bT_a}{U_b + h_{fp} + h_{r,pc}} \quad \text{…4.7c}$$

### 4.1.3Counter flow solar air heater without porous matrix

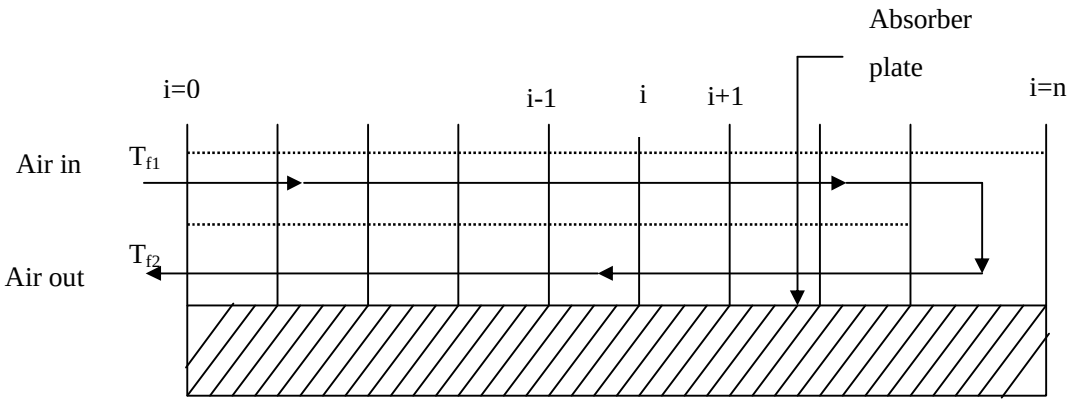


**Fig 4.3 Computational domain for counter-flow air heater without porous matrix**

**For top glass cover:**

G.E.: $I\alpha_c = h_a(T_{c1} - T_a) + h_{fc1}(T_{c1} - T_{f1}) + h_{r.cc}(T_{c1} - T_{c2})$ …4.8a

F.D.E.: $I\alpha_c = h_a(T_{c1}[i] - T_a) + h_{fc1}(T_{c1}[i] - T_{f1}[i]) + h_{r.cci}(T_{c1}[i] - T_{c2}[i])$ …4.8b

$$T_{c1}[i] = \frac{I\alpha_c + h_aT_a + h_{f1c1}T_{f1}[i] + h_{r,cc}T_{c2}[i]}{h_a + h_{f1c1} + h_{r,cc}} \quad \text{…4.8c}$$

**For down flow air stream:**

G.D.E.: $m' c\frac{dT_{f1}}{dx} = h_{f.c1}(T_{c1} - T_{f1}) + h_{fc2}(T_{c2} - T_{f1})$ …4.9a

F.D.E.: $m^{'}c\frac{T_{f1}[i+1]-T_{f1}[i]}{\Delta x}=h_{f.c1}(T_{c1}[i]-T_{f1}[i])+h_{fc2}(T_{c2}[i]-T_{f1}[i])$ …4.9b

$$T_{f1}[i+1]=\left(1-\frac{(h_{f1c1}+h_{f1c2})\Delta x}{m^{'}c}\right)T_{f1}[i]+\frac{(h_{f1c1}T_{c1}[i]+h_{f1c2}T_{c2}[i])\Delta x}{m^{'}c} \quad \ldots 4.9c$$

**For second glass cover:**

G.E.:

$$I\alpha_c\tau_c=h_{r.cc}(T_{c2}-T_{c1})+h_{f1c2}(T_{c2}-T_{f1})+h_{f2c2}(T_{c2}-T_{f2})+h_{r.pc}(T_{c2}-T_p)$$

…4.10a

F.D.E.:

$$I\alpha_c\tau_c=h_{r.cc}(T_{c2}[i]-T_{c1}[i])+h_{f1c2}(T_{c2}[i]-T_{f1}[i])+h_{f2c2}(T_{c2}[i]-T_{f2}[i])$$

$$+h_{r.pc}(T_{c2}[i]-T_p[i]) \quad \ldots 4.10b$$

$$T_{c2}[i]=\frac{I\alpha_c\tau_c+h_{f2c2}T_{f2}[i]+h_{f1c2}T_{f1}[i]+h_{r,cc}T_{c1}[i]+h_{r,pc}T_p[i]}{h_{f2c2}+h_{f1c2}+h_{r,cc}+h_{r,pc}} \quad \ldots 4.10c$$

**For up flow air stream:**

G.D.E.: $m^{'}c\frac{dT_{f2}}{dx}=h_{f2c2}(T_{c2}-T_{f2})+h_{f2p}(T_p-T_{f2})$ …4.11a

F.D.E.: $m^{'}c\frac{T_{f2}[i+1]-T_{f2}[i]}{\Delta x}=h_{f2c2}(T_{c2}[i]-T_{f2}[i])+h_{f2p}(T_p[i]-T_{f2}[i])$

…4.11b

$$T_{f2}[i+1]=\left(1+\frac{(h_{f2p}+h_{f2c2})\Delta x}{m^{'}c}\right)T_{f2}[i]-\frac{(h_{f2c2}T_{c2}[i]+h_{f2p}T_p[i])\Delta x}{m^{'}c} \quad \ldots 4.11c$$

**For absorber plate:**

G.E.: $I\alpha_p\tau_c\tau_c=h_{f2p}(T_p-T_{f2})+h_{r.pc}(T_p-T_{c2})+U_b(T_p-T_a)$ …4.12a

F.D.E.: $I\alpha_p\tau_c\tau_c=h_{f2p}(T_p[i]-T_{f2}[i])+h_{r.pc}(T_p[i]-T_{c2}[i])+U_b(T_p[i]-T_a)$

…4.12b

$$T_p[i]=\frac{I\alpha_p\tau_c\tau_c+U_bT_a+h_{f2p}T_{f2}[i]+h_{r,pc}T_{c2}[i]}{U_b+h_{f2p}+h_{r,pc}} \quad \ldots 4.12c$$

### 4.1.4 Counter flow solar air heater with porous matrix

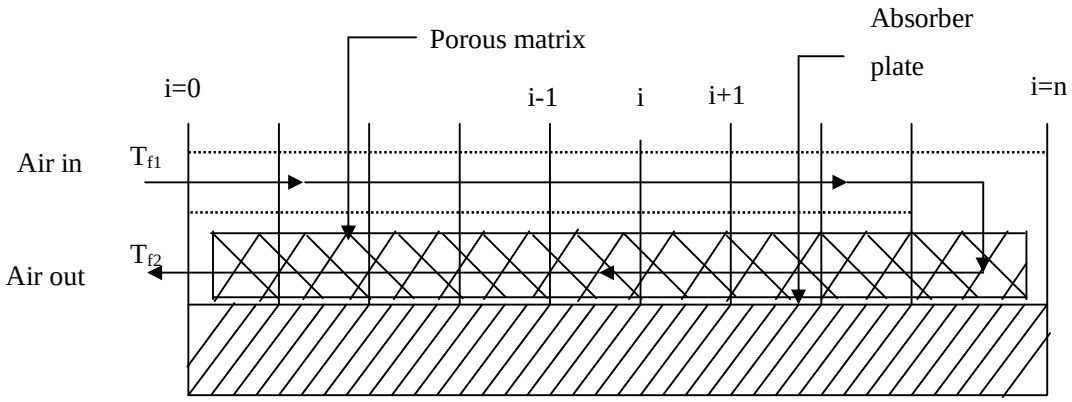


**Fig 4.4 Computational domain for counter-flow air heater with porous matrix**

**For top glass cover:**

G.E.: $I\alpha_c = h_a(T_{c1} - T_a) + h_{fc1}(T_{c1} - T_{f1}) + h_{r.cc}(T_{c1} - T_{c2})$ …4.13a

F.D.E.: $I\alpha_c = h_a(T_{c1}[i] - T_a) + h_{fc1}(T_{c1}[i] - T_{f1}[i]) + h_{r.cci}(T_{c1}[i] - T_{c2}[i])$ …4.13b

$$T_{c1}[i] = \frac{I\alpha_c + h_a T_a + h_{f1c1} T_{f1}[i] + h_{r,cc} T_{c2}[i]}{h_a + h_{f1c1} + h_{r,cc}} \quad \text{…4.13c}$$

**For down flow air stream:**

G.D.E.: $m'c\frac{dT_{f1}}{dx} = h_{f.c1}(T_{c1} - T_{f1}) + h_{fc2}(T_{c2} - T_{f1})$ ...4.14a

F.D.E.: $m'c\frac{T_{f1}[i+1] - T_{f1}[i]}{\Delta x} = h_{f.c1}(T_{c1}[i] - T_{f1}[i]) + h_{fc2}(T_{c2}[i] - T_{f1}[i])$

…4.14b

$$T_{f1}[i+1] = \left(1 - \frac{(h_{f1c1} + h_{f1c2})\Delta x}{m'c}\right) T_{f1}[i] + \frac{(h_{f1c1} T_{c1}[i] + h_{f1c2} T_{c2}[i])\Delta x}{m'c} \quad \text{…4.14c}$$

**For second glass cover:**

G.E.:

$$I\alpha_c\tau_c = h_{r.cc}(T_{c2} - T_{c1}) + h_{f1c2}(T_{c2} - T_{f1}) + h_{f2c2}(T_{c2} - T_{f2}) + h_{r.pc}(T_{c2} - T_{f2})$$

…4.15a

F.D.E. $I\alpha_c\tau_c = h_{r.cc}(T_{c2}[i]-T_{c1}[i]) + h_{f1c2}(T_{c2}[i]-T_{f1}[i]) + h_{f2c2}(T_{c2}[i]-T_{f2}[i])$

$+ h_{r.pc}(T_{c2}[i]-T_{f2}[i])$ …4.15b

$$T_{c2}[i] = \frac{I\alpha_c\tau_c + h_{f2c2}T_{f2}[i] + h_{f1c2}T_{f1}[i] + h_{r,cc}T_{c1}[i] + h_{r,pc}T_{f2}[i]}{h_{f2c2} + h_{f1c2} + h_{r,cc} + h_{r,pc}} \quad \text{…4.15c}$$

**For up flow air stream:**

G.D.E.:

$$m'c\frac{dT_{f2}}{dx} = K_{eff}\frac{d^2T_{f2}}{dx^2} + h_{f2c2}(T_{c2}-T_{f2}) + U_b(T_a-T_{f2}) + I\alpha_p\tau_c\tau_c$$

…4.16a

F.D.E.: $$m'c\frac{T_{f2}[i+1]-T_{f2}[i]}{\Delta x} = K_{eff}\frac{T_{f2}[i+1]-T_{f2}[i-1]}{2\Delta x} + h_{f2c2}(T_{c2}[i]-T_{f2}[i])$$

$+ U_b(T_a - T_{f2}[i]) + I\alpha_p\tau_c\tau_c$ …4.16b

$$T_{f2}(i+1) = T_{f2}(i)\left[\left(\frac{2m'c}{2m'c+k_{eff}}\right) - \left(\frac{2\Delta x}{2m'c+k_{eff}}\right)\left(h_{f2c2}+U_b\right)\right] - \frac{T_{f2}(i-1)}{2m'c+k_{eff}}$$

$$+\left(\frac{2\Delta x}{2m'c+k_{eff}}\right)\left(h_{f2c2}T_{c2}(i)\right) + U_bT_a + I\alpha_p\tau_c\tau_c \quad \text{…4.16c}$$

**Boundary conditions:**

B.C: $T_{f1}[0] = T_i$ …4.17

B.C: $T_{f2}[0] = T_i + \lambda$ …4.18

where $\lambda$ is temperature rise in the down flow of air stream during the first pass between the two glass plates.

For the sake of convenience the heat transfer coefficients between the air stream and the covers and between the air stream and the absorber plate are assumed equal and can be calculated as follows:

$$h_{f1c1} = h_{f1c2} = h_{f2c2} = h_{f2p} = h_f$$

The air density $\rho = \frac{P_a}{RT_a}$ …4.19

Kinematic viscosity: $\nu = \frac{\mu}{\rho}$ …4.20

Thermal diffusivity: $\alpha = \frac{k}{\rho C_p}$ …4.21

Prandtl number: $P_r = \frac{\nu}{\alpha}$ …4.22

Hydraulic diameter: $D_h = \frac{4A_f}{p} = 2D$ …4.23

Reynolds number: $R_e = \frac{\rho U D_h}{\mu} = \frac{2m'}{\mu}$ …4.24

Nusselt number: $Nu = 0.0333\,\mathrm{Re}^{0.8}\,\mathrm{Pr}^{1/3}$ …4.25

Convective heat transfer coefficient: $h_f = \frac{Nuk}{2D}$ …4.26

The radiative heat transfer coefficient between any two surfaces

$$h_{r12} = \frac{\sigma (T_1 + T_2)(T_1^2 + T_2^2)}{1/\varepsilon_1 + 1/\varepsilon_2 - 1}$$ …4.27

So far as pressure drop (pumping power) is concerned, the counter flow solar air heater has a U-turn section and extra-length for air passage compared with conventional solar heaters. Hence the extra pressure drop is introduced by this design. The pressure drop in the u-section can be calculated as

$$\Delta p = \frac{Km^2}{2\rho D^2}$$ …4.28

K=1 for U-section

The pumping power can be calculated as

$$W = \frac{m\Delta p}{\rho}$$ …4.29

**Table 4.1 Values of various input parameters and constants**

| S.No. | Input Parameters | Values |
|---|---|---|
| 1. | Ambient air temperature, $T_a$(K) | 288 |
| 2. | Ambient air pressure, $p_a$(bar) | 1 |
| 3. | Specific gas constant for air, R(J/kgK) | 287 |
| 4. | Dynamic viscosity for air, $\mu$ (kg/ms) | $1.824 \times 10^{-5}$ |
| 5. | Specific heat for air, $c_p$(J/kgK) | 1006.4 |
| 6. | Thermal conductivity for air, $k_f$ (W/mk) | 0.2624 |
| 7. | Thermal conductivity of solid matrix, k(W/mK) | 386.0 |
| 8. | Length of solar air heater, L(m) | 2.0 |
| 9. | Width of solar air heater, w(m) | 1.0 |
| 10. | Depth of solar air heater, D(cm) | 2.5,5.0,10.0 |
| 11. | Emissivity of glass covers, $\varepsilon_c$ | 0.92 |
| 12. | Emissivity of absorber plate and packed bed, $\varepsilon_p$ | 0.92 |
| 13. | Transmissivity of glass cover and absorber, $\tau_c$ or $\tau_p$ | 0.92 |
| 14. | Absorptivity of glass cover, $\alpha_c$ | 0.06 |
| 15. | Absorptivity of absorber, $\alpha_p$ | 0.92 |
| 16. | Stephan-Boltzmann constant, $\sigma$ ($W/m^2K^4$) | $5.67 \times 10^{-6}$ |
| 17. | Overall bottom loss coefficient, $U_b$($W/m^2K$) | 1 |
| 18. | Intensity of solar radiation, I($W/m^2$) | 750,900 |
| 19. | Effective thermal conductivity, $k_{eff}$ (W/mK) | 0.3 |
| 20. | Heat transfer coefficient between top cover and ambient air(convection + radiation), $h_a$($W/m^2K$) | 10 |
| 21. | Inlet air temperature, Ti(K) | 288,303 |
| 22. | Air mass flow rate per unit width, m' (kg/m.s) | 0.01-0.2 |

## 4.2 ALGORITHM FOR COMPUTER PROGRAM

Following steps are involved in the simulation of any of the solar air heaters:

**Step I:** Enter the values of m', L, D, $T_a$, $p_a$, R, $h_a$, $\mu$ , $U_b$, $\alpha_c$ , $\alpha_p$ , $\tau_c$ , $\sigma$ , $c_p$, $k_f$

**Step II:** Select the type of heater.

**Step III:** Calculate v, Pr, Re, Nu, $h_f$.

**Step IV:** Initialize with $T_f[0]=T_i$, $h_{r,cc}[i]=5$, $h_{r,pc}[i]=5$ for all i.

**Step V:** Solving the finite difference equations for a given solar air heater to calculate the nodal temperatures $T_c[i]$, $T_{c1}[i]$, $T_{c2}[i]$, $T_f[i]$, $T_{f1}[i]$, $T_{f2}[i]$, $T_p[i]$ by using the appropriate boundary conditions and gauss elimination method for solving the simultaneous equations as described above. After that following parameters are calculated.

$\Delta T=T_o-Ti;$

$\Delta T_g=\max(T_c[i]-T_a);$

$\Delta T_{pf}=\max(T_p[i]-T_f[i]);$

$$\eta = \frac{mc_p\Delta T}{IA}$$

**Step VI:** Once all these temperatures are obtained, the following performance characteristics are obtained:

1. $\Delta T_g$ Vs m'
2. $\Delta T_{pf}$ Vs m'
3. $\eta$ Vs m'
4. $\Delta T / I$ Vs m'

## 4.3 FLOWCHART FOR THE SIMULATION OF SOLAR AIR HEATERS

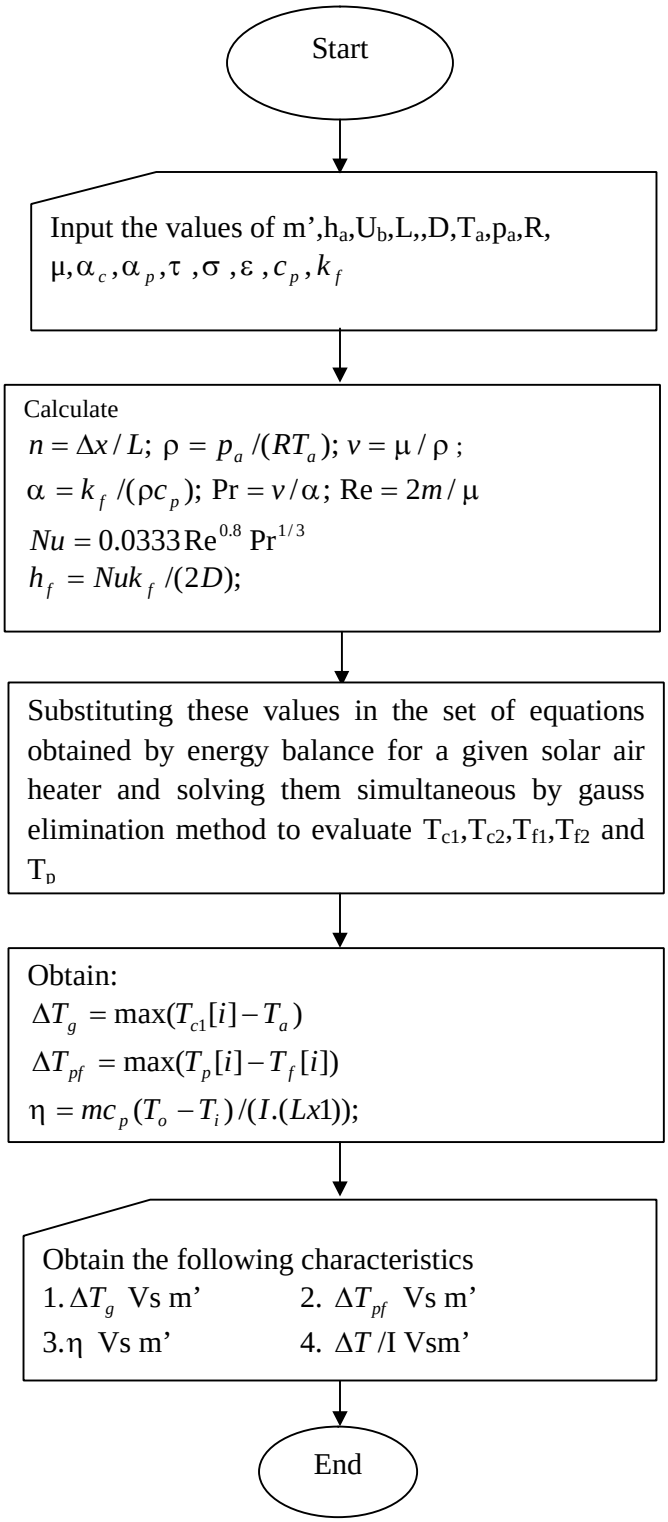


**Fig. 4.5 Flowchart**

# CHAPTER 5
# RESULTS AND DISCUSSIONS

A program in C++ has been developed to simulate the different type of solar air heaters i.e. single glazing air heater, double glazing air heater, counter flow without porous matrix air heater and counter flow with porous matrix air heater. Purely numerical approach has been applied to solve the energy equations for different type of solar air heaters. Mass has been varied from 0.01kg/m.s-0.2 kg/m.s with the increment of 0.01 kg/m.s. The effect of duct depth (as shown in Fig. 5.1) 2.5, 5.0 and 10.0, inlet air temperature 288 K and 303 K, intensity of solar radiation 750W/m$^2$ and 900 W/m$^2$ on the variation of maximum temperature difference between top glass cover temperature and ambient temperature ($\Delta T_g$), the maximum temperature difference between absorber plate temperature and flowing air stream temperature ($\Delta T_{pf}$), the thermal efficiency and $\Delta T / I$ have been studied in the present work. Later the work is been carried out on ANSYS software as it is standard software and widely acceptable. The modeling of single glazing, double glazing and counter flow without porous matrix air heaters is done and after applying the loads and constraints we get the results for the proposed models.

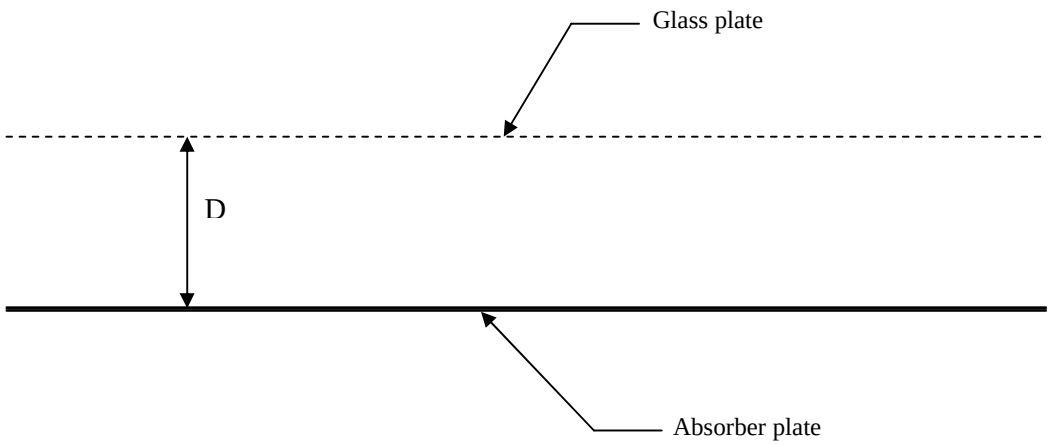


**Figure 5.1 Difference between the absorber plate and glass plate (Duct depth)**

## 5.1 EFFECT OF CHANGING VARIOUS PARAMETERS ON $\Delta T_g$

Figure 5.2, 5.6, 5.10, 5.14, 5.18 and 5.22 shows the variation of the maximum temperature difference between the top glass cover temperature and ambient temperature ($\Delta T_g$) with mass flow rates. $\Delta T_g$ reduces rapidly for mass flow rates between 0.01 kg/m.s -0.05 kg/m.s after that gradual reduction is there for further mass flow rates. As we know the heat transfer coefficient ($h_f$) is the function of fluid velocity, so it increases with higher mass flow rates and consequently higher heat transfer is there for higher velocities. Hence, the rise in ($\Delta T_g$) is small at higher mass flow rates. This rise is least in case of counter flow with porous matrix because of its design, which aids in achieving high transfer rate. As we increase the duct depths from 2.5cm to 5cm and 10cm the velocity for same mass flow rate decreases hence the heat transfer coefficient decreases. Therefore, $\Delta T_g$ is maximum for D=10 cm, where the glass temperature increases because of the radiation heat exchange between the absorber plate and the glass cover and convective heat transfer is decreased by increasing the spacing between the glass cover and the absorber (D). The value of $\Delta T_g$ is less than $5^0$C for counter flow solar air heaters for the normal operating mass flow rates. The local heat losses are reduced by the collector cover to ambient in case of counter flow heaters.

## 5.2 EFFECTS OF CHANGING PARAMETERS ON $\Delta T_{pf}$

Figure 5.3, 5.7, 5.11, 5.15, 5.19 and 5.23 shows the variation of maximum temperature difference between the absorber plate temperature and air stream temperature ($\Delta T_{pf}$) with mass flow rate. As like $\Delta T_g$ it also reduces rapidly for mass flow rates 0.01kg/m.s-0.05kg/m.s the reason is same as discussed above for $\Delta T_g$. As we increase the duct depth from 2.5cm to 5cm and 10cm the value of $\Delta T_{pf}$ increases for a given mass flow rates due to low velocities and consequently convective heat transfer coefficient decreases.

With the increase in inlet temperature from $15^0$C to $30^0$C the value of $\Delta T_{pf}$ increases. Increasing the solar radiation from 750 to 900w/$m^2$ also increases the value of $\Delta T_{pf}$ because the heat input to the system is increased.

One of the drawbacks with the conventional solar air heater is that the poor convection from the absorber plate to the air stream. Hence the temperature of the absorber plate becomes much higher than that of air stream. Increased absorber temperature increases the heat losses by radiation (top) and heat conduction (bottom). The maximum value of $\Delta T_{pf}$ occurs at the outlet of heaters. Single glass cover solar air heater allow a higher temperature difference for normal operating conditions, m>0.05 kg/m.s. For counter flow solar air heater with porous matrix it is assumed that the temperature of air stream is equal to the temperature of the solid matrix because of the high volumetric heat transfer coefficient.

## 5.3 EFFECT OF CHANGING PARAMETERS ON THERMAL EFFICIENCY

Figure 5.4, 5.8, 5.12, 5.16, 5.20 and 5.24 shows the variation in thermal efficiency with mass flow rate. First the efficiency increases rapidly for mass flow rate 0.01kg/m.s to 0.1 kg/m.s then it rise is almost constant. This is because the useful heat gain is directly proportional to the mass flow rate and the thermal efficiency is the ratio of useful gain to the total solar radiation incident on it. The thermal efficiency is maximum for counter flow solar air heater with porous matrix. Adding a porous matrix to a counter flow heater increases the efficiency drastically, with efficiency above 75% for normal operating range and exceeding 80% for high flow rates. The thermal efficiency is maximum for entire range of mass flow rate for a counter flow solar air heater and least for single glazing conventional solar air heater.

As mentioned earlier, increasing duct depth(D) decreases the flow velocity thereby reducing the heat transfer coefficient and hence, the heat transfer rate. Therefore changing the spacing between the absorber plate and the glass cover has a significant effect on the performance of the different type of air heaters. The thermal efficiency of counter flow heater is found to increase 10 to 20% higher than double glazing conventional air heater.

## 5.4 EFFECT OF CHANGING PARAMETERS ON $\Delta T / I$

Figure 5.5, 5.9, 5.13, 5.17, 5.21 and 5.25 depicts the variation of $\Delta T / I$ with mass flow rate. $\Delta T / I$ decreases rapidly initially but becomes almost constant after the mass flow rate of 0.1 kg/m.s. Changing depth, inlet air temperature and intensity of solar radiation doesn't have much effect on this ratio.

Results obtained from the simulation study of various solar air heaters under consideration are tabulated below:

**Table 5.1 Single glazing air heater (D=2.5cm, I=750W/m$^2$, Ti=150$^0$C)**

| m'(kg/s.m) | $T_f$(K) | $T_p$(K) | $\Delta T_g$(K) | $\Delta T_{pf}$(K) | $\eta$ (%) | $\Delta$T/I |
|---|---|---|---|---|---|---|
| 0.01 | 345.12 | 392.92 | 41.44 | 47.80 | 38.29 | 0.076 |
| 0.02 | 328.56 | 368.88 | 32.53 | 40.31 | 54.39 | 0.054 |
| 0.03 | 319.58 | 354.28 | 26.77 | 34.69 | 63.53 | 0.042 |
| 0.04 | 313.91 | 344.42 | 22.78 | 30.51 | 69.49 | 0.034 |
| 0.05 | 309.98 | 337.30 | 19.85 | 27.31 | 73.71 | 0.029 |
| 0.06 | 307.10 | 331.88 | 17.60 | 24.78 | 76.85 | 0.025 |
| 0.07 | 304.89 | 327.62 | 15.82 | 22.72 | 79.30 | 0.022 |
| 0.08 | 303.15 | 324.17 | 14.37 | 21.02 | 81.26 | 0.020 |
| 0.09 | 301.73 | 321.32 | 13.17 | 19.58 | 82.86 | 0.018 |
| 0.10 | 300.55 | 318.91 | 12.16 | 18.35 | 84.20 | 0.016 |
| 0.11 | 299.57 | 316.86 | 11.29 | 17.29 | 85.33 | 0.015 |
| 0.12 | 298.72 | 315.08 | 10.55 | 16.35 | 86.31 | 0.014 |
| 0.13 | 297.99 | 313.53 | 9.89 | 15.53 | 87.15 | 0.013 |
| 0.14 | 297.36 | 312.15 | 9.32 | 14.79 | 87.89 | 0.012 |
| 0.15 | 296.80 | 310.93 | 8.80 | 14.13 | 88.55 | 0.011 |
| 0.16 | 296.30 | 309.84 | 8.35 | 13.53 | 89.13 | 0.011 |
| 0.17 | 295.86 | 308.85 | 7.94 | 12.99 | 89.65 | 0.010 |
| 0.18 | 295.46 | 307.96 | 7.56 | 12.49 | 90.13 | 0.009 |
| 0.19 | 295.10 | 307.15 | 7.22 | 12.04 | 90.56 | 0.009 |
| 0.20 | 294.78 | 306.40 | 6.92 | 11.62 | 90.95 | 0.009 |

**Table 5.2 Double glazing air heater (D=2.5cm, I=750 W/m$^2$, Ti=15$^0$C)**

| m'(kg/s.m) | $T_f$(K) | $T_p$(K) | $\Delta T_g$(K) | $\Delta T_{pf}$(K) | $\eta$ (%) | $\Delta$T/I |
|---|---|---|---|---|---|---|
| 0.01 | 349.82 | 430.45 | 35.56 | 80.63 | 41.44 | 0.082 |
| 0.02 | 329.61 | 397.80 | 28.63 | 68.18 | 55.80 | 0.055 |
| 0.03 | 319.78 | 379.05 | 24.43 | 59.26 | 63.93 | 0.042 |
| 0.04 | 313.86 | 366.57 | 21.53 | 52.71 | 69.36 | 0.034 |
| 0.05 | 309.86 | 357.54 | 19.37 | 47.67 | 73.31 | 0.029 |

| | | | | | | |
|---|---|---|---|---|---|---|
| 0.06 | 306.97 | 350.64 | 17.68 | 43.66 | 76.34 | 0.025 |
| 0.07 | 304.78 | 345.16 | 16.31 | 40.38 | 78.77 | 0.022 |
| 0.08 | 303.05 | 340.69 | 15.17 | 37.63 | 80.76 | 0.020 |
| 0.09 | 301.66 | 336.96 | 14.21 | 35.29 | 82.43 | 0.018 |
| 0.10 | 300.51 | 333.78 | 13.38 | 33.27 | 83.87 | 0.016 |
| 0.11 | 299.54 | 331.05 | 12.66 | 31.51 | 85.11 | 0.015 |
| 0.12 | 298.71 | 328.66 | 12.0 | 29.95 | 86.20 | 0.014 |
| 0.13 | 298.00 | 326.56 | 11.45 | 28.56 | 87.16 | 0.013 |
| 0.14 | 297.37 | 324.69 | 10.95 | 27.31 | 88.01 | 0.012 |
| 0.15 | 296.82 | 323.01 | 10.49 | 26.18 | 88.79 | 0.011 |
| 0.16 | 296.34 | 321.50 | 10.07 | 25.16 | 89.48 | 0.011 |
| 0.17 | 295.90 | 320.13 | 9.69 | 24.23 | 90.12 | 0.010 |
| 0.18 | 295.51 | 318.89 | 9.34 | 23.37 | 90.70 | 0.010 |
| 0.19 | 295.16 | 317.74 | 9.02 | 22.58 | 91.23 | 0.009 |
| 0.20 | 294.84 | 316.69 | 8.72 | 21.85 | 91.73 | 0.009 |

**Table 5.3 Counter flow air heater (D=2.5cm, I=750 W/m$^2$, Ti=15$^0$C)**

| **m'(kg/s.m)** | **$T_f$(K)** | **$T_p$(K)** | **$\Delta T_g$(K)** | **$\Delta T_{pf}$(K)** | **$\eta$ (%)** | **$\Delta$T/I** |
|---|---|---|---|---|---|---|
| 0.01 | 349.37 | 397.26 | 3.34 | 47.88 | 41.15 | 0.081 |
| 0.02 | 328.51 | 368.19 | 2.66 | 39.68 | 54.32 | 0.054 |
| 0.03 | 318.57 | 352.52 | 2.25 | 33.94 | 61.49 | 0.040 |
| 0.04 | 312.67 | 342.49 | 1.98 | 29.81 | 66.17 | 0.032 |
| 0.05 | 308.74 | 335.43 | 1.77 | 26.69 | 69.53 | 0.027 |
| 0.06 | 305.92 | 330.16 | 1.61 | 24.24 | 72.08 | 0.023 |
| 0.07 | 303.79 | 326.05 | 1.49 | 22.26 | 74.12 | 0.021 |
| 0.08 | 302.12 | 322.74 | 1.38 | 20.62 | 75.77 | 0.018 |
| 0.09 | 300.78 | 320.02 | 1.29 | 19.23 | 77.10 | 0.017 |
| 0.10 | 299.68 | 317.73 | 1.21 | 18.04 | 78.35 | 0.015 |
| 0.11 | 298.76 | 315.78 | 1.15 | 17.01 | 79.38 | 0.014 |
| 0.12 | 297.97 | 314.09 | 1.09 | 16.11 | 80.28 | 0.013 |
| 0.13 | 297.30 | 312.61 | 1.04 | 15.31 | 81.08 | 0.012 |

| | | | | | | |
|---|---|---|---|---|---|---|
| 0.14 | 296.71 | 311.31 | 0.99 | 14.60 | 81.79 | 0.011 |
| 0.15 | 296.19 | 310.15 | 0.95 | 13.95 | 82.43 | 0.010 |
| 0.16 | 295.73 | 309.11 | 0.91 | 13.37 | 83.01 | 0.010 |
| 0.17 | 295.33 | 308.18 | 0.88 | 12.85 | 83.54 | 0.009 |
| 0.18 | 294.96 | 307.33 | 0.84 | 12.36 | 84.03 | 0.009 |
| 0.19 | 294.63 | 306.55 | 0.82 | 11.92 | 84.48 | 0.008 |
| 0.20 | 294.33 | 305.84 | 0.79 | 11.51 | 84.89 | 0.008 |

**Table 5.4 Counter flow air heater with porous matrix**

**(D=2.5cm, I=750 W/m$^2$, Ti=15$^0$C)**

| m'(kg/s.m) | $\Delta$T | $\Delta$ T$_g$(K) | $\Delta$T/I | $\eta$ (%) |
|---|---|---|---|---|
| 0.01 | 94.57 | 4.11 | 0.126 | 63.41 |
| 0.02 | 52.13 | 3.47 | 0.069 | 69.90 |
| 0.03 | 36.35 | 3.05 | 0.048 | 73.12 |
| 0.04 | 28.04 | 2.73 | 0.037 | 75.21 |
| 0.05 | 22.89 | 2.48 | 0.030 | 76.74 |
| 0.06 | 19.37 | 2.29 | 0.025 | 77.93 |
| 0.07 | 16.81 | 2.12 | 0.022 | 78.91 |
| 0.08 | 14.86 | 1.98 | 0.019 | 79.73 |
| 0.09 | 13.33 | 1.86 | 0.017 | 80.43 |
| 0.10 | 12.08 | 1.76 | 0.016 | 81.05 |
| 0.11 | 11.06 | 1.67 | 0.014 | 81.59 |
| 0.12 | 10.20 | 1.58 | 0.013 | 82.08 |
| 0.13 | 9.46 | 1.51 | 0.012 | 82.53 |
| 0.14 | 8.83 | 1.45 | 0.011 | 82.93 |
| 0.15 | 8.28 | 1.39 | 0.011 | 83.30 |
| 0.16 | 7.79 | 1.33 | 0.010 | 83.65 |
| 0.17 | 7.36 | 1.28 | 0.009 | 83.96 |
| 0.18 | 6.98 | 1.24 | 0.009 | 84.26 |
| 0.19 | 6.63 | 1.19 | 0.008 | 84.53 |
| 0.20 | 6.32 | 1.15 | 0.008 | 84.80 |

**Table 5.5 Single glazing air heater (D=5cm, I=750 W/m$^2$, Ti=15$^0$C)**

| m'(kg/s.m) | $T_f$(K) | $T_p$(K) | $\Delta T_g$(K) | $\Delta T_{pf}$(K) | $\eta$ (%) | $\Delta$T/I |
|---|---|---|---|---|---|---|
| 0.01 | 332.93 | 402.83 | 41.36 | 69.89 | 30.12 | 0.059 |
| 0.02 | 321.18 | 383.01 | 33.90 | 61.83 | 44.49 | 0.044 |
| 0.03 | 314.62 | 369.77 | 28.82 | 55.14 | 53.56 | 0.035 |
| 0.04 | 310.34 | 360.17 | 25.13 | 49.83 | 59.90 | 0.029 |
| 0.05 | 307.28 | 352.83 | 22.30 | 45.54 | 64.65 | 0.025 |
| 0.06 | 304.98 | 347.01 | 20.05 | 42.02 | 68.33 | 0.022 |
| 0.07 | 303.19 | 342.26 | 18.23 | 39.07 | 71.29 | 0.020 |
| 0.08 | 301.74 | 338.30 | 16.72 | 36.56 | 73.71 | 0.018 |
| 0.09 | 300.55 | 334.94 | 15.45 | 34.39 | 75.74 | 0.016 |
| 0.10 | 299.55 | 332.06 | 14.35 | 32.50 | 77.47 | 0.015 |
| 0.11 | 298.70 | 329.54 | 13.41 | 30.84 | 78.95 | 0.014 |
| 0.12 | 297.97 | 327.33 | 12.58 | 29.34 | 80.24 | 0.013 |
| 0.13 | 297.33 | 325.37 | 11.85 | 28.04 | 81.38 | 0.012 |
| 0.14 | 296.77 | 323.62 | 11.20 | 26.84 | 82.39 | 0.011 |
| 0.15 | 296.28 | 322.04 | 10.62 | 25.76 | 83.29 | 0.011 |
| 0.16 | 295.84 | 320.61 | 10.10 | 24.77 | 84.10 | 0.010 |
| 0.17 | 295.44 | 319.31 | 9.62 | 23.87 | 84.82 | 0.009 |
| 0.18 | 295.08 | 318.12 | 9.19 | 23.04 | 85.49 | 0.009 |
| 0.19 | 294.75 | 317.03 | 8.80 | 22.27 | 86.08 | 0.009 |
| 0.20 | 294.46 | 316.02 | 8.44 | 21.56 | 86.65 | 0.008 |

**Table 5.6 Double glazing air heater (D=5cm, I=750 W/m$^2$, Ti=15$^0$C)**

| m'(kg/s.m) | $T_f$(K) | $T_p$(K) | $\Delta T_g$(K) | $\Delta T_{pf}$(K) | $\eta$ (%) | $\Delta$T/I |
|---|---|---|---|---|---|---|
| 0.01 | 333.53 | 450.42 | 37.91 | 116.89 | 30.52 | 0.060 |
| 0.02 | 320.48 | 422.24 | 31.95 | 101.76 | 43.55 | 0.043 |
| 0.03 | 313.70 | 404.33 | 28.06 | 90.63 | 51.70 | 0.034 |
| 0.04 | 309.43 | 391.61 | 25.26 | 82.18 | 57.47 | 0.028 |
| 0.05 | 306.44 | 381.95 | 23.10 | 75.51 | 61.84 | 0.024 |

| | | | | | | |
|---|---|---|---|---|---|---|
| 0.06 | 304.23 | 374.31 | 21.37 | 70.08 | 65.31 | 0.021 |
| 0.07 | 302.52 | 368.06 | 19.94 | 65.54 | 68.14 | 0.019 |
| 0.08 | 301.14 | 362.84 | 18.73 | 61.69 | 70.52 | 0.017 |
| 0.09 | 300.02 | 358.39 | 17.70 | 58.36 | 72.54 | 0.016 |
| 0.10 | 299.08 | 354.53 | 16.79 | 55.45 | 74.31 | 0.014 |
| 0.11 | 298.28 | 351.16 | 16.00 | 52.88 | 75.85 | 0.013 |
| 0.12 | 297.59 | 348.18 | 15.29 | 50.58 | 77.22 | 0.012 |
| 0.13 | 297.01 | 345.51 | 14.65 | 48.51 | 78.45 | 0.012 |
| 0.14 | 296.47 | 343.12 | 14.08 | 46.64 | 79.56 | 0.011 |
| 0.15 | 296.01 | 340.95 | 13.56 | 44.94 | 80.55 | 0.010 |
| 0.16 | 295.59 | 338.98 | 13.08 | 43.38 | 81.47 | 0.010 |
| 0.17 | 295.22 | 337.17 | 12.64 | 41.95 | 82.31 | 0.009 |
| 0.18 | 294.88 | 335.51 | 12.23 | 40.62 | 83.07 | 0.009 |
| 0.19 | 294.57 | 333.97 | 11.86 | 39.40 | 83.79 | 0.008 |
| 0.20 | 294.29 | 332.55 | 11.51 | 38.25 | 84.46 | 0.008 |

**Table 5.7 Counter flow air heater (D=5cm, I=750 W/m$^2$, Ti=15$^0$C)**

| m'(kg/s.m) | $T_f$(K) | $T_p$(K) | $\Delta T_g$(K) | $\Delta T_{pf}$(K) | $\eta$ (%) | $\Delta T/I$ |
|---|---|---|---|---|---|---|
| 0.01 | 341.12 | 414.15 | 4.00 | 73.04 | 35.61 | 0.070829 |
| 0.02 | 324.5 | 387.18 | 3.42 | 62.66 | 48.97 | 0.048 |
| 0.03 | 316.23 | 371.26 | 3.04 | 55.03 | 56.78 | 0.037 |
| 0.04 | 311.15 | 360.47 | 2.76 | 49.31 | 62.10 | 0.030 |
| 0.05 | 307.69 | 352.56 | 2.54 | 44.86 | 66.02 | 0.026 |
| 0.06 | 305.17 | 346.45 | 2.36 | 41.28 | 69.07 | 0.022 |
| 0.07 | 303.24 | 341.56 | 2.28 | 38.32 | 71.53 | 0.020 |
| 0.08 | 301.71 | 337.55 | 2.09 | 35.83 | 73.56 | 0.018 |
| 0.09 | 300.47 | 334.17 | 1.98 | 33.70 | 75.28 | 0.016 |
| 0.10 | 299.45 | 331.89 | 1.88 | 31.84 | 76.76 | 0.015 |
| 0.11 | 298.58 | 328.80 | 1.80 | 30.22 | 78.05 | 0.014 |
| 0.12 | 297.84 | 326.62 | 1.72 | 28.77 | 79.19 | 0.013 |
| 0.13 | 297.20 | 324.69 | 1.66 | 27.49 | 80.19 | 0.012 |

| | | | | | | |
|---|---|---|---|---|---|---|
| 0.14 | 296.64 | 322.97 | 1.59 | 26.32 | 81.10 | 0.011 |
| 0.15 | 296.14 | 321.42 | 1.54 | 25.27 | 81.92 | 0.010 |
| 0.16 | 295.71 | 320.02 | 1.49 | 24.32 | 82.66 | 0.010 |
| 0.17 | 295.31 | 318.75 | 1.44 | 23.44 | 83.34 | 0.009 |
| 0.18 | 294.95 | 317.59 | 1.39 | 22.63 | 83.97 | 0.009 |
| 0.19 | 294.63 | 316.53 | 1.35 | 21.89 | 84.54 | 0.008 |
| 0.20 | 294.34 | 315.55 | 1.32 | 21.20 | 85.06 | 0.008 |

**Table 5.8 Counter flow air heater with porous matrix**

**(D=5cm, I=750 W/m$^2$, Ti=15$^0$C)**

| m'(kg/s.m) | $\Delta$T | $\Delta$ $T_g$(K) | $\Delta$T/I | $\eta$ (%) |
|---|---|---|---|---|
| 0.01 | 114.83 | 4.35 | 0.153 | 76.99 |
| 0.02 | 61.85 | 3.83 | 0.082 | 82.94 |
| 0.03 | 42.60 | 3.47 | 0.056 | 85.69 |
| 0.04 | 32.603 | 3.18 | 0.043 | 87.43 |
| 0.05 | 26.45 | 2.96 | 0.035 | 88.68 |
| 0.06 | 22.28 | 2.77 | 0.029 | 89.64 |
| 0.07 | 19.26 | 2.61 | 0.025 | 90.42 |
| 0.08 | 16.98 | 2.47 | 0.022 | 91.07 |
| 0.09 | 15.18 | 2.359 | 0.020 | 91.62 |
| 0.10 | 13.76 | 2.25 | 0.018 | 92.11 |
| 0.11 | 12.54 | 2.15 | 0.016 | 92.54 |
| 0.12 | 11.54 | 2.07 | 0.015 | 92.91 |
| 0.13 | 10.70 | 1.99 | 0.014 | 93.26 |
| 0.14 | 13.73 | 2.25 | 0.013 | 93.58 |
| 0.15 | 9.33 | 1.85 | 0.012 | 93.86 |
| 0.16 | 8.77 | 1.79 | 0.011 | 94.18 |
| 0.17 | 8.27 | 1.74 | 0.011 | 94.36 |
| 0.18 | 7.83 | 1.69 | 0.010 | 94.59 |
| 0.19 | 7.44 | 1.64 | 0.009 | 94.80 |
| 0.20 | 7.08 | 1.59 | 0.009 | 94.99 |

**Table 5.9 Single glazing air heater (D=10cm, I=750 W/m$^2$, Ti=15$^0$C)**

| m'(kg/s.m) | $T_f$(K) | $T_p$(K) | $\Delta T_g$(K) | $\Delta T_{pf}$(K) | $\eta$ (%) | $\Delta$T/I |
|---|---|---|---|---|---|---|
| 0.01 | 318.82 | 413.15 | 43.65 | 94.32 | 20.66 | 0.041 |
| 0.02 | 311.90 | 398.25 | 37.81 | 86.35 | 32.05 | 0.031 |
| 0.03 | 307.92 | 387.37 | 33.54 | 79.45 | 40.08 | 0.026 |
| 0.04 | 305.22 | 378.90 | 30.22 | 73.67 | 46.19 | 0.022 |
| 0.05 | 303.22 | 372.04 | 27.54 | 68.81 | 51.05 | 0.020 |
| 0.06 | 301.67 | 366.33 | 25.33 | 64.65 | 55.02 | 0.018 |
| 0.07 | 300.43 | 361.48 | 23.46 | 61.05 | 58.36 | 0.016 |
| 0.08 | 299.40 | 357.30 | 21.85 | 57.98 | 61.19 | 0.015 |
| 0.09 | 298.54 | 353.66 | 20.46 | 55.11 | 63.64 | 0.014 |
| 0.10 | 297.81 | 350.44 | 19.24 | 52.62 | 65.78 | 0.013 |
| 0.11 | 297.17 | 347.57 | 18.16 | 50.39 | 67.67 | 0.012 |
| 0.12 | 296.62 | 344.99 | 17.20 | 48.37 | 69.35 | 0.011 |
| 0.13 | 296.13 | 342.67 | 16.33 | 46.54 | 70.86 | 0.010 |
| 0.14 | 295.69 | 340.58 | 15.55 | 44.86 | 72.21 | 0.010 |
| 0.15 | 295.30 | 338.62 | 14.84 | 43.32 | 73.44 | 0.009 |
| 0.16 | 294.95 | 336.87 | 14.20 | 41.90 | 74.56 | 0.009 |
| 0.17 | 294.63 | 335.22 | 13.60 | 40.59 | 75.59 | 0.008 |
| 0.18 | 294.34 | 333.71 | 13.06 | 39.36 | 76.53 | 0.008 |
| 0.19 | 294.06 | 332.30 | 12.56 | 38.23 | 77.40 | 0.008 |
| 0.20 | 293.83 | 331.06 | 12.09 | 37.16 | 78.20 | 0.007 |

**Table 5.10 Double glazing air heater (D=10cm, I=750 W/m$^2$, Ti=15$^0$C)**

| m'(kg/s.m) | $T_f$(K) | $T_p$(K) | $\Delta T_g$(K) | $\Delta T_{pf}$(K) | $\eta$ (%) | $\Delta$T/I |
|---|---|---|---|---|---|---|
| 0.01 | 317.76 | 470.32 | 41.42 | 152.60 | 19.92 | 0.039 |
| 0.02 | 310.57 | 448.39 | 36.74 | 137.81 | 30.27 | 0.030 |
| 0.03 | 306.64 | 432.94 | 33.41 | 126.30 | 37.49 | 0.024 |
| 0.04 | 304.02 | 421.14 | 30.84 | 117.11 | 42.98 | 0.021 |
| 0.05 | 302.13 | 411.70 | 28.78 | 109.57 | 47.36 | 0.018 |

| | | | | | | |
|---|---|---|---|---|---|---|
| 0.06 | 300.67 | 403.90 | 27.06 | 103.23 | 50.98 | 0.016 |
| 0.07 | 299.51 | 397.31 | 25.60 | 97.80 | 54.04 | 0.015 |
| 0.08 | 298.56 | 391.66 | 24.34 | 93.08 | 56.67 | 0.014 |
| 0.09 | 297.77 | 386.69 | 23.24 | 88.92 | 58.97 | 0.013 |
| 0.10 | 297.09 | 382.32 | 22.26 | 85.23 | 61.00 | 0.012 |
| 0.11 | 296.51 | 378.43 | 21.38 | 81.98 | 62.81 | 0.011 |
| 0.12 | 296.01 | 374.93 | 20.59 | 78.92 | 64.44 | 0.010 |
| 0.13 | 295.56 | 371.76 | 19.87 | 76.19 | 65.91 | 0.010 |
| 0.14 | 295.16 | 368.87 | 19.21 | 73.70 | 67.27 | 0.009 |
| 0.15 | 294.81 | 366.22 | 18.61 | 71.41 | 68.50 | 0.009 |
| 0.16 | 294.49 | 363.77 | 18.05 | 69.29 | 69.64 | 0.008 |
| 0.17 | 294.20 | 361.53 | 17.54 | 67.33 | 70.70 | 0.008 |
| 0.18 | 293.93 | 359.44 | 17.06 | 65.51 | 71.67 | 0.007 |
| 0.19 | 293.69 | 357.50 | 16.61 | 63.80 | 72.58 | 0.007 |
| 0.20 | 293.47 | 355.68 | 16.19 | 62.20 | 73.44 | 0.007 |

**Table 5.11 Counter flow air heater (D=10cm, I=750 W/m$^2$, Ti=15$^0$C)**

| m'(kg/s.m) | $T_f$(K) | $T_p$(K) | $\Delta T_g$(K) | $\Delta T_{pf}$(K) | $\eta$ (%) | $\Delta T/I$ |
|---|---|---|---|---|---|---|
| 0.01 | 327.45 | 431.50 | 4.49 | 104.04 | 26.45 | 0.052 |
| 0.02 | 316.70 | 408.57 | 4.06 | 91.87 | 38.48 | 0.038 |
| 0.03 | 310.99 | 393.63 | 3.75 | 82.64 | 46.24 | 0.030 |
| 0.04 | 307.33 | 382.83 | 3.51 | 75.50 | 51.84 | 0.025 |
| 0.05 | 304.74 | 374.53 | 3.31 | 69.78 | 56.14 | 0.022 |
| 0.06 | 302.81 | 367.89 | 3.14 | 65.08 | 59.59 | 0.019 |
| 0.07 | 301.30 | 362.42 | 2.99 | 61.11 | 62.44 | 0.017 |
| 0.08 | 300.09 | 357.81 | 2.87 | 57.72 | 64.8 | 0.016 |
| 0.09 | 299.09 | 353.86 | 2.75 | 54.77 | 66.91 | 0.014 |
| 0.10 | 298.25 | 350.42 | 2.65 | 52.17 | 68.72 | 0.013 |
| 0.11 | 297.53 | 347.40 | 2.56 | 49.86 | 70.3 | 0.012 |
| 0.12 | 296.91 | 344.71 | 2.48 | 47.79 | 71.73 | 0.011 |
| 0.13 | 296.37 | 342.31 | 2.40 | 45.93 | 73.01 | 0.011 |

| | | | | | | |
|---|---|---|---|---|---|---|
| 0.14 | 295.90 | 340.13 | 2.33 | 44.23 | 74.16 | 0.010 |
| 0.15 | 295.47 | 338.16 | 2.27 | 42.68 | 75.21 | 0.009 |
| 0.16 | 295.10 | 336.36 | 2.21 | 41.26 | 76.17 | 0.009 |
| 0.17 | 294.78 | 334.71 | 2.15 | 39.95 | 77.06 | 0.009 |
| 0.18 | 294.45 | 333.19 | 2.10 | 38.74 | 77.87 | 0.008 |
| 0.19 | 294.17 | 331.78 | 2.05 | 37.61 | 78.63 | 0.008 |
| 0.20 | 293.91 | 330.47 | 2.07 | 36.56 | 79.34 | 0.007 |

**Table 5.12 Counter flow air heater with porous matrix**

**(D=10cm, I=750 W/m$^2$, Ti=15$^0$C)**

| **m'(kg/s.m)** | **$\Delta$T** | **$\Delta$ T$_g$(K)** | **$\Delta$T/I** | **$\eta$ (%)** |
|---|---|---|---|---|
| 0.01 | 116.77 | 4.62 | 0.155 | 78.29 |
| 0.02 | 62.03 | 4.23 | 0.082 | 83.14 |
| 0.03 | 42.40 | 3.94 | 0.056 | 85.28 |
| 0.04 | 32.29 | 3.70 | 0.043 | 86.61 |
| 0.05 | 26.12 | 3.51 | 0.034 | 87.56 |
| 0.06 | 21.94 | 3.34 | 0.029 | 88.29 |
| 0.07 | 18.93 | 3.20 | 0.025 | 88.88 |
| 0.08 | 16.66 | 3.07 | 0.022 | 89.38 |
| 0.09 | 14.88 | 2.95 | 0.019 | 89.80 |
| 0.10 | 13.45 | 2.85 | 0.017 | 90.17 |
| 0.11 | 12.27 | 2.76 | 0.016 | 90.50 |
| 0.12 | 11.285 | 2.67 | 0.015 | 90.7 |
| 0.13 | 10.44 | 2.59 | 0.013 | 91.06 |
| 0.14 | 9.72 | 2.52 | 0.012 | 91.30 |
| 0.15 | 9.19 | 2.45 | 0.012 | 91.51 |
| 0.16 | 8.55 | 2.39 | 0.011 | 91.73 |
| 0.17 | 8.06 | 2.33 | 0.010 | 91.91 |
| 0.18 | 7.63 | 2.28 | 0.010 | 92.09 |
| 0.19 | 7.24 | 2.23 | 0.009 | 92.25 |
| 0.20 | 6.89 | 2.18 | 0.009 | 92.40 |

**Table 5.13 Single glazing air heater (D=5cm, I=750 W/m$^2$, Ti=30$^0$C)**

| m'(kg/s.m) | $T_f$(K) | $T_p$(K) | $\Delta T_g$(K) | $\Delta T_{pf}$(K) | $\eta$ (%) | $\Delta$T/I |
|---|---|---|---|---|---|---|
| 0.01 | 347.93 | 417.83 | 56.35 | 69.89 | 30.12 | 0.059 |
| 0.02 | 336.18 | 398.01 | 48.90 | 61.83 | 44.49 | 0.048 |
| 0.03 | 329.62 | 384.77 | 43.82 | 55.14 | 53.56 | 0.035 |
| 0.04 | 325.34 | 375.17 | 40.13 | 49.83 | 59.91 | 0.029 |
| 0.05 | 322.27 | 367.83 | 37.38 | 45.54 | 64.68 | 0.025 |
| 0.06 | 319.98 | 362.01 | 35.05 | 42.02 | 68.38 | 0.022 |
| 0.07 | 318.19 | 357.26 | 33.23 | 39.07 | 71.29 | 0.020 |
| 0.08 | 316.74 | 353.30 | 31.72 | 36.56 | 73.71 | 0.018 |
| 0.09 | 315.55 | 349.94 | 30.45 | 34.39 | 75.74 | 0.016 |
| 0.10 | 314.55 | 347.06 | 29.35 | 32.50 | 77.47 | 0.015 |
| 0.11 | 313.70 | 344.54 | 28.41 | 30.84 | 78.95 | 0.014 |
| 0.12 | 312.97 | 342.33 | 27.58 | 29.36 | 80.24 | 0.013 |
| 0.13 | 312.33 | 340.37 | 26.85 | 28.04 | 81.38 | 0.012 |
| 0.14 | 311.77 | 338.62 | 26.20 | 26.84 | 82.39 | 0.011 |
| 0.15 | 311.28 | 337.04 | 25.62 | 25.76 | 83.29 | 0.011 |
| 0.16 | 310.84 | 335.61 | 25.10 | 24.77 | 84.10 | 0.010 |
| 0.17 | 310.44 | 334.31 | 24.62 | 23.87 | 84.82 | 0.009 |
| 0.18 | 310.08 | 333.12 | 24.19 | 23.04 | 85.49 | 0.009 |
| 0.19 | 309.75 | 332.03 | 23.80 | 22.27 | 86.08 | 0.009 |
| 0.20 | 309.46 | 331.02 | 23.44 | 21.56 | 86.65 | 0.008 |

**Table 5.14 Double glazing air heater (D=5cm, I=750 W/m$^2$, Ti=30$^0$C)**

| m'(kg/s.m) | $T_f$(K) | $T_p$(K) | $\Delta T_g$(K) | $\Delta T_{pf}$(K) | $\eta$ (%) | $\Delta$T/I |
|---|---|---|---|---|---|---|
| 0.01 | 348.53 | 465.42 | 52.91 | 116.89 | 30.52 | 0.060 |
| 0.02 | 335.48 | 437.24 | 46.95 | 101.76 | 43.55 | 0.043 |
| 0.03 | 328.70 | 419.33 | 43.06 | 90.63 | 51.70 | 0.034 |
| 0.04 | 324.43 | 406.61 | 40.26 | 82.18 | 57.47 | 0.028 |
| 0.05 | 321.44 | 396.95 | 38.10 | 75.51 | 61.84 | 0.024 |

| | | | | | | |
|---|---|---|---|---|---|---|
| 0.06 | 319.23 | 389.31 | 36.37 | 70.08 | 65.31 | 0.021 |
| 0.07 | 317.52 | 383.06 | 34.94 | 65.54 | 68.14 | 0.019 |
| 0.08 | 316.14 | 377.84 | 33.73 | 61.69 | 70.52 | 0.017 |
| 0.09 | 315.02 | 373.39 | 32.70 | 58.36 | 72.54 | 0.016 |
| 0.10 | 314.08 | 369.53 | 31.79 | 55.45 | 74.31 | 0.014 |
| 0.11 | 313.28 | 366.16 | 31.03 | 52.88 | 75.85 | 0.013 |
| 0.12 | 312.59 | 363.18 | 30.29 | 50.58 | 77.22 | 0.012 |
| 0.13 | 312.08 | 360.51 | 29.65 | 48.51 | 78.45 | 0.012 |
| 0.14 | 311.47 | 358.12 | 29.08 | 46.64 | 79.56 | 0.011 |
| 0.15 | 311.01 | 355.95 | 28.56 | 44.94 | 80.55 | 0.010 |
| 0.16 | 310.59 | 353.98 | 28.08 | 43.38 | 81.47 | 0.010 |
| 0.17 | 310.22 | 352.17 | 27.64 | 41.95 | 82.31 | 0.009 |
| 0.18 | 309.88 | 350.51 | 27.23 | 40.62 | 83.07 | 0.009 |
| 0.19 | 309.57 | 348.97 | 26.86 | 39.40 | 83.79 | 0.008 |
| 0.20 | 309.29 | 347.55 | 26.51 | 38.25 | 84.46 | 0.008 |

**Table 5.15 Counter flow air heater (D=5cm, I=750 W/m$^2$, Ti=30$^0$C)**

| m'(kg/s.m) | $T_f$(K) | $T_p$(K) | $\Delta T_g$(K) | $\Delta T_{pf}$(K) | $\eta$ (%) | $\Delta T/I$ |
|---|---|---|---|---|---|---|
| 0.01 | 356.12 | 429.16 | 19.06 | 73.04 | 35.61 | 0.070 |
| 0.02 | 339.52 | 402.18 | 18.42 | 62.66 | 48.97 | 0.048 |
| 0.03 | 331.23 | 386.26 | 18.04 | 55.03 | 56.78 | 0.037 |
| 0.04 | 326.15 | 375.47 | 17.76 | 49.31 | 62.10 | 0.030 |
| 0.05 | 322.69 | 367.56 | 17.54 | 44.86 | 66.02 | 0.026 |
| 0.06 | 320.17 | 361.45 | 17.36 | 41.28 | 69.05 | 0.022 |
| 0.07 | 318.24 | 356.56 | 17.21 | 38.32 | 71.53 | 0.020 |
| 0.08 | 316.71 | 352.55 | 17.09 | 35.83 | 73.56 | 0.018 |
| 0.09 | 315.47 | 349.17 | 16.98 | 33.70 | 75.28 | 0.016 |
| 0.10 | 314.45 | 346.29 | 16.88 | 31.84 | 76.76 | 0.015 |
| 0.11 | 313.58 | 343.80 | 16.80 | 30.22 | 78.05 | 0.014 |
| 0.12 | 312.84 | 341.62 | 16.72 | 28.77 | 79.19 | 0.013 |
| 0.13 | 312.20 | 339.69 | 16.66 | 27.49 | 80.19 | 0.012 |

| | | | | | | |
|---|---|---|---|---|---|---|
| 0.14 | 311.64 | 337.97 | 16.59 | 26.32 | 81.10 | 0.011 |
| 0.15 | 311.14 | 336.42 | 16.54 | 25.27 | 81.92 | 0.010 |
| 0.16 | 310.70 | 335.02 | 16.49 | 24.32 | 82.66 | 0.010 |
| 0.17 | 310.31 | 333.75 | 16.44 | 23.44 | 83.34 | 0.009 |
| 0.18 | 309.95 | 332.59 | 16.39 | 22.63 | 83.97 | 0.009 |
| 0.19 | 309.63 | 331.53 | 16.35 | 21.89 | 84.54 | 0.008 |
| 0.20 | 309.34 | 330.55 | 16.32 | 21.20 | 85.06 | 0.008 |

**Table 5.16 Counter flow air heater with porous matrix**

**(D=5cm, I=750 W/m$^2$, Ti=30$^0$C)**

| m'(kg/s.m) | $\Delta$T | $\Delta$ $T_g$(K) | $\Delta$T/I | $\eta$ (%) |
|---|---|---|---|---|
| 0.01 | 105.73 | 19.35 | 0.140 | 70.89 |
| 0.02 | 56.99 | 18.83 | 0.075 | 76.42 |
| 0.03 | 39.28 | 18.47 | 0.052 | 79.00 |
| 0.04 | 30.06 | 18.18 | 0.040 | 80.64 |
| 0.05 | 24.40 | 17.96 | 0.032 | 81.81 |
| 0.06 | 20.56 | 17.77 | 0.027 | 82.72 |
| 0.07 | 17.78 | 17.61 | 0.023 | 83.46 |
| 0.08 | 15.67 | 17.47 | 0.020 | 84.07 |
| 0.09 | 14.02 | 17.35 | 0.018 | 84.60 |
| 0.10 | 12.68 | 17.25 | 0.016 | 85.06 |
| 0.11 | 11.58 | 17.15 | 0.015 | 85.46 |
| 0.12 | 10.66 | 17.07 | 0.014 | 85.82 |
| 0.13 | 9.88 | 16.99 | 0.013 | 86.14 |
| 0.14 | 9.21 | 16.92 | 0.012 | 86.44 |
| 0.15 | 8.62 | 16.85 | 0.011 | 86.72 |
| 0.16 | 8.10 | 16.79 | 0.010 | 86.96 |
| 0.17 | 7.6 | 16.74 | 0.010 | 87.19 |
| 0.18 | 7.24 | 16.69 | 0.009 | 87.41 |
| 0.19 | 6.87 | 16.64 | 0.009 | 87.60 |
| 0.20 | 6.54 | 16.59 | 0.008 | 87.80 |

**Table 5.17 Single glazing air heater (D=5cm, I=900 W/m$^2$, Ti=15$^0$C)**

| m'(kg/s.m) | $T_f$(K) | $T_p$(K) | $\Delta T_g$(K) | $\Delta T_{pf}$(K) | $\eta$ (%) | $\Delta$T/I |
|---|---|---|---|---|---|---|
| 0.01 | 341.91 | 425.79 | 49.62 | 83.87 | 30.12 | 0.059 |
| 0.02 | 327.81 | 402.01 | 40.68 | 74.28 | 44.49 | 0.048 |
| 0.03 | 319.95 | 386.12 | 34.59 | 66.17 | 53.56 | 0.035 |
| 0.04 | 314.81 | 374.60 | 30.15 | 59.79 | 59.91 | 0.029 |
| 0.05 | 311.14 | 365.80 | 26.76 | 54.65 | 64.65 | 0.025 |
| 0.06 | 308.38 | 358.81 | 24.07 | 50.42 | 68.33 | 0.022 |
| 0.07 | 306.22 | 353.11 | 21.88 | 46.88 | 71.29 | 0.020 |
| 0.08 | 304.49 | 348.36 | 20.07 | 43.87 | 73.71 | 0.018 |
| 0.09 | 303.06 | 344.33 | 18.54 | 41.27 | 75.75 | 0.016 |
| 0.10 | 301.86 | 340.87 | 17.23 | 39.00 | 77.47 | 0.015 |
| 0.11 | 300.84 | 337.85 | 16.09 | 37.01 | 78.95 | 0.014 |
| 0.12 | 299.96 | 335.20 | 15.10 | 35.23 | 80.24 | 0.013 |
| 0.13 | 299.20 | 332.85 | 14.22 | 33.64 | 81.38 | 0.012 |
| 0.14 | 298.53 | 330.74 | 13.44 | 32.21 | 82.37 | 0.011 |
| 0.15 | 297.93 | 328.85 | 12.75 | 30.91 | 83.28 | 0.011 |
| 0.16 | 297.40 | 327.14 | 12.12 | 29.73 | 84.09 | 0.010 |
| 0.17 | 296.93 | 325.57 | 11.55 | 28.64 | 84.82 | 0.009 |
| 0.18 | 296.50 | 324.15 | 11.03 | 27.65 | 85.48 | 0.009 |
| 0.19 | 296.11 | 322.84 | 10.56 | 26.73 | 86.09 | 0.009 |
| 0.20 | 295.754 | 321.63 | 10.13 | 25.87 | 86.64 | 0.008 |

**Table 5.18 Double glazing air heater (D=5cm, I=900 W/m$^2$, Ti=15$^0$C)**

| m'(kg/s.m) | $T_f$(K) | $T_p$(K) | $\Delta T_g$(K) | $\Delta T_{pf}$(K) | $\eta$ (%) | $\Delta$T/I |
|---|---|---|---|---|---|---|
| 0.01 | 342.64 | 482.91 | 45.49 | 140.22 | 30.53 | 0.060 |
| 0.02 | 326.98 | 449.09 | 38.34 | 122.11 | 43.55 | 0.043 |
| 0.03 | 318.85 | 427.60 | 33.68 | 108.75 | 51.70 | 0.034 |
| 0.04 | 313.71 | 412.33 | 30.31 | 98.61 | 57.47 | 0.028 |
| 0.05 | 310.13 | 400.75 | 27.72 | 90.61 | 61.84 | 0.024 |

| | | | | | | |
|---|---|---|---|---|---|---|
| 0.06 | 307.48 | 391.57 | 25.64 | 84.09 | 65.31 | 0.021 |
| 0.07 | 305.42 | 384.08 | 23.93 | 78.65 | 68.14 | 0.019 |
| 0.08 | 303.77 | 377.81 | 22.48 | 74.03 | 70.51 | 0.017 |
| 0.09 | 302.42 | 372.46 | 21.24 | 70.04 | 72.5 | 0.016 |
| 0.10 | 301.37 | 367.84 | 20.15 | 66.54 | 74.31 | 0.014 |
| 0.11 | 300.34 | 363.79 | 19.20 | 63.45 | 75.85 | 0.013 |
| 0.12 | 299.51 | 360.21 | 18.35 | 60.78 | 77.22 | 0.012 |
| 0.13 | 298.80 | 357.02 | 17.59 | 58.22 | 78.45 | 0.012 |
| 0.14 | 298.17 | 354.14 | 16.90 | 55.97 | 79.55 | 0.011 |
| 0.15 | 297.61 | 351.54 | 16.27 | 53.93 | 80.55 | 0.010 |
| 0.16 | 297.11 | 349.17 | 15.78 | 52.06 | 81.47 | 0.010 |
| 0.17 | 296.66 | 347.00 | 15.17 | 50.34 | 82.31 | 0.009 |
| 0.18 | 296.26 | 345.01 | 14.68 | 48.75 | 83.08 | 0.009 |
| 0.19 | 295.89 | 343.17 | 14.23 | 47.28 | 83.80 | 0.008 |
| 0.20 | 295.55 | 341.47 | 13.81 | 45.91 | 84.45 | 0.008 |

**Table 5.19 Counter flow air heater (D=5cm, I=900 W/m$^2$, Ti=15$^0$C)**

| m'(kg/s.m) | $T_f$(K) | $T_p$(K) | $\Delta T_g$(K) | $\Delta T_{pf}$(K) | $\eta$ (%) | $\Delta$T/I |
|---|---|---|---|---|---|---|
| 0.01 | 351.74 | 439.40 | 4.80 | 87.65 | 35.61 | 0.070 |
| 0.02 | 331.82 | 407.02 | 4.11 | 75.20 | 48.97 | 0.048 |
| 0.03 | 321.88 | 387.91 | 3.65 | 66.03 | 56.78 | 0.037 |
| 0.04 | 315.78 | 374.96 | 3.31 | 59.18 | 62.10 | 0.030 |
| 0.05 | 311.63 | 365.47 | 3.05 | 53.83 | 66.08 | 0.026 |
| 0.06 | 308.60 | 358.14 | 2.83 | 49.54 | 69.07 | 0.022 |
| 0.07 | 306.29 | 352.28 | 2.66 | 45.99 | 71.53 | 0.020 |
| 0.08 | 304.45 | 347.46 | 2.51 | 43.00 | 73.56 | 0.018 |
| 0.09 | 302.97 | 343.41 | 2.38 | 40.44 | 75.2 | 0.016 |
| 0.10 | 301.74 | 339.95 | 2.26 | 38.21 | 76.76 | 0.015 |
| 0.11 | 300.76 | 336.96 | 2.16 | 36.26 | 78.05 | 0.014 |
| 0.12 | 299.81 | 334.34 | 2.07 | 34.53 | 79.18 | 0.013 |
| 0.13 | 299.04 | 332.02 | 1.99 | 32.987 | 80.20 | 0.012 |

| | | | | | | |
|---|---|---|---|---|---|---|
| 0.14 | 298.36 | 329.96 | 1.91 | 31.59 | 81.10 | 0.011 |
| 0.15 | 297.77 | 328.10 | 1.85 | 30.33 | 81.92 | 0.010 |
| 0.16 | 297.24 | 326.43 | 1.78 | 29.18 | 82.66 | 0.010 |
| 0.17 | 296.77 | 324.90 | 1.73 | 28.13 | 83.34 | 0.009 |
| 0.18 | 296.34 | 323.51 | 1.67 | 27.16 | 83.96 | 0.009 |
| 0.19 | 295.96 | 322.23 | 1.63 | 26.27 | 84.54 | 0.008 |
| 0.20 | 295.61 | 321.06 | 1.58 | 25.44 | 85.07 | 0.008 |

**Table 5.20 Counter flow air heater with porous matrix**

**(D=5cm, I=900 W/m$^2$, Ti=15$^0$C)**

| m'(kg/s.m) | $\Delta$T | $\Delta$ $T_g$(K) | $\Delta$T/I | $\eta$ (%) |
|---|---|---|---|---|
| 0.01 | 126.88 | 5.22 | 0.140 | 70.89 |
| 0.02 | 68.39 | 4.6 | 0.075 | 76.42 |
| 0.03 | 47.13 | 4.16 | 0.052 | 79.00 |
| 0.04 | 36.08 | 3.82 | 0.040 | 80.67 |
| 0.05 | 29.28 | 3.55 | 0.032 | 81.81 |
| 0.06 | 24.67 | 3.33 | 0.027 | 82.72 |
| 0.07 | 21.34 | 3.14 | 0.023 | 83.46 |
| 0.08 | 18.81 | 2.97 | 0.020 | 84.07 |
| 0.09 | 16.82 | 2.83 | 0.018 | 84.60 |
| 0.10 | 15.22 | 2.7 | 0.016 | 85.05 |
| 0.11 | 13.90 | 2.58 | 0.015 | 85.46 |
| 0.12 | 12.80 | 2.48 | 0.014 | 85.82 |
| 0.13 | 11.86 | 2.39 | 0.013 | 86.15 |
| 0.14 | 11.05 | 2.3 | 0.012 | 86.44 |
| 0.15 | 10.34 | 2.22 | 0.011 | 86.71 |
| 0.16 | 9.72 | 2.15 | 0.010 | 86.94 |
| 0.17 | 9.18 | 2.09 | 0.010 | 87.19 |
| 0.18 | 8.69 | 2.02 | 0.009 | 87.41 |
| 0.19 | 8.25 | 1.97 | 0.009 | 87.61 |
| 0.20 | 7.85 | 1.91 | 0.008 | 87.79 |

**Table 5.21 Single glazing air heater (D=10cm, I=900 W/m$^2$, Ti=15$^0$C)**

| m'(kg/s.m) | $T_f$(K) | $T_p$(K) | $\Delta T_g$(K) | $\Delta T_{pf}$(K) | $\eta$ (%) | $\Delta$T/I |
|---|---|---|---|---|---|---|
| 0.01 | 324.99 | 438.18 | 52.38 | 113.19 | 20.66 | 0.041 |
| 0.02 | 316.68 | 420.31 | 45.37 | 103.62 | 32.05 | 0.038 |
| 0.03 | 311.91 | 407.25 | 40.25 | 95.34 | 40.08 | 0.031 |
| 0.04 | 308.67 | 397.08 | 36.26 | 88.41 | 46.19 | 0.027 |
| 0.05 | 306.24 | 388.84 | 33.05 | 82.57 | 51.05 | 0.024 |
| 0.06 | 304.41 | 381.99 | 30.39 | 77.58 | 55.02 | 0.021 |
| 0.07 | 302.92 | 376.18 | 28.15 | 73.26 | 58.36 | 0.019 |
| 0.08 | 301.69 | 371.17 | 26.22 | 69.48 | 61.19 | 0.018 |
| 0.09 | 300.65 | 366.79 | 24.56 | 66.13 | 63.64 | 0.016 |
| 0.10 | 299.77 | 362.92 | 23.09 | 63.15 | 65.78 | 0.015 |
| 0.11 | 299.01 | 359.48 | 21.8 | 60.47 | 67.67 | 0.014 |
| 0.12 | 298.34 | 356.39 | 20.64 | 58.05 | 69.35 | 0.013 |
| 0.13 | 297.75 | 353.60 | 19.60 | 55.85 | 70.86 | 0.013 |
| 0.14 | 297.23 | 351.07 | 18.66 | 53.83 | 72.22 | 0.012 |
| 0.15 | 296.76 | 348.75 | 17.81 | 51.99 | 73.44 | 0.011 |
| 0.16 | 296.34 | 346.62 | 17.04 | 50.28 | 74.56 | 0.011 |
| 0.17 | 295.95 | 344.66 | 16.33 | 48.70 | 75.59 | 0.010 |
| 0.18 | 295.61 | 342.85 | 15.67 | 47.24 | 76.53 | 0.010 |
| 0.19 | 295.29 | 341.17 | 15.07 | 45.87 | 77.40 | 0.009 |
| 0.20 | 294.99 | 339.60 | 14.51 | 44.60 | 78.20 | 0.009 |

**Table 5.22 Double glazing air heater (D=10cm, I=900 W/m$^2$, Ti=15$^0$C)**

| m'(kg/s.m) | $T_f$(K) | $T_p$(K) | $\Delta T_g$(K) | $\Delta T_{pf}$(K) | $\eta$ (%) | $\Delta$T/I |
|---|---|---|---|---|---|---|
| 0.01 | 323.65 | 506.78 | 49.70 | 183.12 | 19.92 | 0.039 |
| 0.02 | 315.09 | 480.47 | 44.09 | 165.38 | 30.27 | 0.036 |
| 0.03 | 310.36 | 461.93 | 40.09 | 151.56 | 37.49 | 0.029 |
| 0.04 | 307.23 | 447.77 | 37.01 | 140.53 | 42.98 | 0.025 |
| 0.05 | 304.95 | 436.44 | 34.53 | 131.48 | 47.36 | 0.022 |

| | | | | | | |
|---|---|---|---|---|---|---|
| 0.06 | 303.20 | 427.08 | 32.47 | 123.87 | 50.98 | 0.020 |
| 0.07 | 301.81 | 419.18 | 30.72 | 117.36 | 54.04 | 0.018 |
| 0.08 | 300.68 | 412.37 | 29.21 | 111.69 | 56.67 | 0.016 |
| 0.09 | 299.72 | 406.43 | 27.88 | 106.71 | 58.97 | 0.015 |
| 0.10 | 298.91 | 401.19 | 26.71 | 102.27 | 61.00 | 0.014 |
| 0.11 | 298.22 | 396.52 | 25.66 | 98.29 | 62.81 | 0.013 |
| 0.12 | 297.61 | 392.31 | 24.71 | 94.70 | 64.44 | 0.012 |
| 0.13 | 297.07 | 388.51 | 23.84 | 91.43 | 65.92 | 0.012 |
| 0.14 | 296.6 | 385.04 | 23.06 | 88.44 | 67.27 | 0.011 |
| 0.15 | 296.17 | 381.87 | 22.33 | 85.69 | 68.50 | 0.010 |
| 0.16 | 295.79 | 378.94 | 21.66 | 83.15 | 69.64 | 0.010 |
| 0.17 | 295.44 | 376.24 | 21.04 | 80.80 | 70.69 | 0.009 |
| 0.18 | 295.12 | 373.73 | 20.47 | 78.61 | 71.67 | 0.009 |
| 0.19 | 294.83 | 371.40 | 19.93 | 76.56 | 72.59 | 0.009 |
| 0.20 | 294.57 | 369.22 | 19.43 | 74.65 | 73.43 | 0.008 |

**Table 5.23 Counter flow air heater (D=5cm, I=900 W/m$^2$, Ti=15$^0$C)**

| m'(kg/s.m) | $T_f$(K) | $T_p$(K) | $\Delta T_g$(K) | $\Delta T_{pf}$(K) | $\eta$ (%) | $\Delta T/I$ |
|---|---|---|---|---|---|---|
| 0.01 | 335.35 | 460.20 | 5.38 | 124.85 | 26.45 | 0.052 |
| 0.02 | 322.43 | 432.68 | 4.87 | 110.24 | 38.48 | 0.045 |
| 0.03 | 315.58 | 414.76 | 4.50 | 99.17 | 46.24 | 0.036 |
| 0.04 | 311.19 | 401.80 | 4.21 | 90.60 | 51.84 | 0.030 |
| 0.05 | 308.09 | 391.84 | 3.97 | 83.74 | 56.14 | 0.026 |
| 0.06 | 305.77 | 383.87 | 3.77 | 78.09 | 59.59 | 0.023 |
| 0.07 | 303.96 | 377.30 | 3.59 | 73.34 | 62.44 | 0.021 |
| 0.08 | 302.50 | 371.77 | 3.44 | 69.26 | 64.85 | 0.019 |
| 0.09 | 301.30 | 367.033 | 3.31 | 65.72 | 66.91 | 0.017 |
| 0.10 | 300.30 | 362.90 | 3.18 | 62.60 | 68.72 | 0.016 |
| 0.11 | 299.44 | 359.28 | 3.07 | 59.83 | 70.32 | 0.015 |
| 0.12 | 298.7 | 356.05 | 2.97 | 57.35 | 71.73 | 0.014 |
| 0.13 | 298.05 | 353.17 | 2.88 | 55.11 | 73.01 | 0.013 |

| | | | | | | |
|---|---|---|---|---|---|---|
| 0.14 | 297.48 | 350.56 | 2.80 | 53.08 | 74.16 | 0.012 |
| 0.15 | 296.97 | 348.20 | 2.72 | 51.22 | 75.21 | 0.011 |
| 0.16 | 296.52 | 346.04 | 2.65 | 49.52 | 76.17 | 0.011 |
| 0.17 | 296.11 | 344.06 | 2.58 | 47.94 | 77.05 | 0.010 |
| 0.18 | 295.74 | 342.23 | 2.52 | 46.49 | 77.88 | 0.010 |
| 0.19 | 295.40 | 340.54 | 2.46 | 45.13 | 78.63 | 0.009 |
| 0.20 | 295.14 | 338.97 | 2.40 | 43.87 | 79.33 | 0.009 |

**Table 5.24 Counter flow air heater with porous matrix**

**(D=10cm, I=900 W/m$^2$, Ti=15$^0$C)**

| m'(kg/s.m) | $\Delta T$ | $\Delta T_g$(K) | $\Delta T/I$ | $\eta$ (%) |
|---|---|---|---|---|
| 0.01 | 140.12 | 5.54 | 0.155 | 78.29 |
| 0.02 | 74.40 | 5.08 | 0.082 | 83.14 |
| 0.03 | 50.88 | 4.73 | 0.056 | 85.28 |
| 0.04 | 38.75 | 4.44 | 0.043 | 86.61 |
| 0.05 | 31.34 | 4.21 | 0.034 | 87.56 |
| 0.06 | 26.33 | 4.01 | 0.029 | 88.29 |
| 0.07 | 22.72 | 3.84 | 0.025 | 88.88 |
| 0.08 | 19.99 | 3.68 | 0.022 | 89.38 |
| 0.09 | 17.86 | 3.55 | 0.019 | 89.80 |
| 0.10 | 16.14 | 3.42 | 0.017 | 90.17 |
| 0.11 | 14.72 | 3.31 | 0.016 | 90.50 |
| 0.12 | 13.54 | 3.21 | 0.015 | 90.79 |
| 0.13 | 12.53 | 3.11 | 0.013 | 91.06 |
| 0.14 | 11.67 | 3.03 | 0.012 | 91.29 |
| 0.15 | 10.92 | 2.95 | 0.012 | 91.52 |
| 0.16 | 10.26 | 2.87 | 0.011 | 91.72 |
| 0.17 | 9.67 | 2.8 | 0.010 | 91.91 |
| 0.18 | 9.15 | 2.73 | 0.010 | 92.09 |
| 0.19 | 8.69 | 2.67 | 0.009 | 92.25 |
| 0.20 | 8.27 | 2.61 | 0.009 | 92.416 |

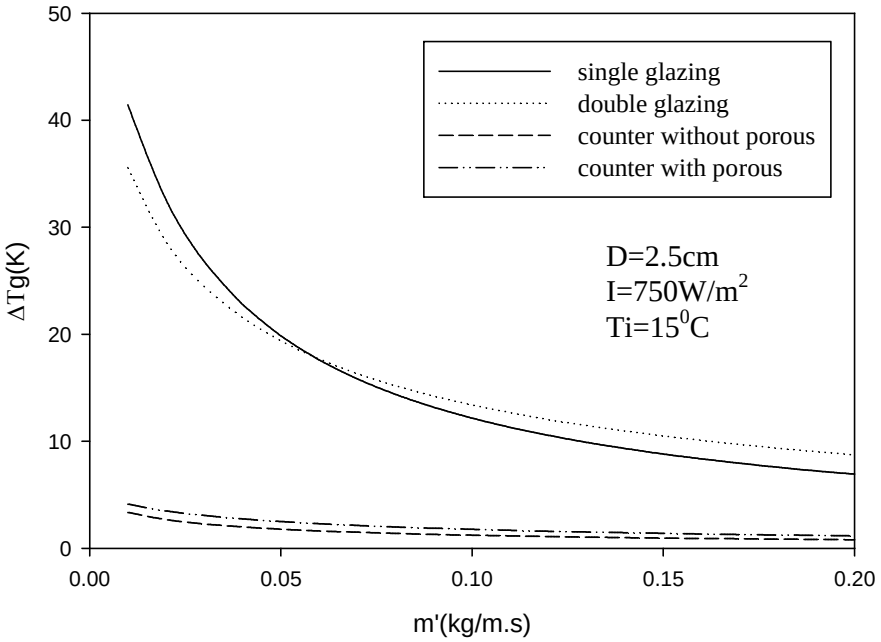


**Fig. 5.1 Variation of max. temp. difference between top cover and anbient air with mass flow rate**

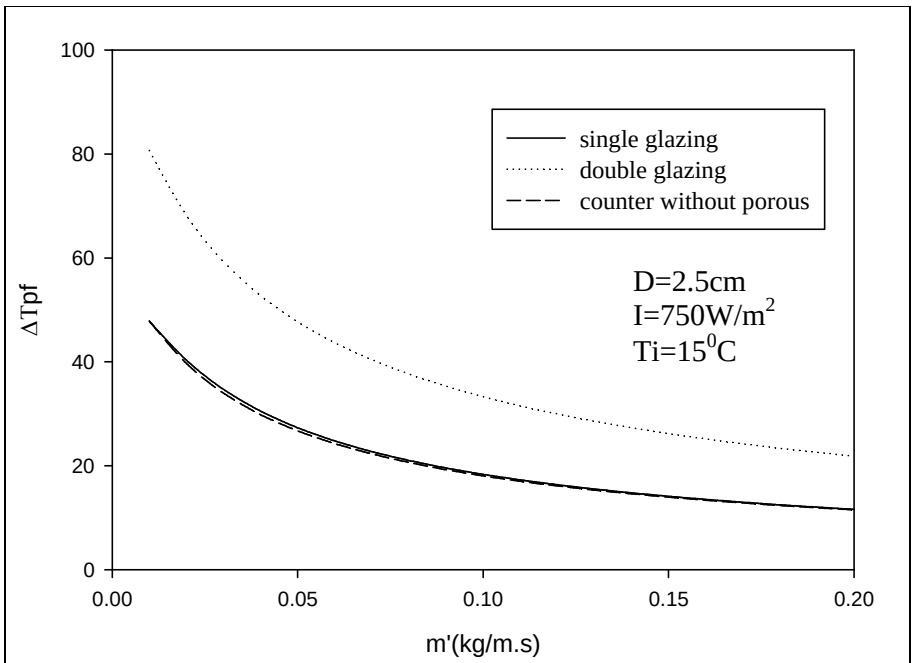


**Fig. 5.2 Variation of max. temp. difference between air stream and absorber plate with mass flow rate**

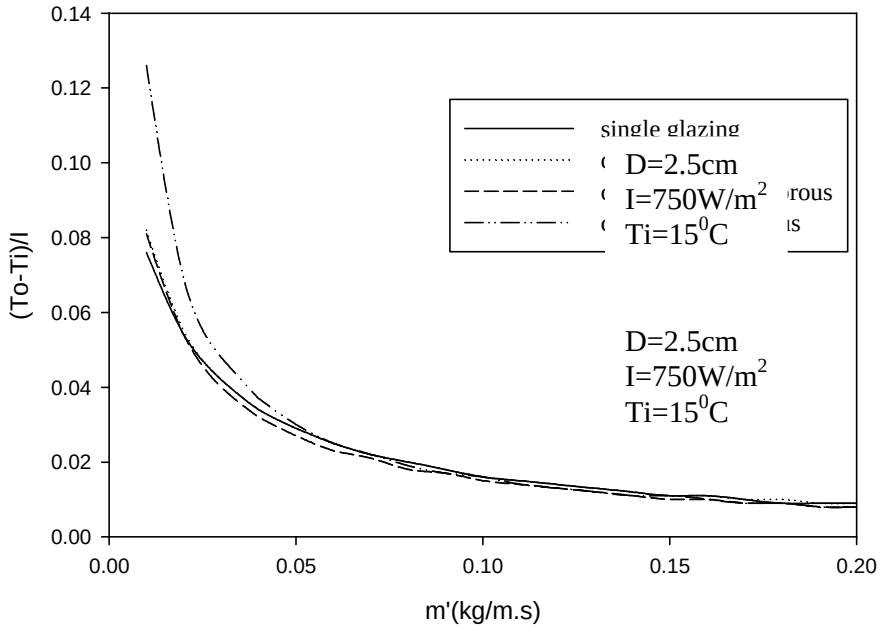


**Fig. 5.4 (T0-Ti)/I Vs mass flow rate**

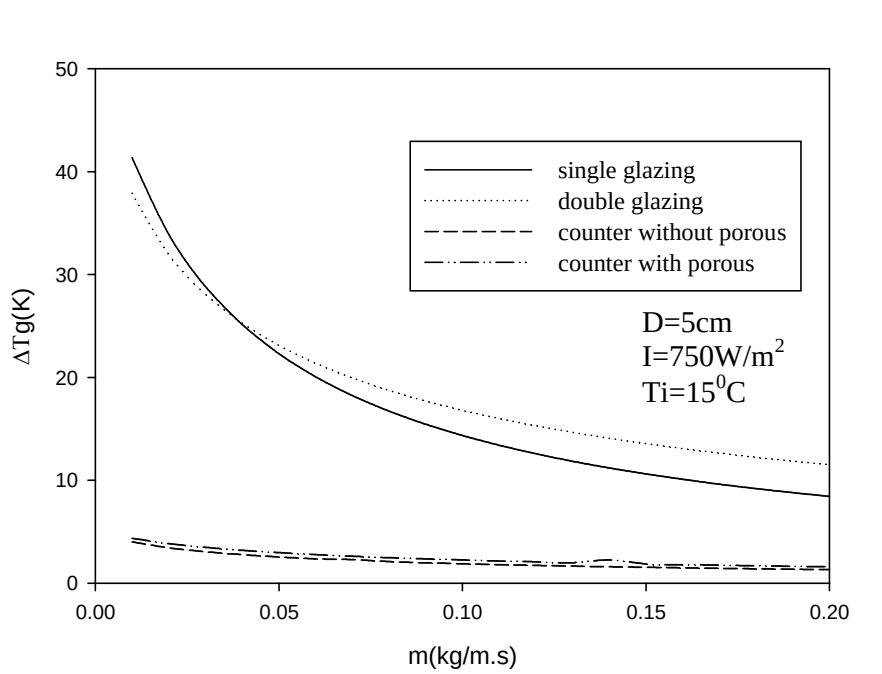


**Fig. 5.5 Variation in max. temp. difference between top cover and ambient air with mass flow rate**

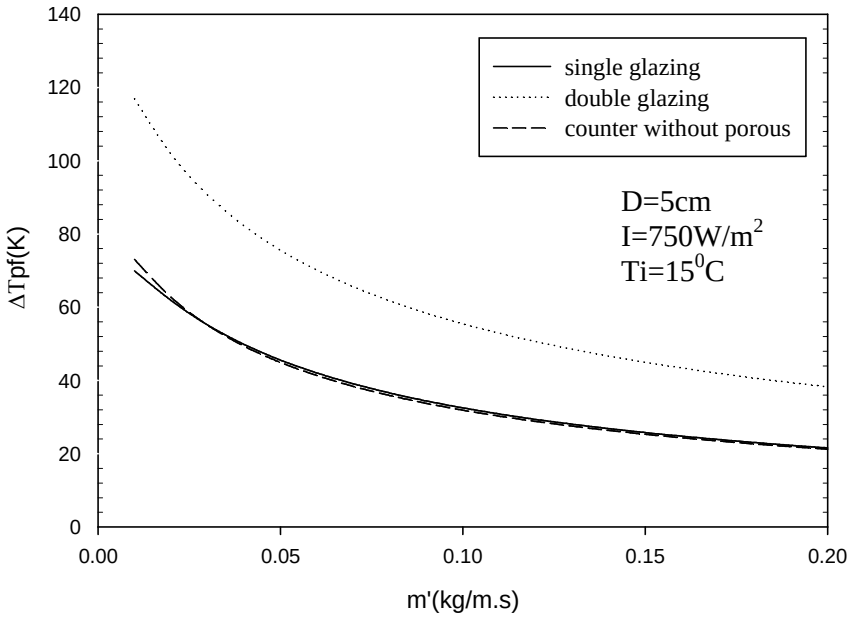


**Fig. 5.6 Variation in max. temp. difference between air stream and the absorber plate with mass flow rate**

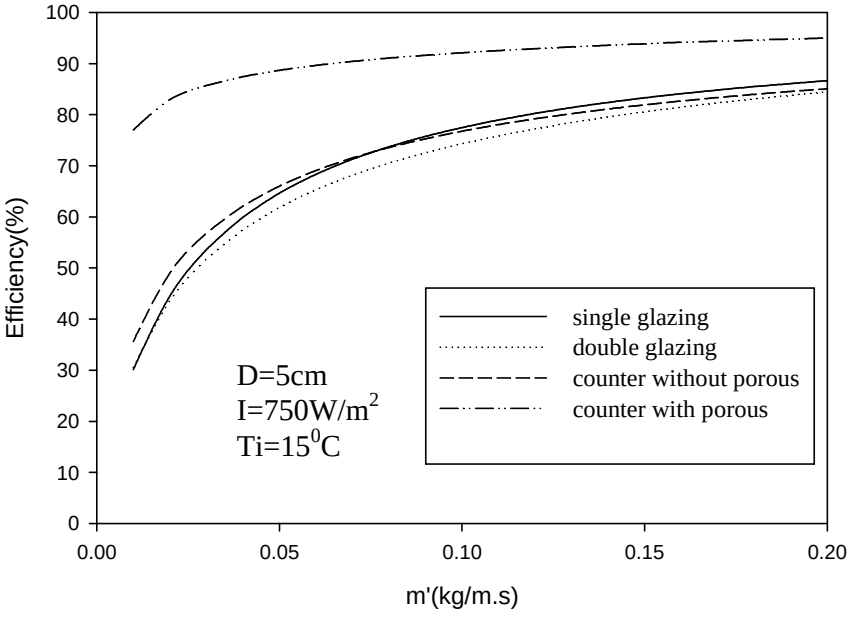


**Fig. 5.7 Variation of thermal efficiency with mass flow rate**

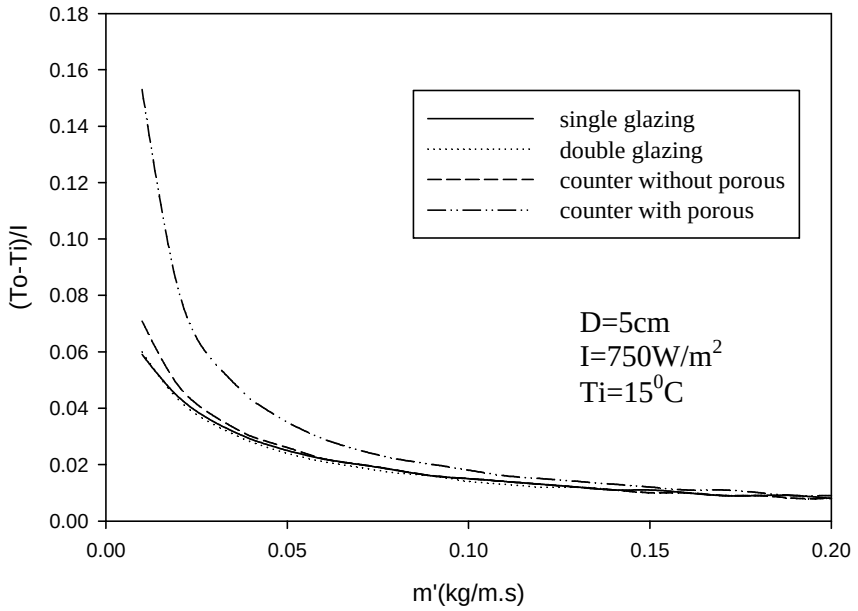


**Fig. 5.8 (To-Ti)/I vs m'**

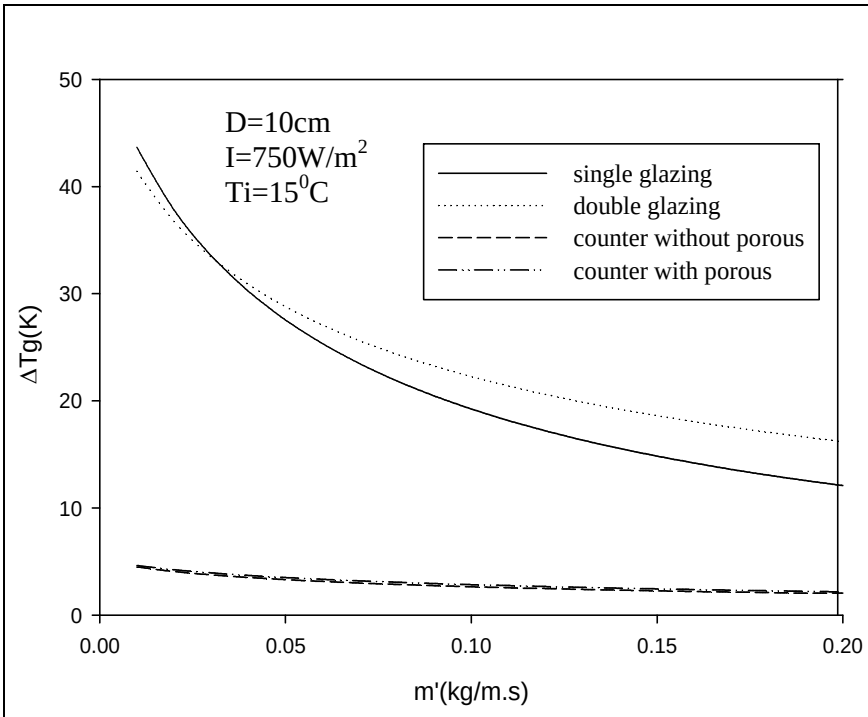


**Fig. 5.9 Variation of max. temp. difference between top cover and ambient air with mass flow rate**

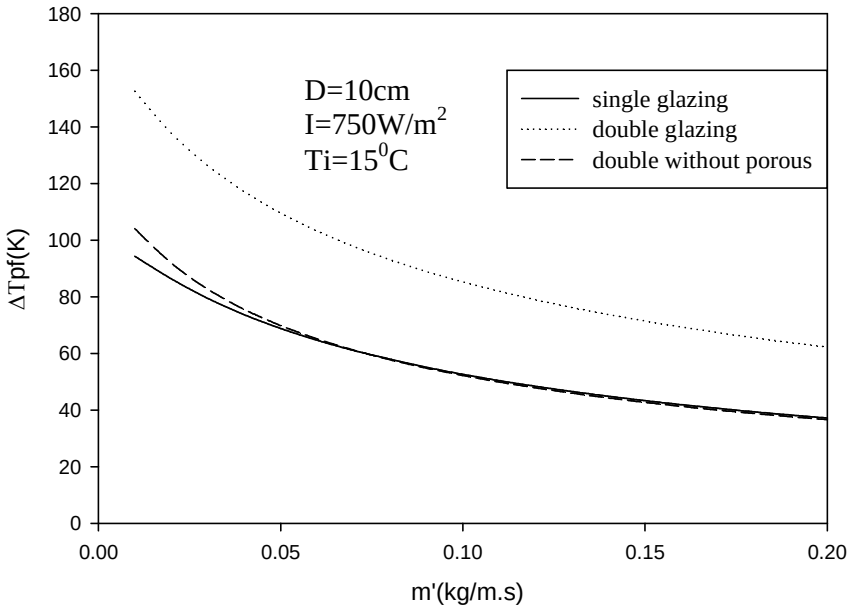


**Fig. 5.10 Variation in max. temp. difference between air stream and the absorber plate with mass flow rate**

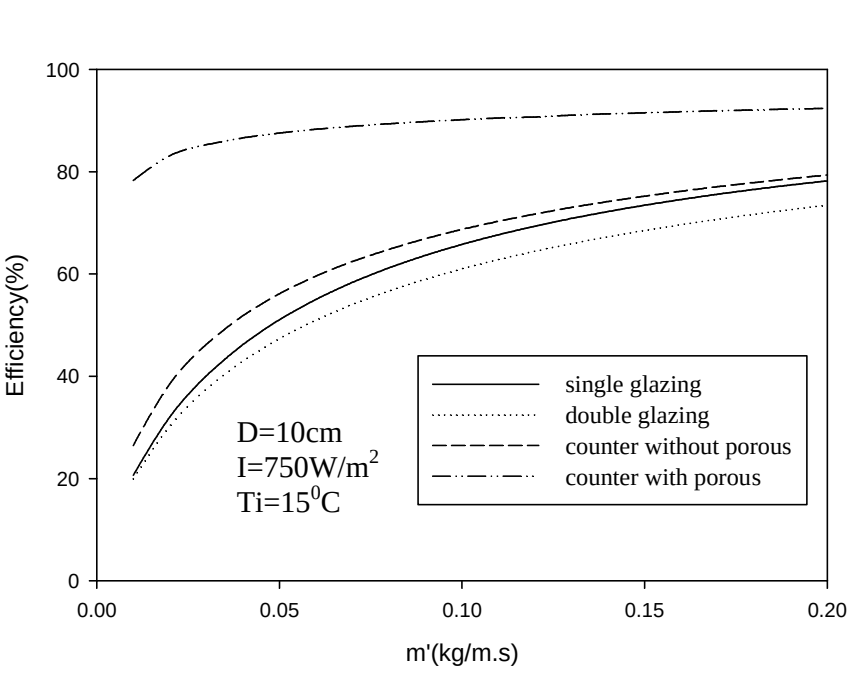


**Fig. 5.11 Variation of thermal efficiency with mass flow rate**

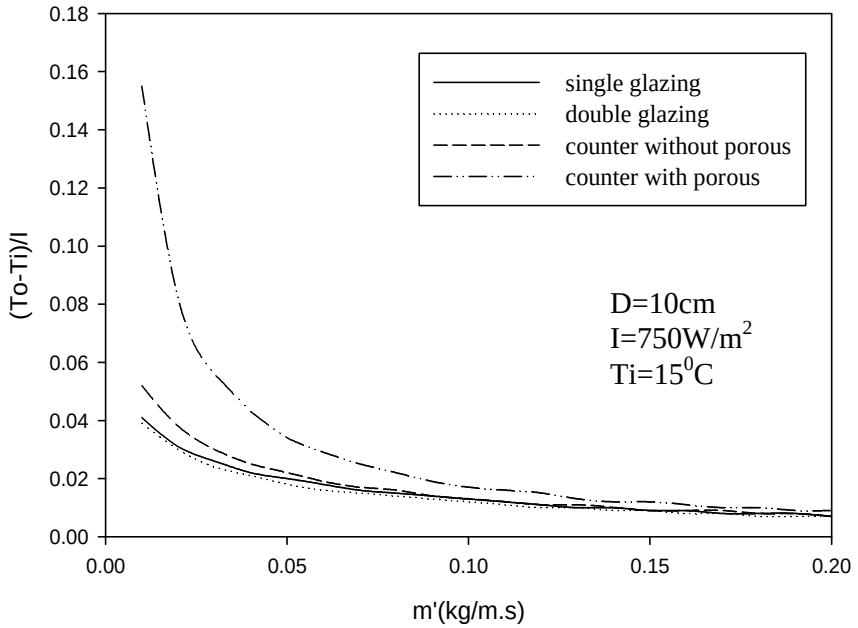


**Fig. 5.12 (To-Ti)/I Vs m'**

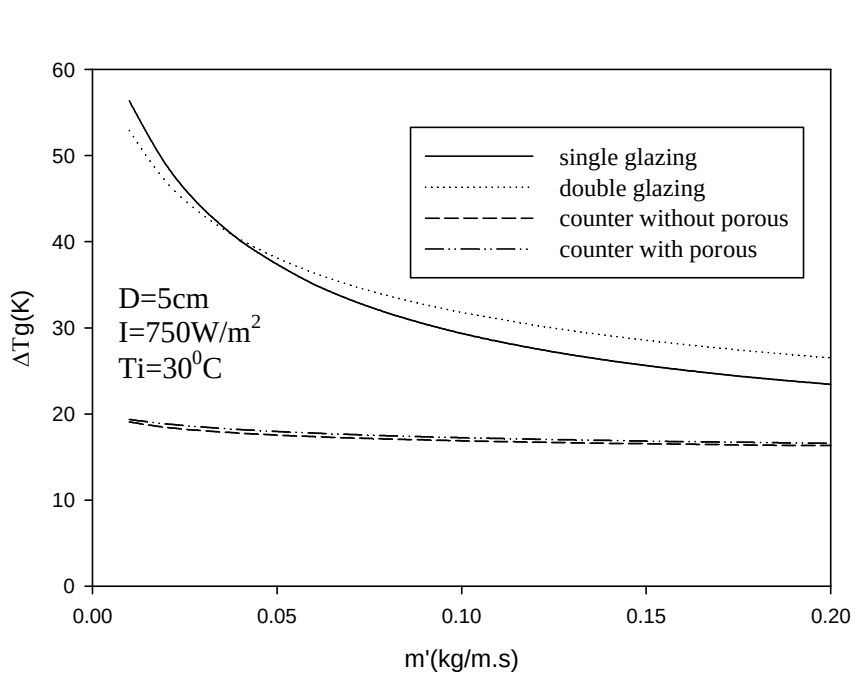


**Fig. 5.13 Variation of max. temp. difference between top cover and anbient air with mass flow rate**

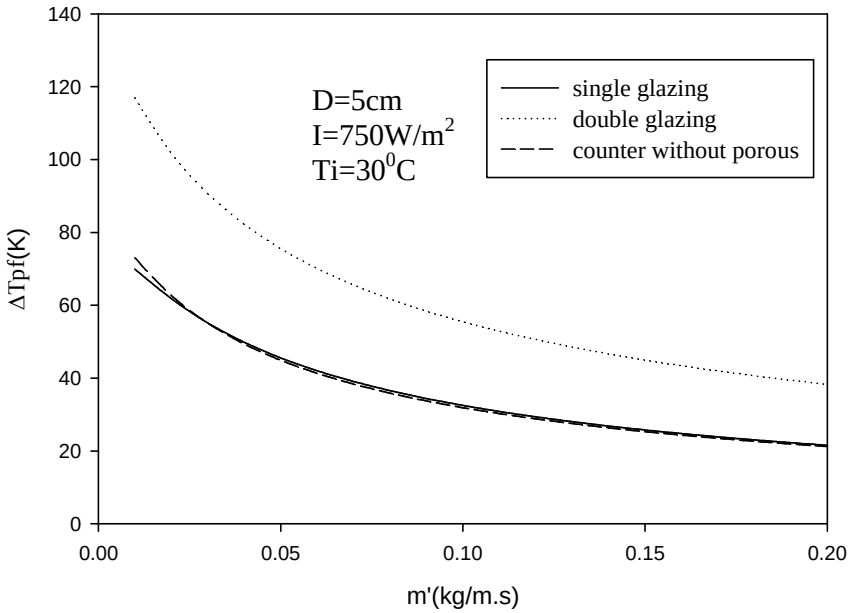


**Fig. 5.14 Variation of max. temp. difference between air stream and absorber plate with mass flow rate**

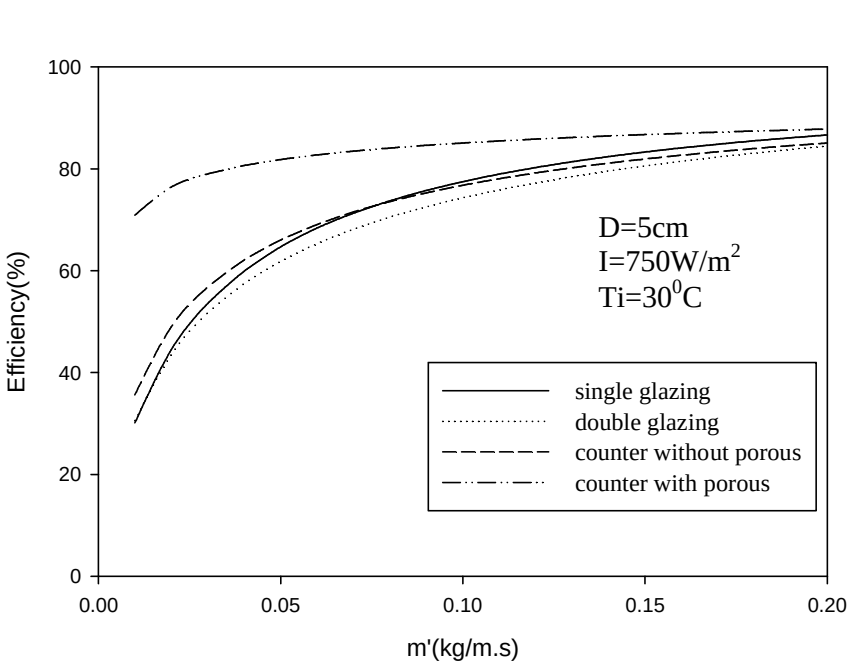


**Fig. 5.15 Variation of thermal efficiency with mass flow rate**

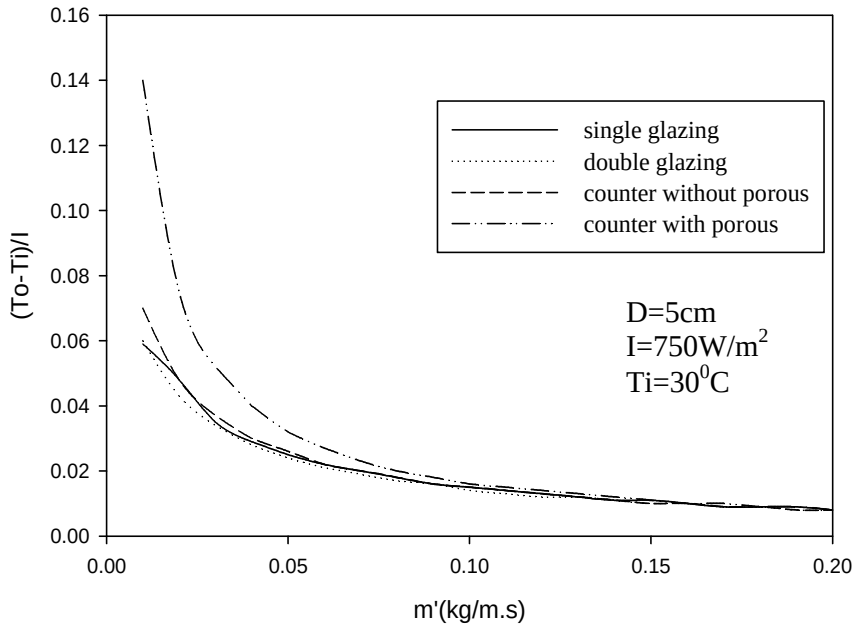


**Fig. 5.16 (To-Ti)/I Vs mass flow rate**

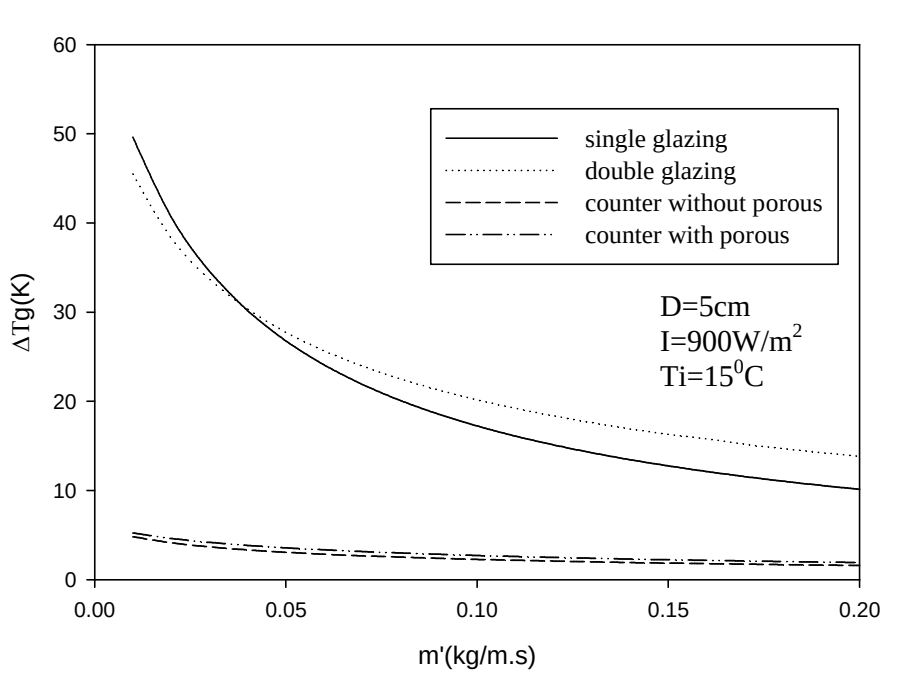


**Fig. 5.17 Variation of max. temp. difference between top cover and anbient air with mass flow rate**

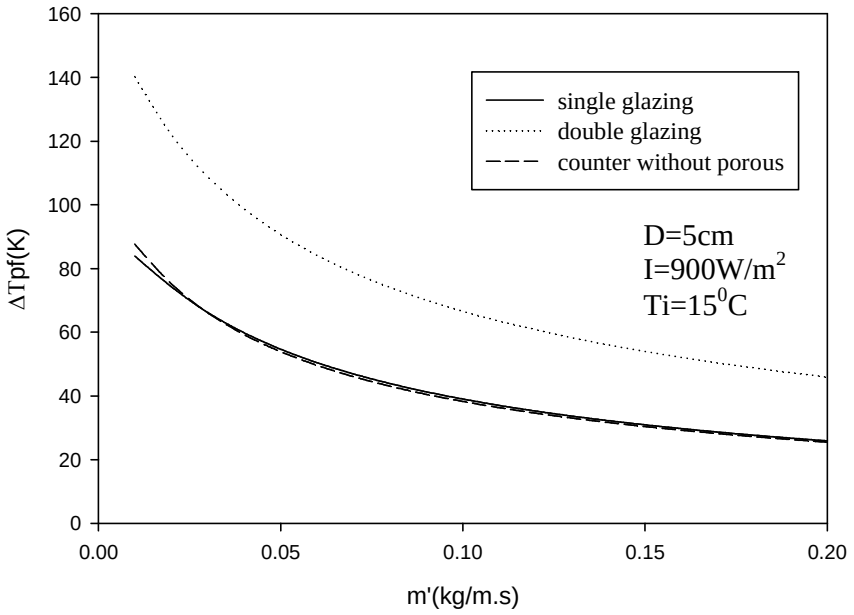


**Fig. 5.18 Variation of max. temp. difference between air stream and absorber plate with mass flow rate**

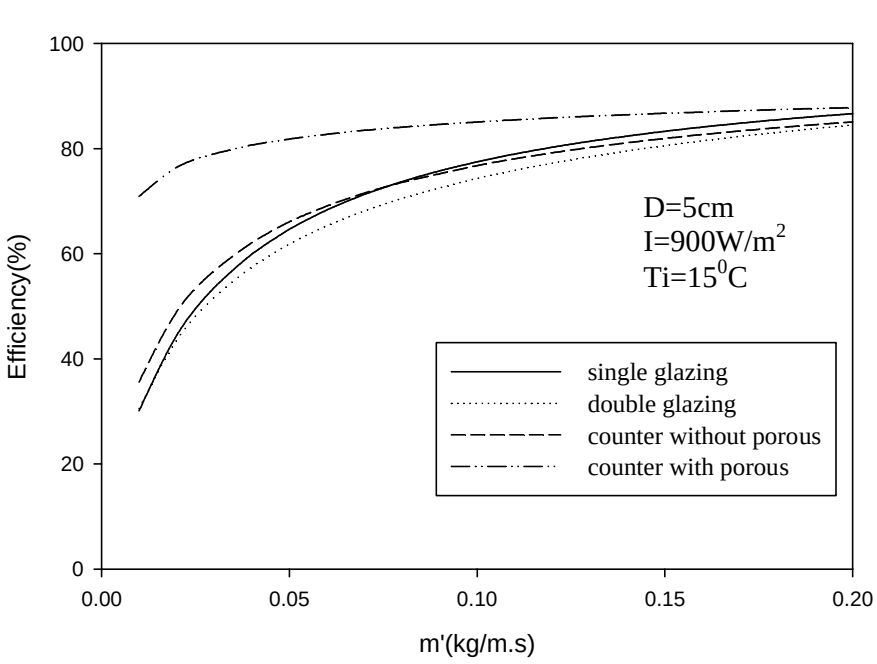


**Fig. 5.19 Variation of thermal efficiency with mass flow rate**

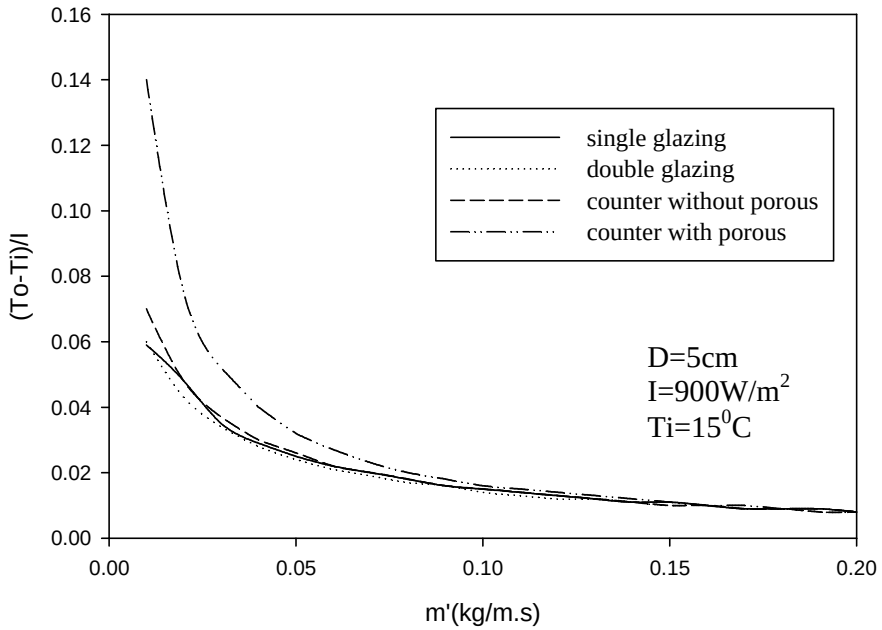


**Fig. 5.20 (T0-Ti)/I Vs mass flow rate**

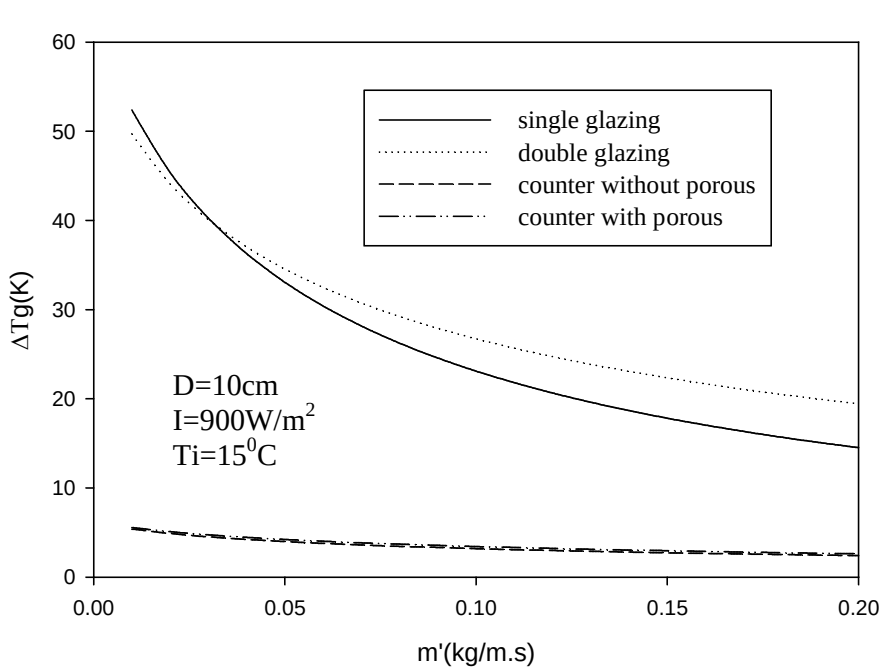


**Fig. 5.21 Variation of max. temp. difference between top cover and anbient air with mass flow rate**

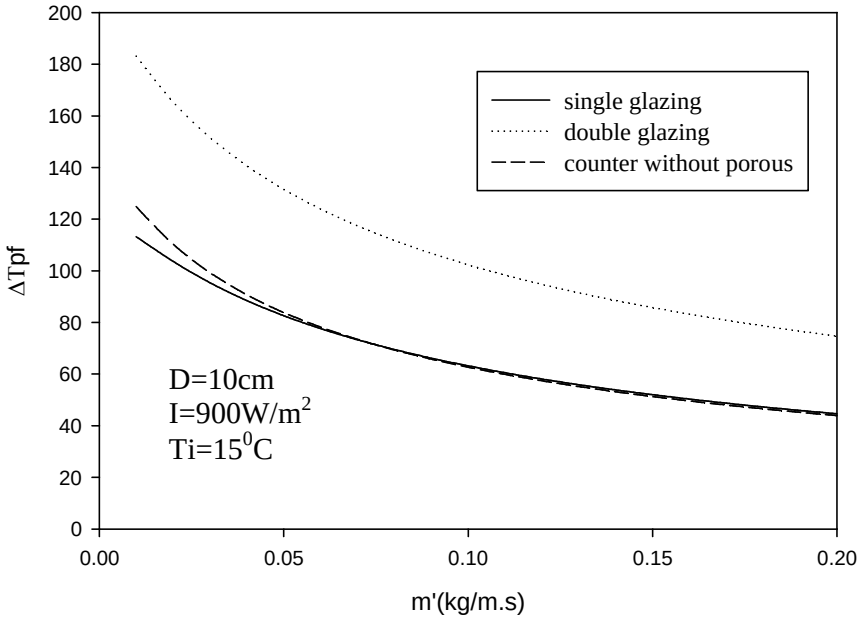


**Fig. 5.22 Variation of max. temp. difference between air stream and absorber plate with mass flow rate**

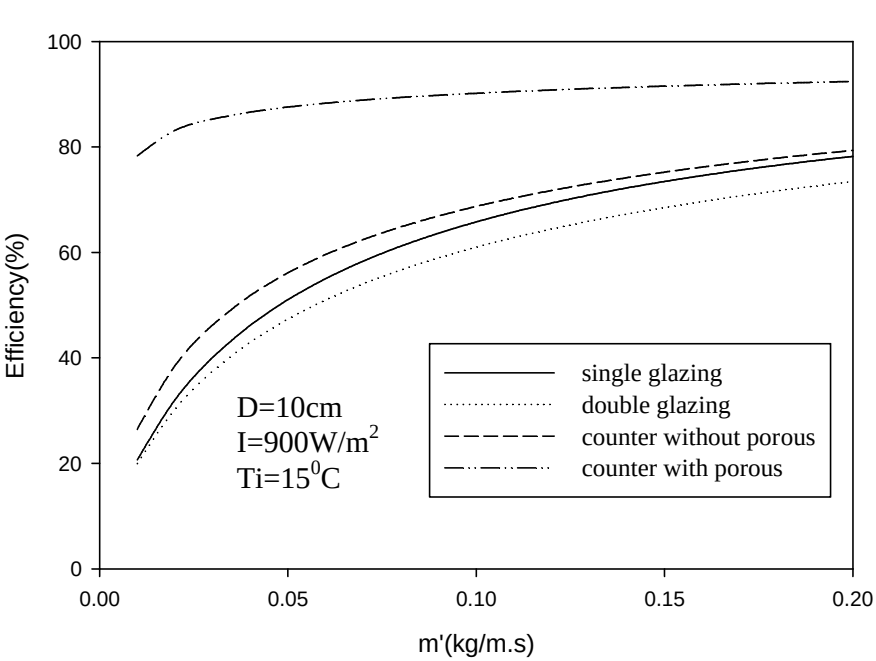


**Fig. 5.23 Variation of thermal efficiency with mass flow rate**

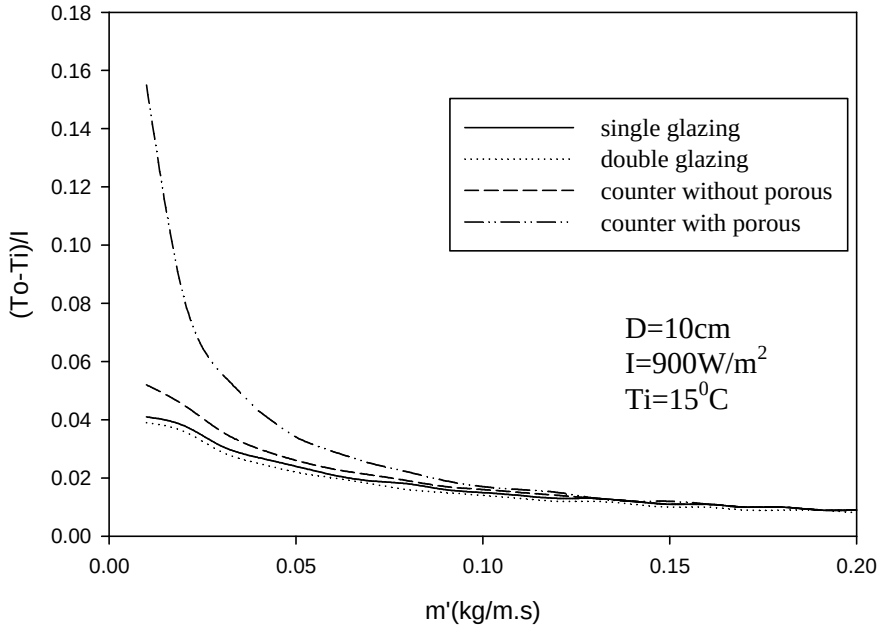


**Fig. 5.24 (T0-Ti)/I Vs mass flow rate**

## 5.5 ANSYS MODELING

ANSYS is standard software and results from ANSYS are widely acceptable. So for present work this software is used for the modeling and analysis of our proposed models of air heaters with different geometries. In the present study problem is converted into 2-D problem along the length of the air heaters. The different elements used are listed below

a) **Link 32:** Link 32 is a uniaxial element with the ability to conduct heat between its nodes. The element has a single degree of freedom, temperature, at each node point. The conducting bar is applicable to a 2-D (plane or axisymmetric), steady-state or transient thermal analysis.

b) **Plane 55:** Plane 55 can be used as a plane element or as an axisymmetric ring element with a 2-D thermal conduction capability. The element has four nodes with a single degree of freedom, temperature, at each node.

c) **Matrix 50:** This superelement is a group of previously assembled elements that is treated as a single element. The superelement, once generated, may be included in any Ansys model and used in any analysis type for which it is applicable.

### 5.5.1 Steps involved in ANSYS modeling

For the three types of solar air heaters the modeling is started by creating the key points along the length and joining them, then the area is being created for the geometry of solar air heaters. Then the meshing is done using above mentioned elements and constraints are applied. Fig. 5.25-Fig. 5.28, Fig. 5.29-Fig. 5.32 and Fig. 5.33- Fig. 5.38 shows the modeling, meshing and constraints for single glazing air heater, double glazing air heater and counter flow solar air heater respectively.

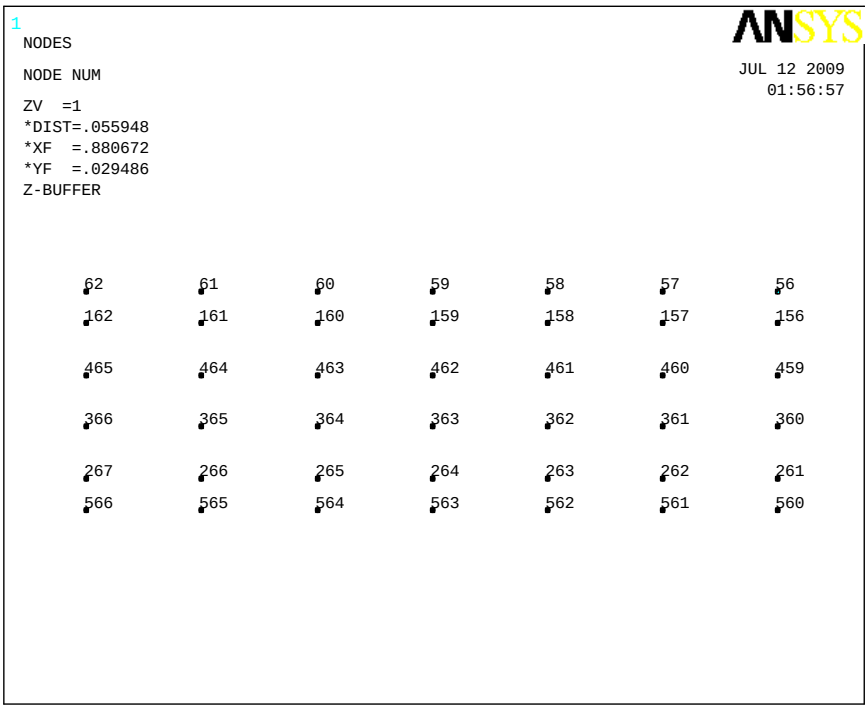


**Fig. 5.26 Key points for single glazing air heater**

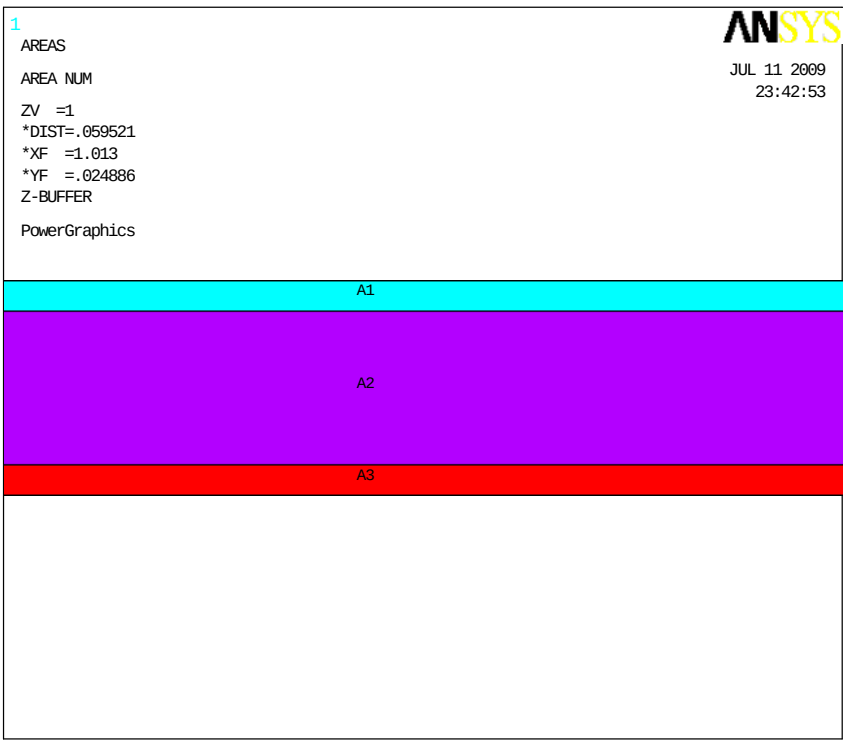


**Fig. 5.27 Areas of single glazing air heater**

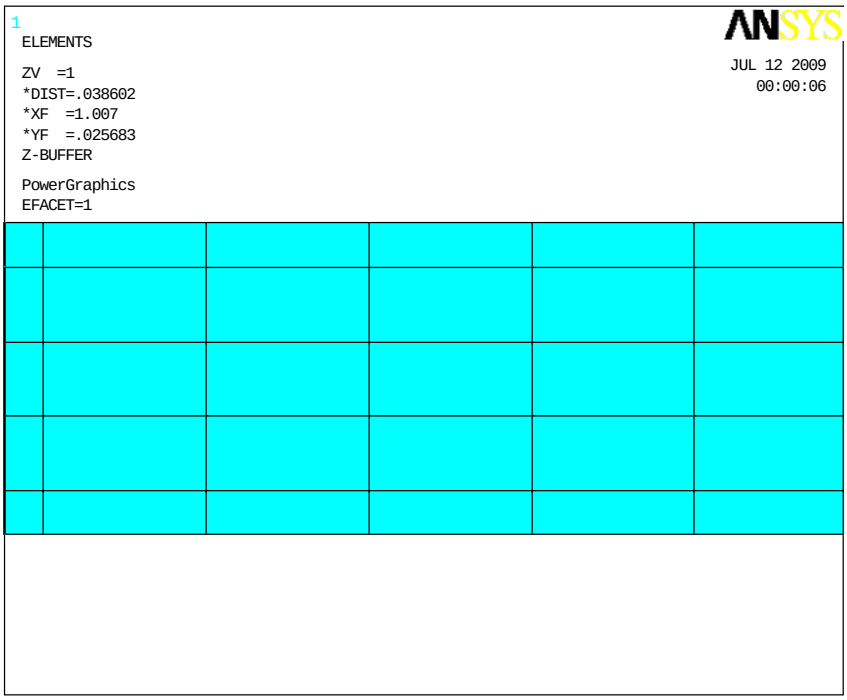


**Fig. 5.28 Meshing of single glazing air heater**

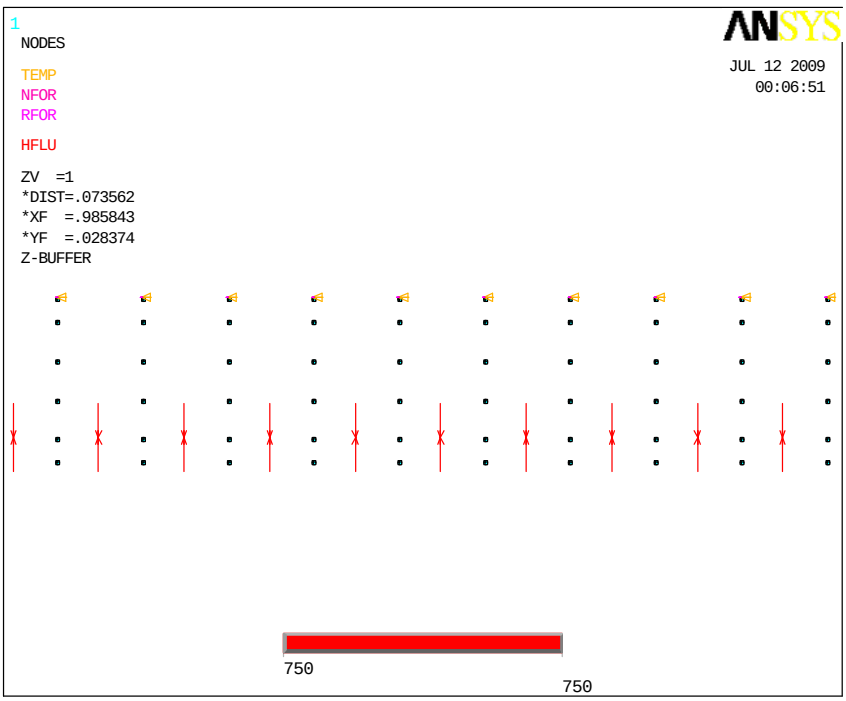


**Fig. 5.29 Constraints for single glazing air heater**

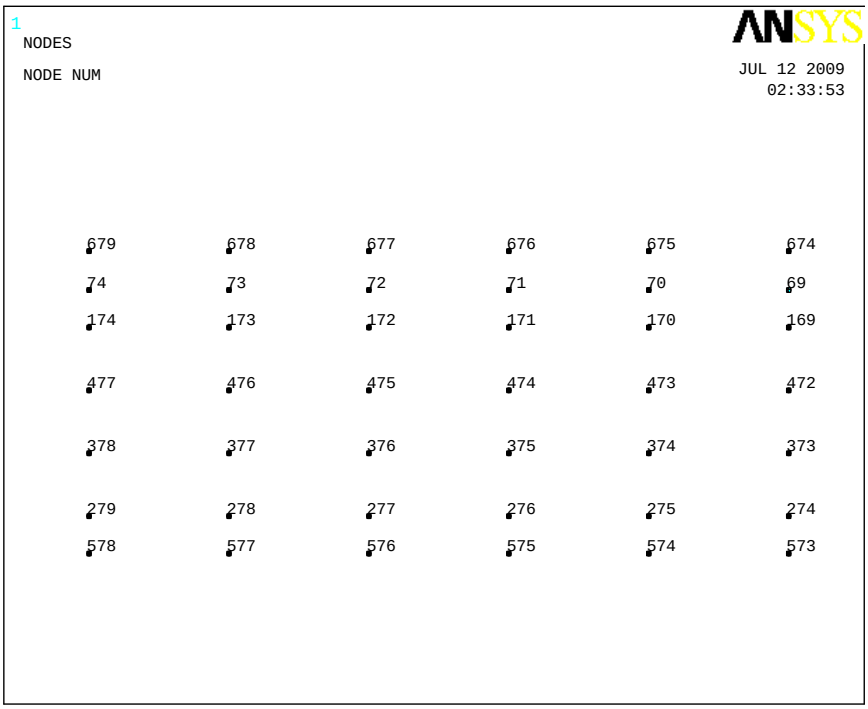


**Fig. 5.30 Key points for double glazing air heater**

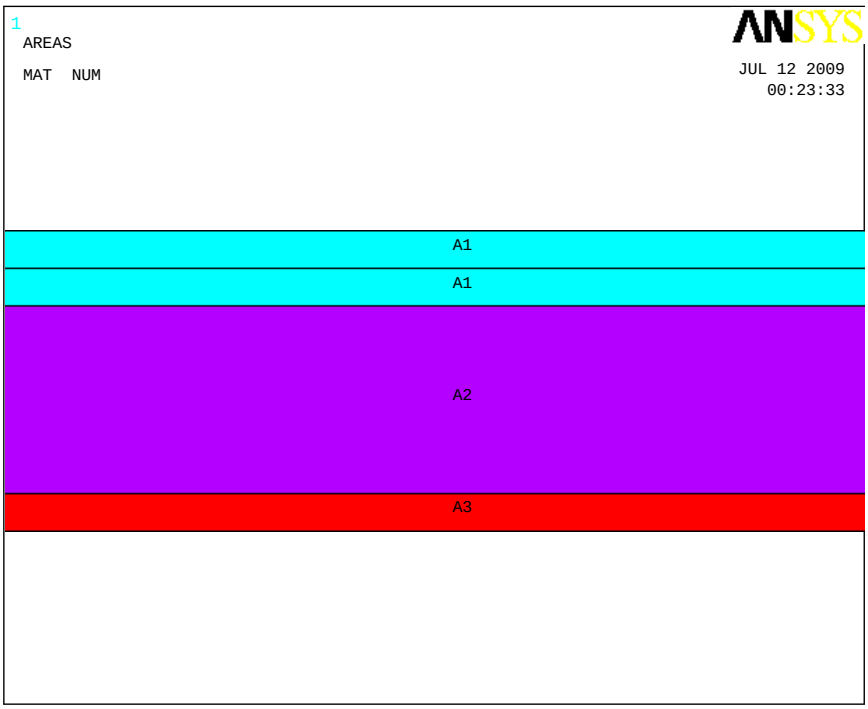


**Fig. 5.31 Areas of double glazing air heater**

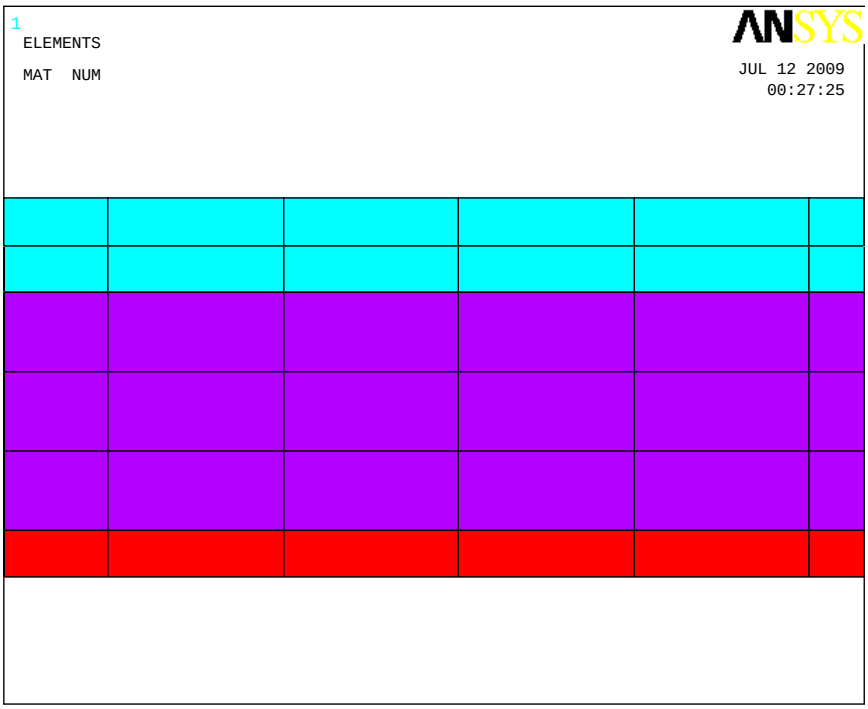


**Fig. 5.32 Meshing of double glazing air heater**

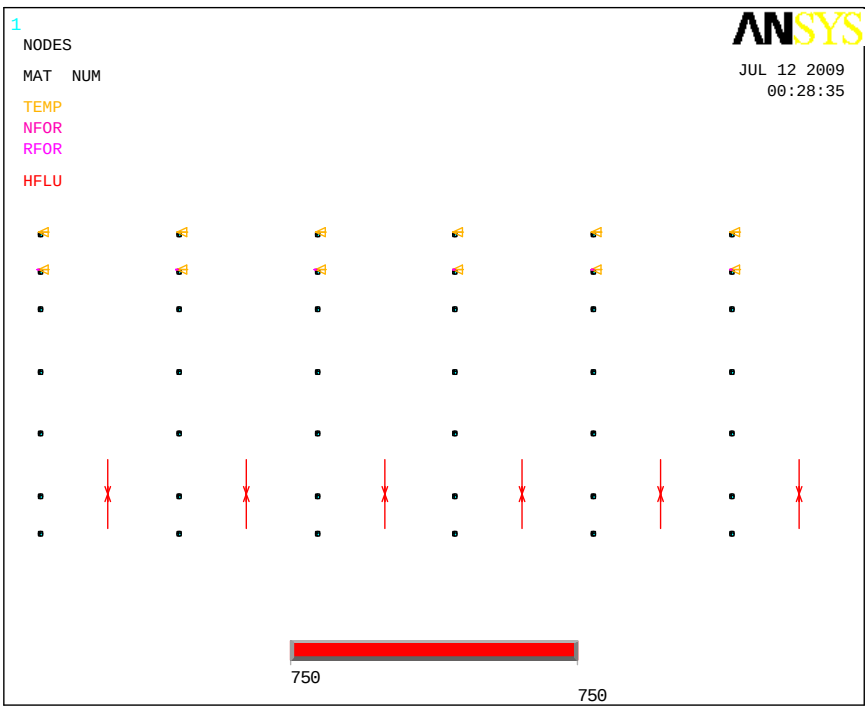


**Fig. 5.33 Constraints for double glazing air heater**

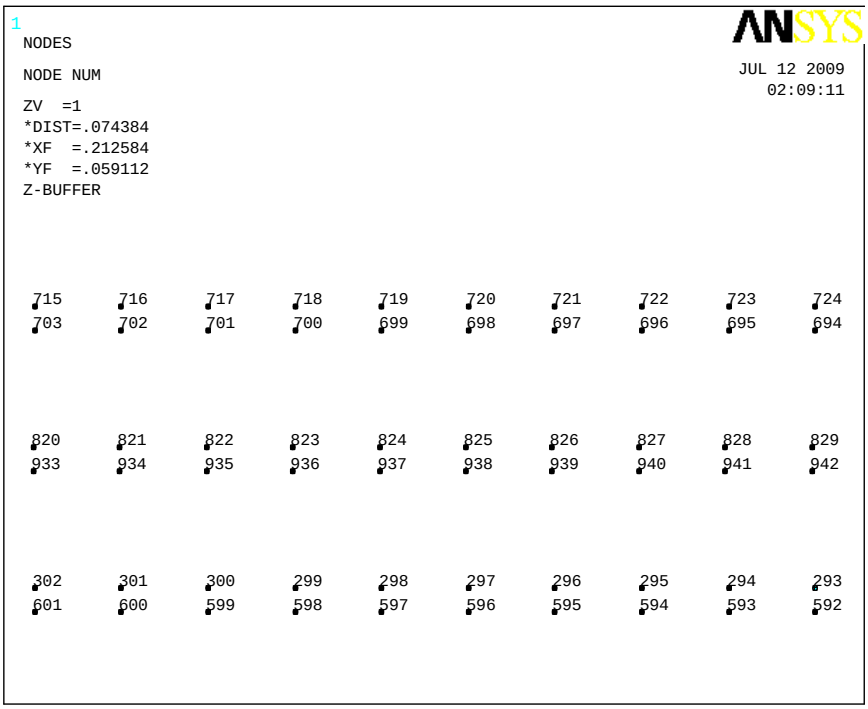


**Fig. 5.34 Key points for counter flow air heater**

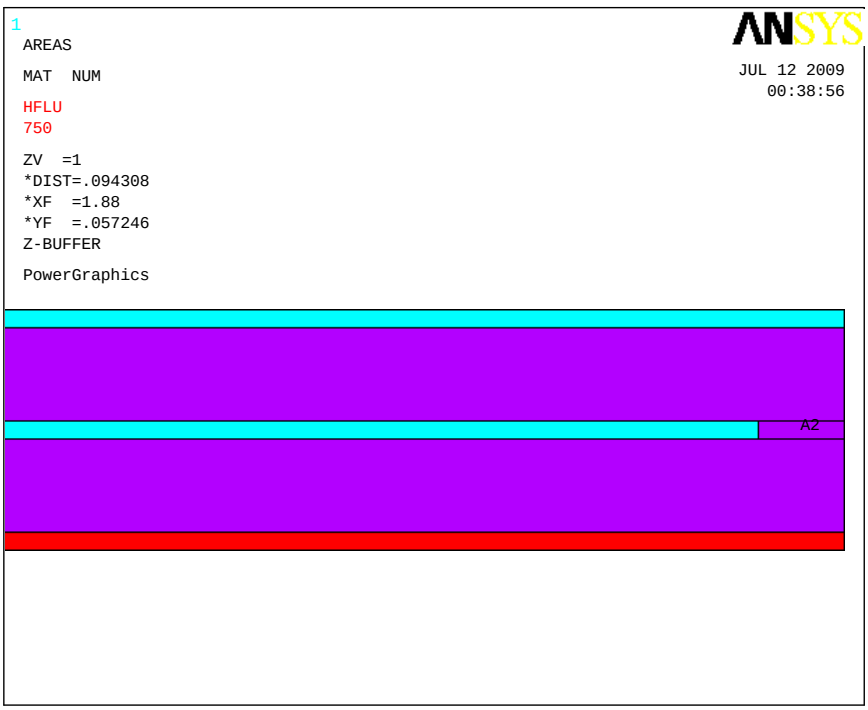


**Fig. 5.35 Areas of counter flow air heater**

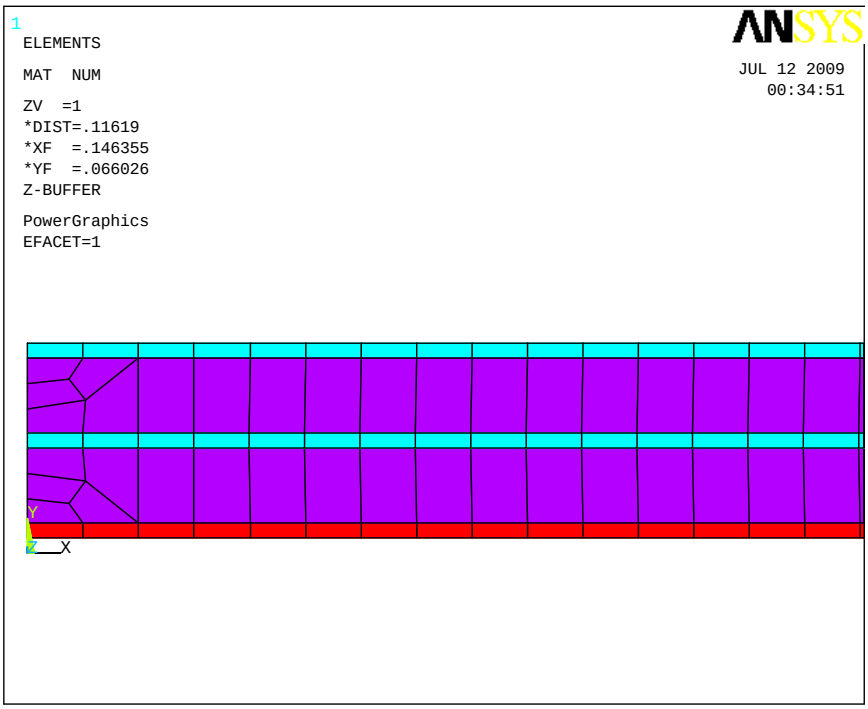


**Fig. 5.36 Meshing at inlet of counter flow air heater**

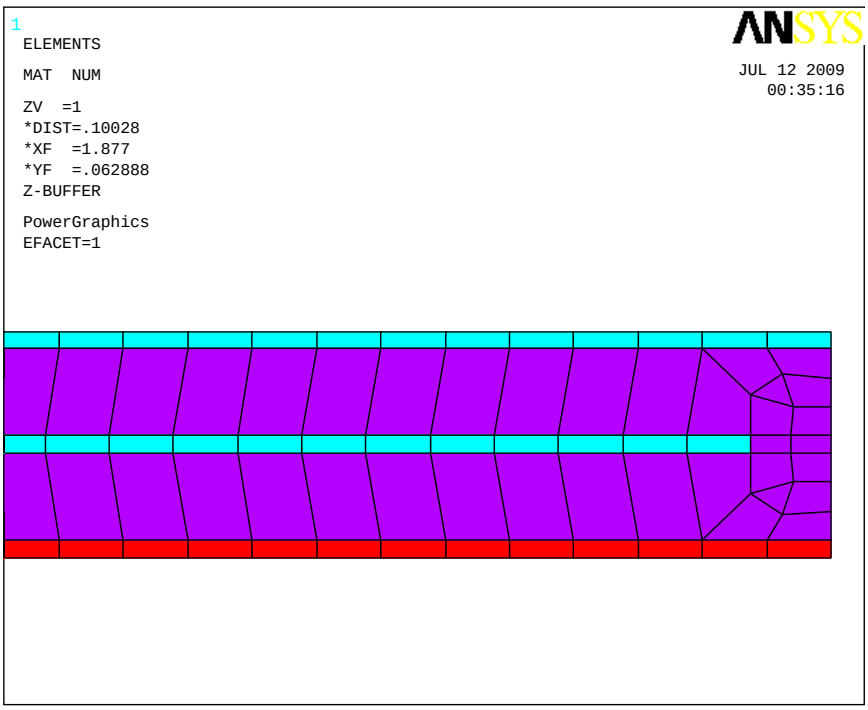


**Fig. 5.37 Meshing at outlet of counter flow air heater**

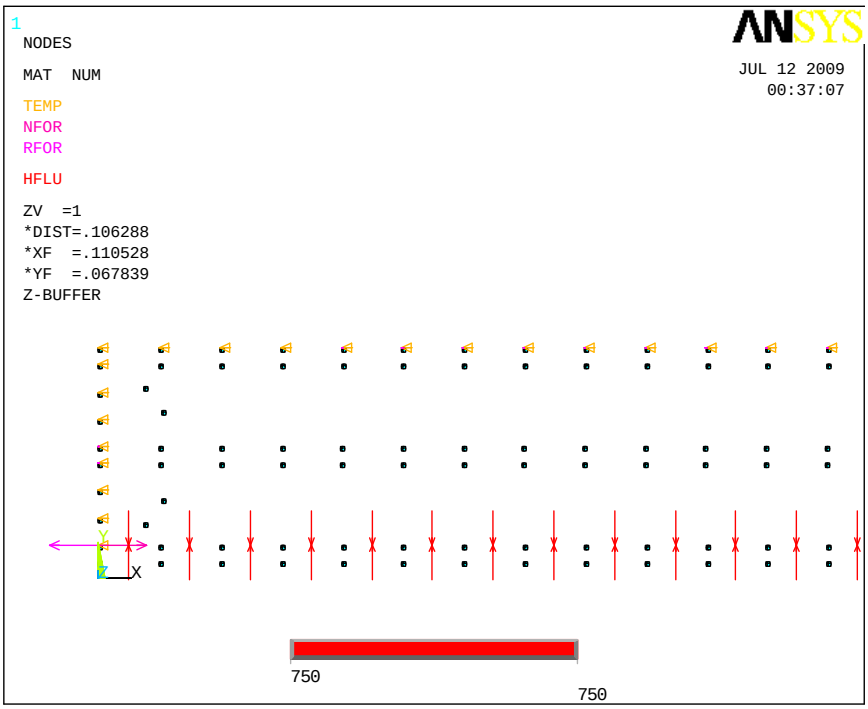


**Fig. 5.38 Constraints at inlet for counter flow air heater**

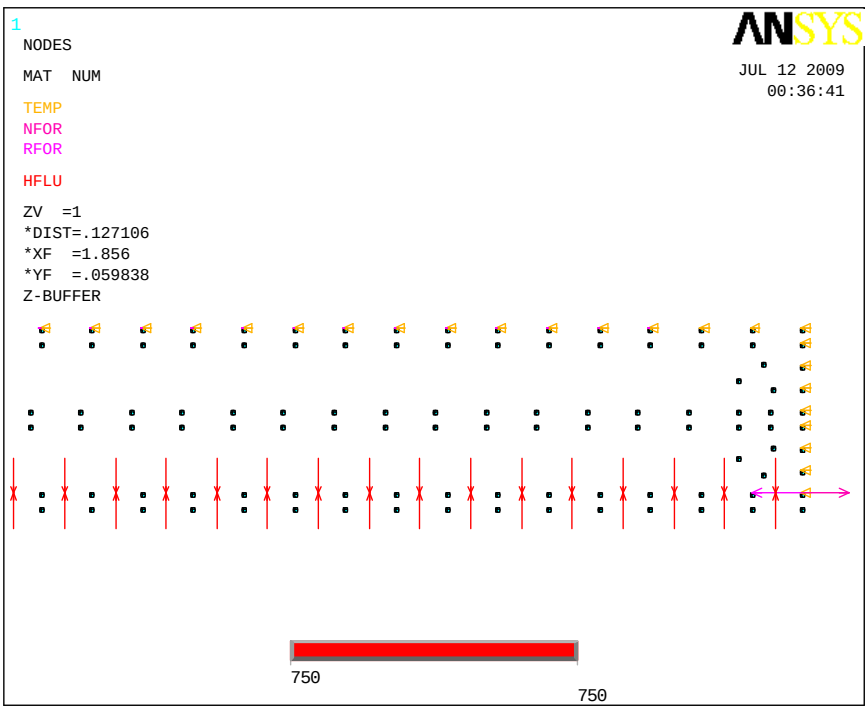


**Fig. 5.39 Constraints at outlet for counter flow air heater**

## 5.6 ANSYS RESULTS

After solving all the three cases in ANSYS we get temperature variation for the three types of solar air heater i.e. single glazing, double glazing and counter flow with porous matrix air heater. The temperature variation for single glazing and double glazing is almost same as shown in Fig. 5.39-Fig. 5.44 and temperature is highest at the center of the air heaters along the length. Fig.5.45-Fig. 5.47 shows the average temperature of absorber plate in counter flow air heater which is maximum as compare to conventional air heaters.

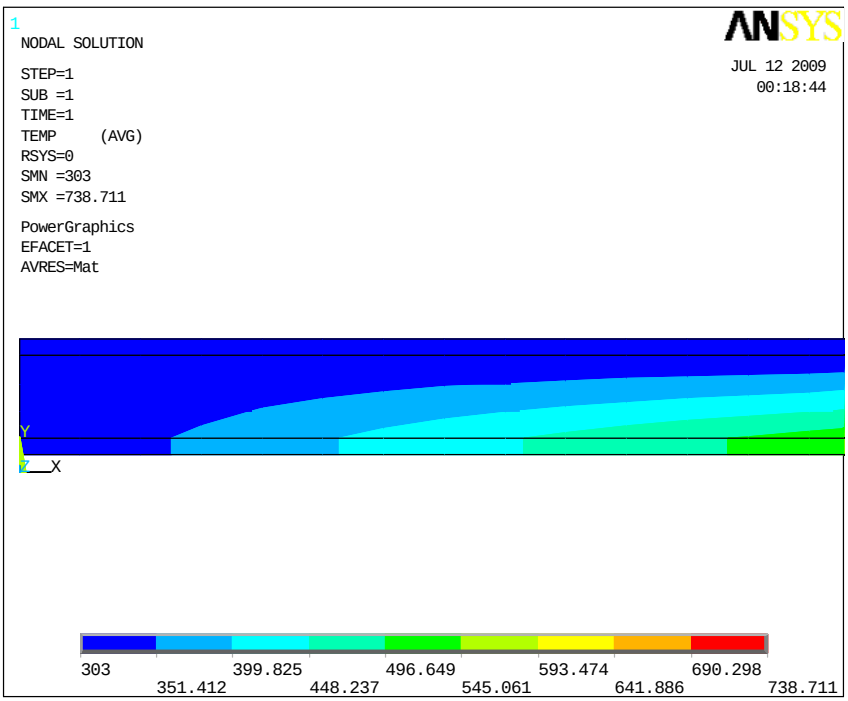


**Fig. 5.40 Temperature variation for single glazing air heater at inlet**

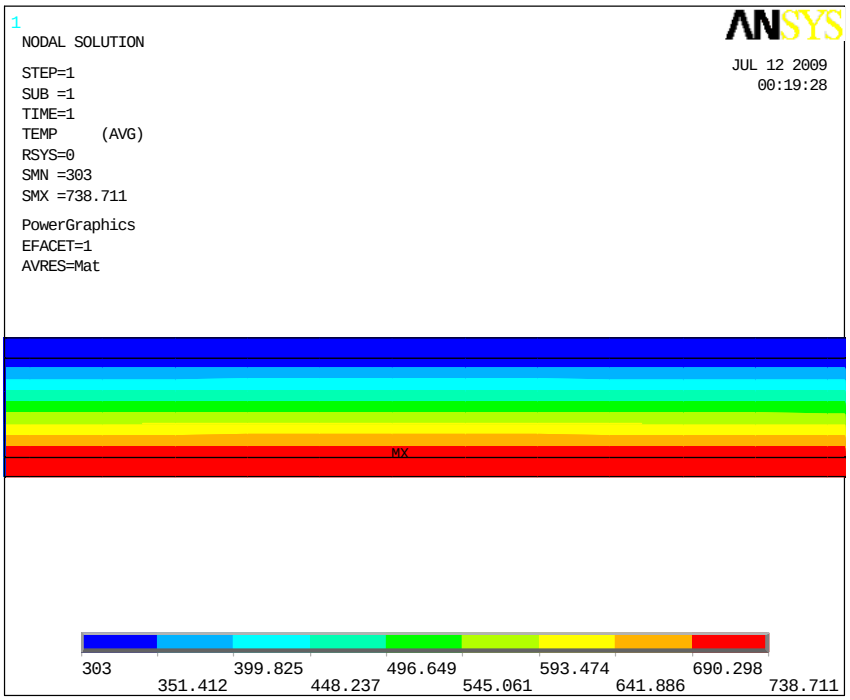


**Fig. 5.41 Temperature variation for single glazing air heater at center**

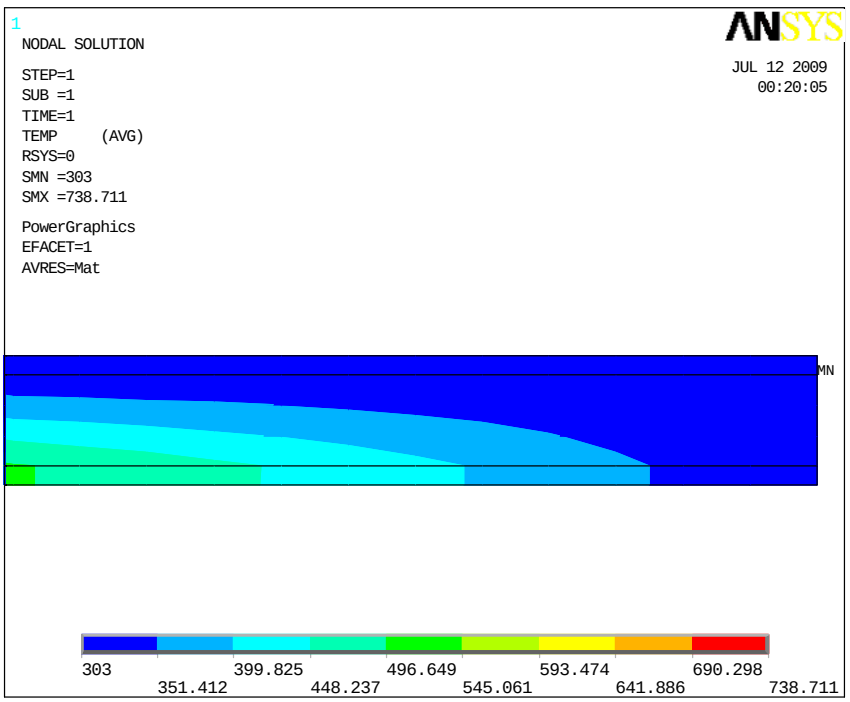


**Fig. 5.42 Temperature variation for single glazing air heater at outlet**

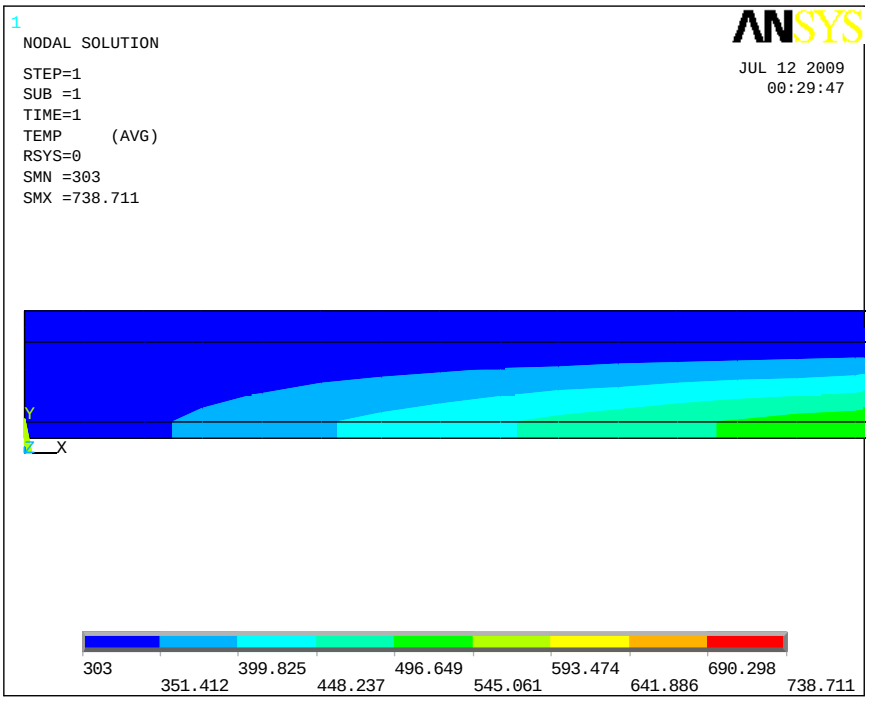


**Fig. 5.43 Temperature variation for double glazing air heater at inlet**

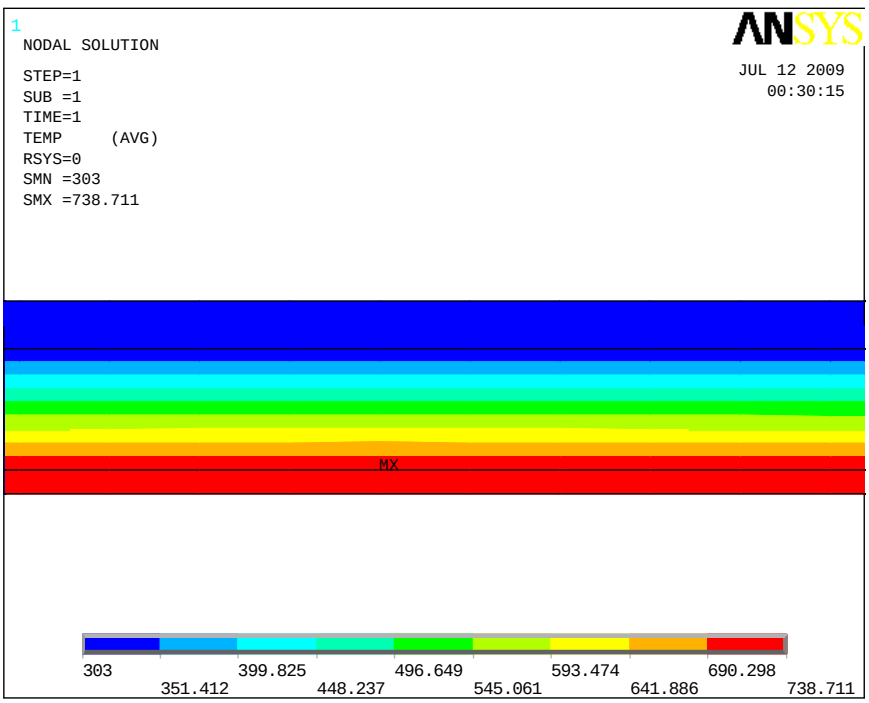


**Fig. 5.44 Temperature variation for double glazing air heater at center**

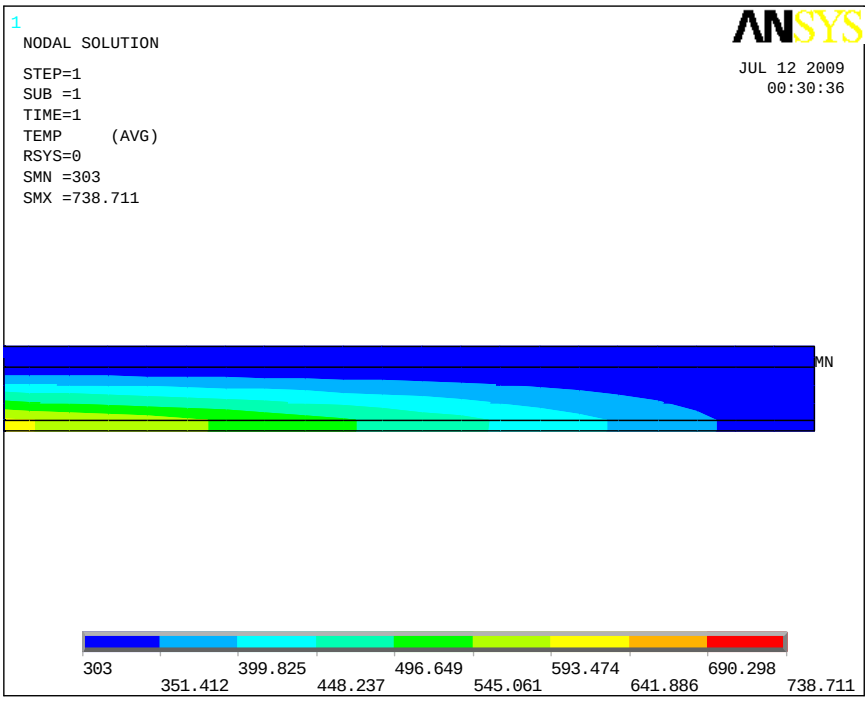


**Fig. 5.45 Temperature variation for double glazing air heater at outlet**

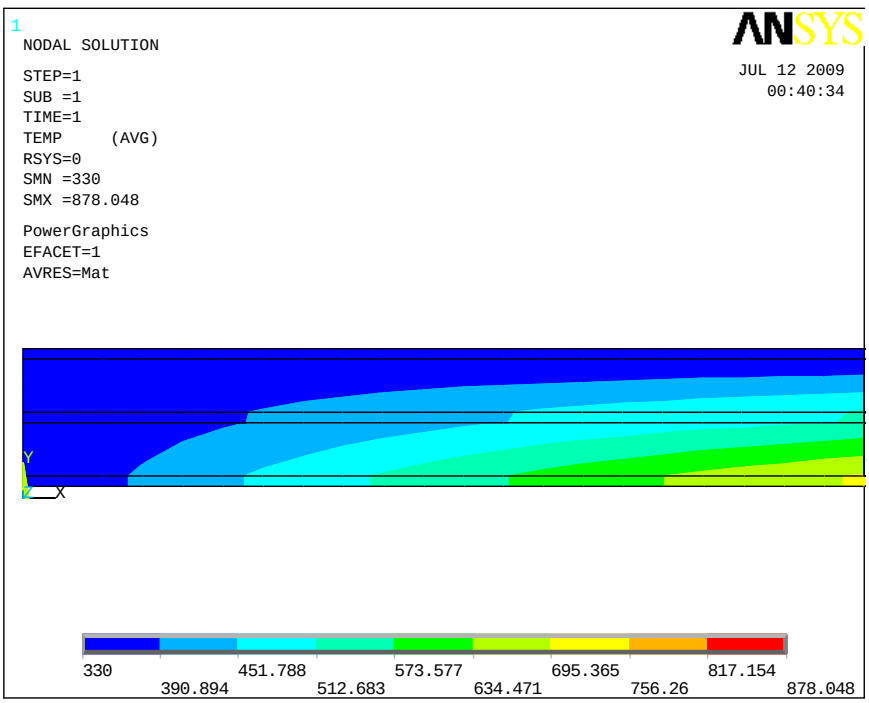


**Fig. 5.46 Temperature variation for counter flow air heater at inlet**

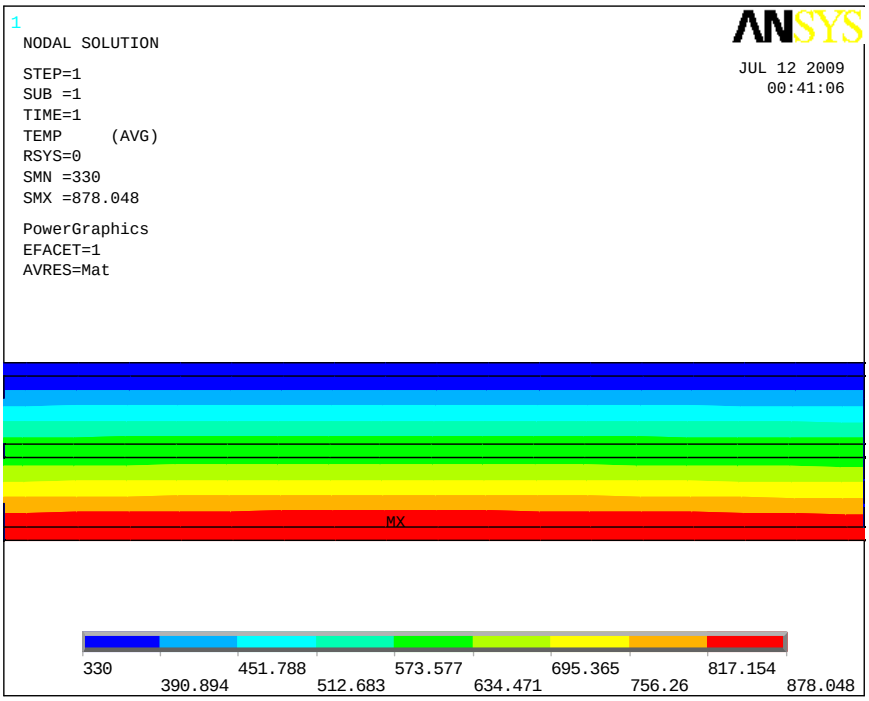


**Fig. 5.47 Temperature variation for counter flow air heater at center**

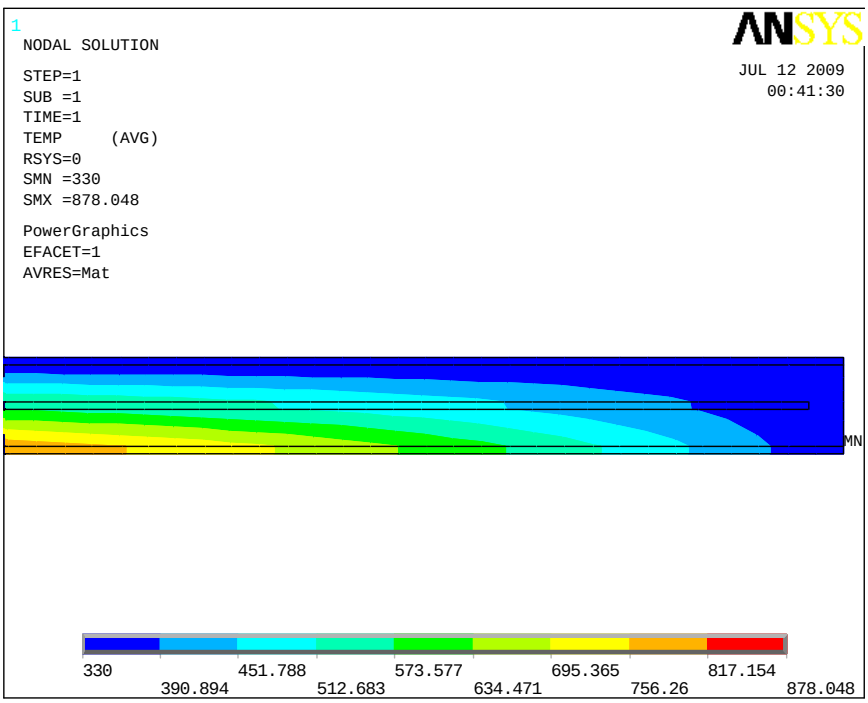


**Fig. 5.48 Temperature variation for counter flow air heater at outlet**

# CHAPTER 6
# CONCLUSION AND SCOPE OF FUTURE WORK

## 6.1 CONCLUSION

Following conclusions can be drawn from the present work:

1. In the present work the drawbacks of the conventional solar heaters i.e. single glazing solar air heater and double glazing solar air heater are identified, which are heat loss to the surrounding through the front cover and the poor convective heat transfer from the absorber to the air.
2. The performance of counter flow air heater is compared with the conventional solar air heaters for the mass flow range 0.01kg/m.s-0.02kg/m.s. The heat loss from the top cover is reduced in case of counter flow solar air heater for the entire range of mass flow rate. The efficiency of counter flow solar air heater is further increased by adding porous matrix to the air heater in second air pass. The path of the air travel is increased in case of counter flow solar air heater resulting higher outlet temperature of the same mass flow rate. This collector minimizes the heat losses to the ambient and maximizes the heat transfer to the air stream.
3. The thermal efficiency of counter flow solar air heater is more than conventional solar air heater of same construction cost.
4. The only problem with the counter flow heater is that the higher pressure drop is encountered at high flow rates.
5. Increasing the duct depth increases $\Delta T_g$ and $\Delta T_p$ for given mass flow rate.

## 6.2 SCOPE OF FUTURE WORK

The work can be extended for varying solar radiations instead of constant solar radiation as in the present work.

# REFERENCES


1. Zhao, Q., Salder, G.W., Leonardo, J.J., "Transient simulation of flat-plate solar collectors", Solar Energy, Vol.40, pp.167-174, 1988.

2. Choudhury, C., Anderson, S.L., Rekstad, J., "A solar air heater for low temperature applications", Solar Energy, Vol. 40, pp. 335-344, 1988.

3. Nasr, K.J., Ramadhyani, S., Viskanta, R., "Numerical studies of forced convection heat transfer from a cylinder embedded in a packed bed", Int., J., Heat and Mass Transfer, Vol.38, pp2353-2366, 1995.

4. Gupta, D., Solanki, S.C., Saini, J.S., "Thermo-hydraulic performance of solar air heaters with roughened absorber plates", Solar Energy, Vol. 61, pp.33-42, 1997.

5. Jannot, Y., Coulibaaly, Y., "Radiative heat transfer in a solar air heater covered with a plastic film", Solar Energy, Vol. 60, pp. 35-40, 1997.

6. Mohamad, A.A., "High efficiency solar air heater", Solar energy Vol. 60, pp. 71-76, 1997

7. Akhtar, N., Mullick, S.C., "Appropriate method for computation of glass cover temperature and top heat-loss coefficient of solar collectors with single glazing", Solar Energy, Vol. 66, pp. 349-354,1999.

8. Kolb, A., Winter, E.R.F., Viskanta, R., "Experimental studies on a solar air collector with metal matrix absorber", Solar Energy, Vol. 65, pp. 91-98, 1999.

9. Karwa, Rajendra, "Need for reliable heat transfer coefficient correlation for Transition flow regime in rectangular duct of smooth plate solar air heater" Heat and Mass Transfer HMT, pp. 399-402, 2000.

10. Muluwork, K.B., "Study of heat transfer and friction in solar air heaters with staggered discrete ribs", Heat and Mass Transfer HMT, pp. 391-397, 2000.

11. Mittal, M.K., Varshney, L., "Optimal thermo hydraulic performance of a wire mesh packed solar air heater", Solar Energy, Vol. 80 pp. 1112-1120, 2005.

12. Mittal, M.K., Varun., Saini, R.P., Singhal, S.K., "Effective efficiency of solar air heaters having different types of roughness elements on the absorber plate", Energy, Vol. 32, pp. 739-745, 2007.

13. Aharwal, K., R., Gandhi, B., K., Saini, J., S., "Experimental investigation on heat-transfer enhancement due to a gap in an inclined continuous rib arrangement in a rectangular duct of solar air heater", Renewable Energy, Vol. 33 pp. 585-596, 2007.

14. Sparrow, E.M., and Tien, K.K., "Forced convection heat transfer at an inclined and yawed square plate application to solar collectors", Heat transfer, Vol. 99 pp. 507-522, 1977.

15. Sukhatme S.P., "Solar energy", 3rd ed., 1984, Tata Mcgraw Hill, New delhi.

# APPENDIX

```
#include "stdafx.h"

void gauss_ele(double a[2][2],double b[2],double x[2],double &Tc1,double &Tc2);
void gauss_ele(double a1[3][3],double b1[3],double x1[3],double &Tc1,double
&Tc2,double &Tp);
double Ta = 288;    //Air inlet temperature
double I=750;        // Solar radiation
double b = 0.025;   // Duct depth
double Pa = 100000;
double rhoa=1.1885;
double mua=0.000018249;
double ka = 0.025743;
double cp=1006.4;
double ha=10;
double alpha_c=0.06;
double tau_c=0.92;
double alpha_p=0.92;
double Ub=1;
double d=1;
double L = 2.0;
double ec=0.06;
double ep=0.92;
double sigma=0.0000000567;

void main()
{
int i,j,n,n1,no;
double division;
double Tc,Tp,Tc1,Tc2,T[1000],Tc1_new[1000]={0},Tf2[1000],Tc2_new,Keff=0.3;
double hr;
double m[10];
double v[10];
double re[10];
double nu[10];
double hf[10];
double A=b*d;
double p=2*(b+d);
double de=(4*A)/p;
double pr=(mua*cp)/ka;
double a[2][2], b[2],x[2],a1[3][3], b1[3],x1[3];
cout<<"enter 1 for single glass air heater"<<"\n"<<"enter 2 for double glass air
heater"<<"\n"
```

```
<<"enter 3 for counter flow air heater"<<"\n"<<"enter 4 for counter flow air heater with
porous matrix";
cin>>n1;
        switch(n1)
        {
        case 1: //For single glass cover air heater
                cout<<"enter the number of mass u want to enter";
                cin>>n;
                for ( i=0;i<n;i++)
                {
                cout<<"enter the value of mass m"<<i+1<<"=";
                cin>>m[i];
                }
                cout<<"Enter th no. of division=";
                cin>>division;

                        for(i=0;i<n;i++)
                        {
                                Tc=Ta,Tp=Ta,T[0]=Ta;

                                for ( j=0;j<=division;j++)
                                {
                                v[i]=m[i]/(rhoa*A);
                                re[i]=(rhoa*v[i]*de)/mua;
                                nu[i]=0.0333*(pow(re[i],0.8))*(pow(pr,0.33));
                                hf[i]=nu[i]*ka/de;
                                hr=5;
                                a[0][0]=(ha+hf[i])+hr;
                                a[0][1]=-hr;
                                a[1][0]=-hr;
                                a[1][1]=hf[i]+hr+Ub;
                                b[0]=(I*alpha_c)+(ha*Ta)+(hf[i]*T[j]);
                                b[1]=(I*tau_c*alpha_p)+(hf[i]*T[j])+(Ub*Ta);
                                gauss_ele(a,b,x,Tc,Tp);
                                double G=rhoa*v[i];
                                double dz=(2/division);
                                T[j+1]=T[j]+((dz*hf[i])*((Tc-T[j])+(Tp-T[j])))/(G*A*cp);
                                }

                                cout<<"Values of temperatur cooresponding to mass
                                m"<<i+1<<"\n";
                                cout<<"value of Tc="<<Tc<<"\n"<<"value of
                                Tp="<<Tp<<"\n";
                                cout<<"Tf="<<T[j];
```

```
                    }
                    break;

case 2: //For double glass cover air heater
                cout<<"enter the number of mass u want to enter";
                cin>>n;
                for ( i=0;i<n;i++)
                {
                cout<<"enter the value of mass m"<<i+1<<"=";
                cin>>m[i];
                }
                cout<<"Enter th no. of division=";
                cin>>division;
                        for(i=0;i<n;i++)
                        {
                        Tc1=Ta,Tc2=Ta,Tp=Ta,T[0]=Ta;

                                for ( j=0;j<=division;j++)
                                {
                                v[i]=m[i]/(rhoa*A);
                                re[i]=(rhoa*v[i]*de)/mua;
                                nu[i]=0.0333*(pow(re[i],0.8))*(pow(pr,0.33));
                                hf[i]=nu[i]*ka/(2*de);
                                hr=5;
                                a1[0][0]=(ha+hf[i])+hr;
                                a1[0][1]=-(hf[i]+hr);
                                a1[0][2]=0;
                                a1[1][0]=-(hf[i]+hr);
                                a1[1][1]=2*hf[i]+2*hr;
                                a1[1][2]=-hr;
                                a1[2][0]=0;
                                a1[2][1]=-hr;
                                a1[2][2]=Ub+hf[i]+hr;
                                b1[0]=(I*alpha_c)+(ha*Ta);
                                b1[1]=(I*tau_c*alpha_c)+(hf[i]*T[j]);
                                b1[2]=(I*tau_c*alpha_p)+(hf[i]*T[j])+(Ub*Ta);
                                gauss_ele(a1,b1,x1,Tc1,Tc2,Tp);
                                double G=rhoa*v[i];
                                double dz=(2/division);
                                T[j+1]=T[j]+((dz*hf[i])*((Tc2-T[j])+(Tp-T[j])))/(G*A*cp);
                                }
                                cout<<"Values of temperatur cooresponding to mass
                                m"<<i+1<<"\n";
                                cout<<"tc1="<<Tc1<<"\n"<<"tc2="<<Tc1<<
                                "\n"<<"tp="<<Tp<<"\n";
                                cout<<"T="<<T[j];
```

```
                cout<<"\n";
            }
            break;
case 3: //For counter flow air heater without porous matrix
        cout<<"enter the number of mass u want to enter";
        cin>>n;

        for ( i=0;i<n;i++)
        {
        cout<<"enter the value of mass m"<<i+1<<"=";
        cin>>m[i];

        }
        cout<<"Enter th no. of division=";
        cin>>division;
        no=division;
            for(i=0;i<n;i++)
            {
            Tc1=Ta;
            Tc2=Ta;
            Tc2_new=Ta;
            Tp=Ta;
            for ( j=0;j<=division;j++)
            {
            T[0]=Ta;
            v[i]=m[i]/(rhoa*A);
             re[i]=(rhoa*v[i]*de)/mua;
            nu[i]=0.0333*(pow(re[i],0.8))*(pow(pr,0.33));
            hf[i]=nu[i]*ka/de;
            hr=5;
            a[0][0]=(ha+hf[i])+hr;
            a[0][1]=-hr;
            a[1][0]=-hr;
            a[1][1]=2*(hf[i]+hr);
            b[0]=(I*alpha_c)+(ha*Ta)+(hf[i]*T[j]);
            b[1]=(I*tau_c*alpha_c)+(hf[i]*T[j])+(hf[i]*Ta)+(hr*Ta);
            gauss_ele(a,b,x,Tc1,Tc2);
            Tc1_new[no-j]=Tc1;
            double G=rhoa*v[i];
            double dz=(2/division);
            T[j+1]=T[j]+((dz*hf[i])*((Tc1-T[j])+(Tc2-T[j])))/(G*A*cp);
            if(j==division)
            Tf2[0]=T[j+1];
            }
            for (j=0;j<=division;j++)
            {
```

```
                T[0]=Ta;
                v[i]=m[i]/(rhoa*A);
                re[i]=(rhoa*v[i]*de)/mua;
                nu[i]=0.0333*(pow(re[i],0.8))*(pow(pr,0.33));
                hf[i]=nu[i]*ka/de;
                hr=5;
                a[0][0]=2*(hf[i]+hr);
                a[0][1]=-hr;
                a[1][0]=-hr;
                a[1][1]=(hr+hf[i])+Ub;
                b[0]=(I*tau_c*alpha_c)+(Tc1_new[j]*hr)+
                (hf[i]*Tf2[j])+(hf[i]*Tf2[j]);
                b[1]=(I*tau_c*alpha_p)+(hf[i]*Tf2[j])+(Ub*Ta);
                gauss_ele(a,b,x,Tc2_new,Tp);
                double G=rhoa*v[i];
                double dz=(2/division);
                Tf2[j+1]=Tf2[j]+((dz*hf[i])*((Tc2_new-Tf2[j])+(Tp-
                Tf2[j])))/(G*A*cp);

                }
                cout<<"Values of temperatur cooresponding to mass
                m"<<i+1<<"\n";
                cout<<"Tc1="<<Tc1<<"\n"<<"Tp="<<Tp<<"\n";
                cout<<"Tf="<<Tf2[j];
                cout<<"\n";
                }
                cout<<"\n";
        break;

case 4: //For counter flow air heater with porous matrix
        cout<<"enter the number of mass flow rates u want to enter";
        cin>>n;

        for ( i=0;i<n;i++)
        {
        cout<<"enter the value of mass flow rates m"<<i+1<<"=";
        cin>>m[i];

        }
        cout<<"Enter th no. of division=";
        cin>>division;
        no=division;
        for(i=0;i<n;i++)
        {
                Tc1=Ta;
                Tc2=Ta;
```

```
Tc2_new=Ta;
Tp=Ta;
for ( j=0;j<=division;j++)
{
T[0]=Ta;
v[i]=m[i]/(rhoa*A);
 re[i]=(rhoa*v[i]*de)/mua;
nu[i]=0.0333*(pow(re[i],0.8))*(pow(pr,0.33));
hf[i]=nu[i]*ka/de;
hr=5;
a[0][0]=(ha+hf[i])+hr;
a[0][1]=-hr;
a[1][0]=-hr;
a[1][1]=2*(hf[i]+hr);
b[0]=(I*alpha_c)+(ha*Ta)+(hf[i]*T[j]);
b[1]=(I*tau_c*alpha_c)+(hf[i]*T[j])+(hf[i]*Ta)+(hr*Ta);
gauss_ele(a,b,x,Tc1,Tc2);
Tc1_new[no-j]=Tc1;
double G=rhoa*v[i];
double dz=(2/division);
T[j+1]=T[j]+((dz*hf[i])*((Tc1-T[j])+(Tc2-T[j])))/(G*A*cp);
if(j==division)
Tf2[1]=T[j+1];
}


for (j=0;j<=division;j++)
{
v[i]=m[i]/(rhoa*A);
re[i]=(rhoa*v[i]*de)/mua;
nu[i]=0.0333*(pow(re[i],0.8))*(pow(pr,0.33));
hf[i]=nu[i]*ka/de;
hr=5;
Tf2[0]=Tf2[1];
Tc2=((I*tau_c*alpha_c)+(hf[i]*Tf2[j])+(hf[i]*Tf2[1])+
        (hr*Tc1_new[no-j])+(hr*Tf2[j]))/(2*(hf[i]+hr));
double G=rhoa*v[i];
double dz=(2/division);
Tf2[j+1]=((Tf2[j]*((G*A*cp*dz)-(2*Keff)))+(Keff*Tf2[j-1])+
(hf[i]*dz*dz*(Tc2_new-Tf2[j]))+(Ub*dz*dz*(Ta-Tf2[j]))+
(I*dz*dz*tau_c*alpha_p))/(G*A*cp*dz-Keff);
}
cout<<"Values of temperatur cooresponding to mass
m"<<i+1<<"\n";
cout<<"Tc1="<<Tc1<<"\n";
cout<<"Tf="<<Tf2[j];
```

```
                        cout<<"\n";

                }
        cout<<"\n";
        break;
        }
}
// Function for Gauss elimination method
void gauss_ele(double a[2][2],double b[2],double x[2],double &Tc,double &Tp)
{
        int n=2;
        for(int k=0;k<n-1;k++)
        {
                for(int i=k+1;i<n;i++)
                {
                        double c=a[i][k]/a[k][k];
                        for(int j=k;j<n;j++)
                        {
                                a[i][j]-=c*a[k][j];
                        }
                        b[i]-=c*b[k];
                }
        }
        for(k=n-1;k>=0;k--)
        {
                for(int i=n-1;i>k;i--)
                {
                b[k]=b[k]-(a[k][i]*x[i]);
                }
                x[k]=b[k]/a[k][k];
        }
                Tc=x[0];
                Tp=x[1];
}
void gauss_ele(double a1[3][3],double b1[3],double x1[3],double &Tc1,double
&Tc2,double &Tp)
{
        int n=3;
        for(int k=0;k<n-1;k++)
        {
                for(int i=k+1;i<n;i++)
                {
                        double c=a1[i][k]/a1[k][k];
                        for(int j=k;j<n;j++)
                        {
                                a1[i][j]-=c*a1[k][j];
```

```
                    }
                    b1[i]-=c*b1[k];
                }
        }
        for(k=n-1;k>=0;k--)
        {
                for(int i=n-1;i>k;i--)
                {
                b1[k]=b1[k]-(a1[k][i]*x1[i]);
                }
                x1[k]=b1[k]/a1[k][k];
        }

                Tc1=x1[0];
                Tc2=x1[1];
                Tp=x1[2];
}
```